

**NON-EQUILIBRIUM STEADY STATE  
PHASE TRANSITIONS OF VARIOUS  
STATISTICAL MODELS**

A DISSERTATION SUBMITTED TO  
THE DEPARTMENT OF PHYSICS  
AND THE GRADUATE SCHOOL OF ENGINEERING AND SCIENCE  
OF BILKENT UNIVERSITY  
IN PARTIAL FULFILLMENT OF THE REQUIREMENTS  
FOR THE DEGREE OF  
DOCTOR OF PHILOSOPHY

By  
Başak Renkliođlu  
June, 2013

I certify that I have read this thesis and that in my opinion it is fully adequate, in scope and in quality, as a dissertation for the degree of Doctor of Philosophy.

---

Prof. Dr. M. Cemal Yalabık(Advisor)

I certify that I have read this thesis and that in my opinion it is fully adequate, in scope and in quality, as a dissertation for the degree of Doctor of Philosophy.

---

Prof. Dr. Bilal Tanatar

I certify that I have read this thesis and that in my opinion it is fully adequate, in scope and in quality, as a dissertation for the degree of Doctor of Philosophy.

---

Assoc. Prof. Dr. Azer Kerimov

I certify that I have read this thesis and that in my opinion it is fully adequate, in scope and in quality, as a dissertation for the degree of Doctor of Philosophy.

---

Assoc. Prof. Dr. M. Özgür Oktel

I certify that I have read this thesis and that in my opinion it is fully adequate, in scope and in quality, as a dissertation for the degree of Doctor of Philosophy.

---

Prof. Dr. Tacettin Altanhan

Approved for the Graduate School of Engineering and Science:

---

Prof. Dr. Levent Onural  
Director of the Graduate School

# ABSTRACT

## NON-EQUILIBRIUM STEADY STATE PHASE TRANSITIONS OF VARIOUS STATISTICAL MODELS

Başak Renklioğlu

Ph.D. in Physics

Supervisor: Prof. Dr. M. Cemal Yalabık

June, 2013

Non-equilibrium phase transitions of a number of systems are investigated by several methods. These systems are in contact with thermal baths with different temperatures and taken to be driven to the non-equilibrium limits by spin exchange (Kawasaki) dynamics.

First of all, the criticality of the two-finite temperature spin-1/2 Ising model with a conserved order parameter on a square lattice is studied through a real space renormalization group transformation. The dynamics of the non-equilibrium system are characterized by means of different temperatures ( $T_x$  and  $T_y$ ), and also different time-scale constants, ( $\alpha_x$  and  $\alpha_y$ ) for spin exchanges in the  $x$  and  $y$  directions. Based on the RG flows, the critical surface of the system is obtained as a function of these exchange parameters. This is the first study in which the full critical surface displaying various universality classes of this system is reported.

Secondly, steady state phase transitions of the eight-vertex model, formulated by two interlaced two-dimensional Ising models on square lattices, are studied through four independent Monte Carlo simulations, each with  $60 \times 10^6$  Monte Carlo steps on  $N \times N$  lattices with  $N = 32, 40, 80, 100$ . To obtain an isotropic system, the spin exchanges are considered to occur within the sublattices. We observe non-universal behavior for non-equilibrium transitions around the equilibrium transitions, and Ising like behavior when one of the bath temperature becomes very large.

*Keywords:* Non-Equilibrium Phase Transitions, Renormalization Group Theory, Monte Carlo Simulations, Critical Point, Critical Exponent, Universality.

## ÖZET

# FARKLI İSTATİSTİKSEL MODELLERDE DENGE DIŐI FAZ GEÇİŐLERİ

BaŐak Renkliođlu

Fizik, Doktora

Tez Yöneticisi: Prof. Dr. M. Cemal Yalabık

Haziran, 2013

Farklı sistemlerin denge dıŐı faz geçiŐleri deđiŐik yollarla incelenmiŐtir. Bu sistemler farklı sıcaklıklılı ısı banyoları ile etkileŐmekte olup, denge dıŐı limitlerine Kawasaki-tipi (spin deđiŐimi) stokastik dinamiđi ile eriŐmektedirler.

İlk olarak, kare örgüli, iki-sıcaklıklılı ve korunumlu düzen parametrelili spin-1/2 Ising modelinin kritiklik durumu, konum uzayı renormalizasyon grup metodu kullanılarak incelenmiŐtir. Denge dıŐı dinamikler, farklı sıcaklıklar ( $T_x$  ve  $T_y$ ) ve  $x$  ile  $y$  yönlerinde gerçekteŐen spin deđiŐimleri için farklı zaman ölçek sabitleri ( $\alpha_x$  ve  $\alpha_y$ ) ile sađlanmıŐtır. Bu çalıŐma ile sisteme ait çok parametrelili kritik yüzey ilk defa sunulmuŐtur. İlgili kritik üsteller elde edilmiŐ olup, sürer durumlar için elde edilen üstellerin denge dıŐı faz geçiŐlerinin farklı evrensellik sınıfı özelliđini gösterdiđi tespit edilmiŐtir.

Ayrıca, iki-boyutlu kare örgüli iç içe geçmiŐ iki adet Ising modelinden oluŐan sekiz-köŐe modelinin sürer durum faz geçiŐleri Monte Carlo simülasyonu yolu ile çalıŐılmıŐtır. Birbirinden bađımsız dört farklı  $60 \times 10^6$  Monte Carlo adımı içeren simülasyonlardan yararlanılmıŐtır. Sistem dinamiklerini oluŐturan spin deđiŐimleri alt örgüler içerisinde gerçekteŐmektedir. Denge durumu faz geçiŐ noktaları etrafında incelenen denge dıŐı faz geçiŐlerinin evrensellik özelliđi taŐımadıđı gözlenmiŐtir. Ayrıca ısı banyolarından birinin sıcaklıđı çok büyük olduđunda faz geçiŐlerinin denge durumu Ising benzeri bir davranıŐ sergilediđi görülmektedir.

*Anahtar sözcükler:* Denge Olmayan Faz GeçiŐleri, Renormalizasyon Grup Teorisi, Monte Carlo Simülasyonu, Kritik Nokta, Kritik Üstel, Evrensellik.

To my beloved family...

## Acknowledgement

Completing my PhD degree is probably the most challenging activity of my life. The best and worst moments of my doctoral journey have been shared with many people. It has been a great privilege to spend several years in the Department of Physics at Bilkent University, and its members will always remain dear to me.

My first debt of gratitude must go to my advisor, Prof. Dr. M. Cemal Yalabık. He patiently provided the vision, encouragement and advice necessary for me to proceed through the doctoral program and complete my dissertation. I want to thank Prof. Dr. M. Cemal Yalabık for his unflagging encouragement and serving as a role model to me as a junior member of academia. He has been a strong and supportive adviser to me throughout my graduate school career, but he has always given me great freedom to pursue independent work.

Special thanks to my committee, Prof. Dr. Bilal Tanatar, Assoc. Dr. Azer Kerimov, Assoc. Prof. Dr. M. Özgür Oktel, and Prof. Dr. Tacettin Altanhan for their guidance and helpful suggestions. Their guidance has served me well and I owe them my heartfelt appreciation. I would also like to express my gratitude to Turkish Academy of Sciences (TUBA) for the financial support they provided during my research.

My friends in İstanbul and Ankara were sources of laughter, joy, and support. Thanks to Esra Ülkü for visiting me constantly, Ayşe Ferhan Yeşil for being an awesome companion in all of our travels and Ece Demirci for not making me feel alone in the way of the Ph.D. misery. Special thanks go to my roommate Hatice Çalık for being supportive, encouraging, and patient during all those years. I am very happy that, in many cases, my friendships with you have extended well beyond our shared time in Bilkent.

I wish to thank my parents, Mehmet and Hasibe Renklioğlu and my brother Cihan Renklioğlu. Their love provided my inspiration and was my driving force. I owe them everything and wish I could show them just how much I love and appreciate them.

# Contents

<b>1</b>	<b>Introduction</b>	<b>1</b>
1.1	Master Equation . . . . .	2
1.2	Equilibrium Dynamics . . . . .	4
1.3	Non-Equilibrium Dynamics . . . . .	6
1.4	Critical Exponents . . . . .	6
1.4.1	Critical Exponents of Equilibrium Systems . . . . .	7
1.4.2	Dynamic Critical Exponents . . . . .	12
1.5	Universality: “Out of-Equilibrium” Classes . . . . .	13
1.5.1	Dynamical Ising Classes . . . . .	13
1.5.2	Kinetic Ising Model - Near Equilibrium . . . . .	14
1.5.3	Kinetic Ising Model - Out of-Equilibrium . . . . .	17
<b>2</b>	<b>Literature Review</b>	<b>20</b>
<b>3</b>	<b>Global Phase Diagram of the Two-Temperature Ising Model with Kawasaki Dynamics from Real Space Renormalization Group</b>	

<b>Theory</b>	<b>24</b>
3.1 The Model . . . . .	25
3.2 The RG Transformation . . . . .	26
3.2.1 The Concepts of Renormalization Group Theory . . . . .	26
3.2.2 General Remarks . . . . .	30
3.2.3 Previous Work on RSRG Transformation . . . . .	31
3.3 Our RG Transformation . . . . .	33
3.4 Results and Conclusion . . . . .	40
3.5 Discussion on the Suitability of Proposed Transformation . . . . .	47
<b>4 A Monte Carlo Study on the Steady State Phase Transitions of the Eight-Vertex Model with Conserved Order Dynamics</b>	<b>52</b>
4.1 The Model . . . . .	53
4.2 Monte Carlo Simulations . . . . .	56
4.3 Data Collapse . . . . .	59
4.4 Results and Conclusion . . . . .	61
<b>5 Further Considerations: Full Phase Diagram of the Non-Equilibrium Eight-Vertex Model with Conserved Order Dynamics</b>	<b>66</b>
5.1 The Model . . . . .	67
5.2 Preliminary Results . . . . .	70
5.2.1 Single Temperature Variation: . . . . .	70

5.2.2 Two Temperature Variation: . . . . .	72
5.3 Discussion . . . . .	74
<b>6 Summary and Conclusion</b>	<b>76</b>
<b>A Finite Size and Truncation Effects for the Non-Conserved RG Transformation</b>	<b>89</b>
<b>B Spline Interpolation</b>	<b>91</b>
<b>C Code-1: RSRG Transformation</b>	<b>94</b>
<b>D Code-2: Monte Carlo Simulations</b>	<b>121</b>
<b>E Code-3: Finite Size Scaling</b>	<b>134</b>

# List of Figures

1.1	Detailed balance condition: <i>Case 1</i> : The total change in the probability current is zero because transitions between the microstates, substantiated with the convenient rates such as $\omega_{m \rightarrow n}$ and $\omega_{n \rightarrow m}$ , are equilibrated by the corresponding reverse process. <i>Case 2</i> : Probability current does not vanish as the transitions occur only one direction. System is out-of equilibrium, even in its stationary state. Detailed balance condition is violated. . . . .	5
1.2	An illustration for Glauber dynamics. System evolution depends on the individual spins $s_i$ which change their states randomly with a transition probability $w_I(s_i)$ . Possible states of these spins are indicated by $\bullet$ and $\circ$ . . . . .	15
1.3	An illustration for Kawasaki dynamics. Based on an exchange between the spin pairs $s_i$ and $s_j$ with a transition rate $w_{I \rightarrow J}$ , the energy of the system changes. Here, $\bullet$ and $\circ$ denote different states of the spins of the system. The energy interaction constants used in equation (1.58) are represented by solid lines. . . . .	16
3.1	The original $4 \times 4$ system is in contact with heat baths at different finite temperatures $T_x$ and $T_y$ . Up (down) spin variables are indicated by $\bullet$ and $\circ$ , respectively. Spin exchanges occur along the $x$ ( $y$ ) direction under the effect of the temperature $T_x$ ( $T_y$ ) with the transition rate $\omega_x$ ( $\omega_y$ ). . . . .	26

- 3.2 A  $b = 2$  renormalization scheme: The original lattice is split into two groups of spins denoted by  $\bullet$  and  $\circ$ . The dark circles  $\bullet$  indicate the spins that are eliminated by the transformation while the open circles  $\circ$  represent the remaining spins after the RG process. In the renormalized lattice, the remaining spins lie on square lattice with the nearest-neighbor distance increased by a factor of 2. The emergent next nearest neighbors links are denoted by dashed lines. 29
- 3.3 RG flows for the Ising model in high dimensional parameter space.  $C$  represents the unstable (relevant) critical fixed point while  $F1$  and  $F2$  indicate the stable (irrelevant) fixed points of the system.  $K_x$  and  $K_y$  are the unitless interaction constants along the the  $x$  and  $y$  directions, respectively. For the case of  $K_x = K_y$ , Onsager introduced an exact solution for this system [1] . . . . . 30
- 3.4 Block-spin transformation utilized in this study.  $\bullet$  and  $\circ$  indicate the  $\pm 1$  spins of the two dimensional spin-1/2 Ising model. The parameters of the original system are transformed into the ones of the rescaled system. Transfer matrix is denoted by  $T$ . . . . . 34
- 3.5 Possible 6 rescaled states of the renormalized  $2 \times 2$  system with  $M' = 0$ . Spin exchange can be accepted only for a single direction for the first four ordered states. The allowed exchange in (a) and (b) can occur along the  $y$  direction. Similarly, in (c) and (d) exchange can be seen along the  $x$  direction. However, spin exchange along both directions can be observed in (e) and (f). (Reproduced with kind permission of The European Physical Journal (EPJ) and Springer Science and Business Media) Copyright © Springer 2012 35

- 3.6 A schematic drawing of the critical surface of the system.  $C$  and  $E$  indicate the fixed points for the steady-state and the equilibrium, respectively.  $R_1$ ,  $R_2$  and  $P$  denote the critical points for certain limits. Thick lines indicate the RG flows. Thin lines refer to the cross sections at certain values of the variable  $r$ . Surface  $S$  (at  $K_x = K_y$ ) corresponds to the first-order phase transition between the ordered states at low temperatures. (Reproduced with kind permission of The European Physical Journal (EPJ) and Springer Science and Business Media) Copyright © Springer 2012 . . . . . 42
- 3.7 The phase diagram for various values of the parameter  $r$ .  $P$  represents the disordered paramagnetic phase, while  $O1$  and  $O2$  are the two symmetric ordered phases separated from one another by the first order transition line at the upper right corner. The inner most phase boundary is the result of Monte Carlo work reported [2] for  $r = 0$ . The diagram and the inset are further explained in the text. (Reproduced with kind permission of The European Physical Journal (EPJ) and Springer Science and Business Media) Copyright © Springer 2012 . . . . . 43
- 4.1 An illustration for the two spin-1/2 Ising model sublattices connected to each other with a four spin coupling constant  $Q$  shown in the plaquette. The spin sites denoted by  $\blacktriangle$  and  $\circ$  belong to the two sublattices. . . . . 55
- 4.2 Finite-size scaling plot of  $\widetilde{C}_v/N^{2\lambda-d}$  versus  $N^\lambda t$  for different values of  $J_q$ . The best collapse obtained from the adjustable parameters  $K_c$ ,  $\lambda$  and  $g$  are indicated by the solid lines. Symbols are as follows:  $N = 32(\bullet)$ ,  $40(\blacksquare)$ ,  $80(\blacklozenge)$ ,  $100(\blacktriangledown)$ . . . . . 58
- 4.3 Plot of  $g$  versus  $\lambda$  for different values of  $J_q$ . Here, dotted points denote all data points, presented in Table 4.2 and the dashed line indicates the existence of the singularity at  $\lambda = 1$  between the curves. 62

4.4	Plot of $\varepsilon$ versus $\lambda$ for different values of $J_q$ . Here, dotted points denote all data points, presented in Table 4.2 and the dashed line indicates the interpolated lines. . . . .	62
5.1	An illustration of the phase space of the non-equilibrium eight-vertex model. In the first case of our study, phase transitions are examined along the direction of the dotted line $F_1$ . The solid line represents the critical Baxter line ( $K_1 = B(Q_1)$ ) in equilibrium and “ $c$ ” denotes a critical point on this line. . . . .	69
5.2	An illustration for the second case of our study, phase transitions are examined along the direction of the dotted line $F_2$ , which does not lie on the $\alpha = 1$ surface, but crosses it at point “ $c$ ”. The solid line represents the critical Baxter line in equilibrium and “ $c$ ” denotes a critical point on this line. . . . .	70
5.3	Plot of $\widehat{C}$ versus $\alpha$ for different four spin coupling constant $Q_1 = Q_{c_B}$ . Symbols are as follows: $N = 32(\bullet), 64(\blacksquare), 96(\blacklozenge), 128(\blacktriangle)$ . Along the solid line, equilibrium phase transitions occur. . . . .	71
5.4	Plot of $\widehat{C}$ versus $\delta$ for different four spin coupling constant $Q_1 = Q_{c_B}$ . Symbols are as follows: $N = 32(\bullet), 64(\blacksquare)$ . . . . .	73
5.5	An illustration for the critical surface of the non-equilibrium eight vertex model. Here critical surface intersects the critical Baxter line indicated by the solid line at the equilibrium limit represented by $E$ where $\alpha = 1$ ( $T_1 = T_2$ ). Critical exponent varies along the critical surface. . . . .	75

# List of Tables

1.1	Equilibrium critical exponents of the Ising model for different dimensions $d$ . . . . .	14
1.2	Dynamical critical exponents of the Ising model for different dimensions $d$ . “A” and “B” denote the model-A and model-B [3]. Note that for the model-B in $d = 2$ , the value of the dynamical critical exponent $z$ is corrected with regard to the references [4, 5].	17
1.3	Critical exponents of the two-dimensional randomly driven lattice-gas [3] . . . . .	18
3.1	Quantitative results for various phase transition points studied in this work. Results from other studies are also included for comparison. Critical points $P$ , $R_1$ , and $R_2$ belong to steady state, mean-field, and equilibrium universality classes respectively. (Reproduced with kind permission of The European Physical Journal (EPJ) and Springer Science and Business Media) Copyright © Springer 2012 . . . . .	46
4.1	Critical temperature $K_c$ values for different $J_q$ values. . . . .	57
4.2	Quantitative results for the critical exponent $\lambda$ with the minimum errors of the finite size scaling of the specific heat for different $J_q$ values. . . . .	63

4.3	The interpolated line equations $y_1$ and $y_2$ are obtained from the data pairs $(\lambda, error)$ , shown in Table 4.2, for $(\lambda < 1)$ and $(\lambda > 1)$ cases respectively. $R^2$ defines the goodness of this interpolation. . . . .	64
5.1	Correction to scaling results for $Q_1 = 0.5$ . . . . .	72
A.1	Near equilibrium limit, the RSRG results of the Ising model with non-conserved order parameter obtained through the transformation method presented in chapter 3. Different type of interactions are considered in each case. . . . .	90

# Chapter 1

## Introduction

To understand the physical process of our world, studies on non-equilibrium systems play an important role. It is a well-known fact that nature consists of mainly non-equilibrium systems. There are few, if any, substantial equilibrium systems in nature. Research on equilibrium systems gives scientists an extensive knowledge. Moreover, the theoretical and analytical studies on the universality property of the equilibrium systems is quite well-established. Although in most cases structural changes in the systems of the nature occur at non-equilibrium limits, today physicists do not have enough information and comprehension on non-equilibrium systems. The studies on the power law correlations suggest that there is a certain relation between the static and dynamic critical phenomena. In addition, it is considered that the principles of the universality feature can be also applied to the non-equilibrium systems. Because of all these reasons, it is worthy of study and expand our knowledge on the non-equilibrium critical phenomena.

After the great contributions of Boltzmann and Gibbs [6], most of the system observable are defined by the terms of the stationary probability distribution  $\exp(-H/k_B T)$ , where  $k_B$  is the Boltzmann constant,  $H$  is the Hamiltonian and  $T$  is the temperature of the system. As a consequence of this, for equilibrium systems, the corresponding macroscopic quantities can be identified and computed from the microscopic rules. The most significant and distinctive difference between the non-equilibrium systems and the equilibrium ones is that there is

an existence of a “current” in some physical quantity such as energy, particles, mass, *etc* of the non-equilibrium system. Non-equilibrium steady states (NESS) form the basis of the studies on the dynamic critical phenomena. When the system is in NESS, the probability distributions do not change over time. In other words, initial conditions are not remembered any more so that the system is time-translation invariant.

## 1.1 Master Equation

The master equation is one of the most essential methods, utilized in the determination of the probability distribution of a stochastic process. In general, the system can be described by all the possible configurations of the particles  $m$ . Based on the rapid transitions  $m \rightarrow n$  with certain rates  $\omega_{m \rightarrow n} \geq 0$ , the system changes in time. Here, the unit of the transition rate  $\omega_{m \rightarrow n}$  is  $[\text{time}]^{-1}$ . Hereby, the stochastic process is identified by the initial state, the transition rates and the set of all configurations of the system.

Theoretically, although the configuration of the system transforms unpredictably in time because of the stochastic process, the change in the probability of finding the system in a state  $m$  at a certain time  $t$ , defined as  $P_t(m)$  can be obtained from a linear set of differential equations. Note that, the normalization condition implies that  $\sum_m P_t(m) = 1$ . This set of equations is known in literature as “master equation”. We have the general relation

$$\frac{\partial P_t(m)}{\partial t} = \text{gain} - \text{loss}, \quad (1.1)$$

where “gain” and “loss” include all transitions  $n \rightarrow m$  and  $m \rightarrow n$  respectively, defined as

$$\text{gain} = \sum_n \omega_{n \rightarrow m} P_t(n), \quad (1.2)$$

$$\text{loss} = \sum_n \omega_{m \rightarrow n} P_t(m). \quad (1.3)$$

Putting these equations into the equation 1.1, and noting that  $\omega_{m \rightarrow m} = 0$ , we

obtain

$$\frac{\partial P_t(m)}{\partial t} = \sum_n \omega_{n \rightarrow m} P_t(n) - \sum_n \omega_{m \rightarrow n} P_t(m), \quad (1.4)$$

which describes the current of the probability between different configurations. As time progresses, the gain and loss in the probability distribution compensates each other so the conservation of the probability holds. The master equation is also rewritten as

$$\frac{\partial \vec{P}_t}{\partial t} = \mathcal{L} \vec{P}_t, \quad (1.5)$$

where  $\vec{P}_t$  is the vector of all probabilities  $P_t(m)$  and  $\mathcal{L}$  is the Liouville operator given by

$$\mathcal{L}_{m,n} = \omega_{m \rightarrow n} - \delta_{m,n} \sum_k \omega_{m \rightarrow k}. \quad (1.6)$$

The dimension of the Liouville operator matrix is equal to the total number of all configurations of the system. General solution of the master equation 1.5 which consists of a set of linear first-order differential equations is given by

$$P(t) = e^{\mathcal{L}t} P(0), \quad (1.7)$$

where the initial probability distribution is defined as  $P(0) = \sum_m a_m \phi_m$ . According to this general solution, another relation is also defined

$$\mathcal{L} \phi_m = \lambda_m \phi_m, \quad (1.8)$$

where  $\lambda_m$  and  $\phi_m$  represent the eigenvalues and the eigenvectors of the Liouville operator matrix, respectively. These relations lead to

$$P(t) = \sum_m a_m e^{\lambda_m t} \phi_m. \quad (1.9)$$

One of the most important properties of the Liouville operator used in this section is being an “intensity matrix” in which its diagonal elements have negative and real values while the off-diagonal elements are positive [7]. This is a result of the balance between the gain and loss terms in the master equation. Thus, the sum of each column of the Liouville operator matrix is equal to zero,  $\sum_i \mathcal{L}_{ij} = 0$ . This means that the probability is conserved.

The eigenvalues and the eigenvectors obtained from equation 1.8, defines the stochastic process of the system. Although the eigenvalues of the operator matrix can be complex as a result of the system oscillations, the real parts are always nonnegative. In addition to this, condition of the probability conservation ( $\sum_i \mathcal{L}_{ij} = 0$ ) leads to linearly dependent rows for the Liouville matrix. This means that  $\det \mathcal{L} = 0$ . Based on this property, the product of the eigenvalues of the Liouville matrix must be zero,  $\prod_i \lambda_i = 0$ . Consequently, at least one zero mode ( $\mathcal{L}\vec{P}_{eq} = 0$ ) which corresponds to the stationary probability distribution, must be obtained in order to implement the conservation of the probability distribution of the system [7]. This indicates that for equilibrium  $\lambda_0 = 0$  and  $\phi_0 = P_{ss}$ . In addition the “relaxational eigenmodes” of the system are determined by the remaining eigenvalues of the Liouville operator, denoted as  $\{(\lambda_1, \phi_1), (\lambda_2, \phi_2), \dots\}$ . This argument can be easily observed in the relation given by

$$P(t) = \phi_0 + a_1 e^{\lambda_1 t} \phi_1 + a_2 e^{\lambda_2 t} \phi_2 + \dots \quad (1.10)$$

## 1.2 Equilibrium Dynamics

Describing a physical system by using an “ensemble” which provides all possible configurations of the system and the corresponding probabilities, constitutes the basis of the statistical mechanics. In most of the studies on equilibrium phase transitions, the system is in thermal equilibrium with its environment. In other words, as time proceeds, the system reaches a state in which the history of the system is no longer recognizable and the stochastic process becomes independent of time. Usually, the stochastic system is considered to be interacting with the thermal heat bath which changes the energy of the system. The probability of finding a system at temperature  $T$  in a certain state with energy  $E(m)$  according to the Boltzmann distribution is

$$P_{eq}(m) = \frac{e^{-E_m/k_B T}}{\sum_i e^{-E_i/k_B T}} = \frac{e^{-E_m/k_B T}}{Z}, \quad (1.11)$$

where  $Z$  is the partition function of the system and  $T$  is the temperature of the heat bath. Here, apart from equation 1.11 which provides only the equilibrium

probability distribution, this canonical ensemble does not give any information about the relaxational eigenmodes of the system. Due to the fact that the corresponding system has many possible dynamics, and all of these dynamics provide the same state of equilibrium, a unique solution cannot be obtained for the system. Because of this reason, a dynamical rule must be chosen in order to determine the remaining modes of the system. For instance, different dynamics such as heat bath, Metropolis, Glauber, etc. are carried out to the well-known Ising model. For all of these dynamics, the relaxation of the system leads to a stationary state which is equivalent to canonical ensemble of the model.

All systems at thermal equilibrium obey the detailed balance conditions in which the transition rates of the dynamic process are defined as

$$P(m) \omega_{m \rightarrow n} = P(n) \omega_{n \rightarrow m}. \quad (1.12)$$

This indicates that the probability fluxes between the corresponding configurations  $m$  and  $n$  vanish as shown in Figure 1.1.

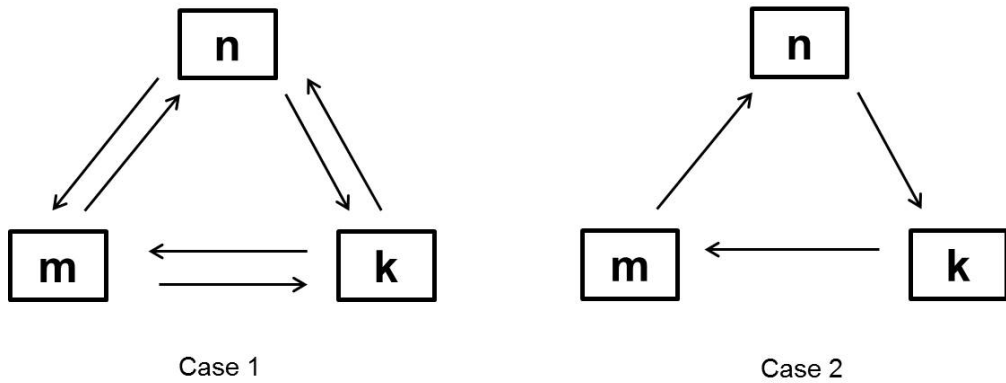


Figure 1.1: Detailed balance condition: *Case 1*: The total change in the probability current is zero because transitions between the microstates, substantiated with the convenient rates such as  $\omega_{m \rightarrow n}$  and  $\omega_{n \rightarrow m}$ , are equilibrated by the corresponding reverse process. *Case 2*: Probability current does not vanish as the transitions occur only one direction. System is out-of equilibrium, even in its stationary state. Detailed balance condition is violated.

## 1.3 Non-Equilibrium Dynamics

Dynamical systems are driven out of the equilibrium by violating the detailed balance condition. The net probability current of the stochastic process can be nonzero based on the transition rates  $\omega$  between the microstates. Difference between an equilibrium system and a non-equilibrium one is the violation of the detailed balance condition.

Non-equilibrium systems can be grouped into two main categories [3];

- (i) Near Equilibrium Systems: Hermitian systems with a stationary state described by the appropriate Boltzmann distribution. In the thermodynamic limit, these systems usually do not relax towards an equilibrium state. Glasses, spin glasses, phase-ordering systems are some of the examples for these systems.
- (ii) Out of Equilibrium Systems: Non-Hermitian systems introduced by transition rates in which the detailed balance condition is violated. Although it is not certain that these systems have a steady state, if it exists, this state cannot be defined as a Gibbs state. These systems are obtained by coupling more than one energy reservoir. This type of systems are referred to as “out-of equilibrium” models.
- (iii) In addition to these, there are also some systems which violate the detailed balance condition so severely that even the proper approximations based on the equilibrium statistical mechanics can no longer be applied. These systems are referred to as “far from equilibrium” models.

## 1.4 Critical Exponents

For the theory of critical phenomena, it is essential to determine the critical exponents of a system. Near the critical point, non-analyticity in the thermodynamic functions such as specific heat, susceptibility, *etc.*, are observed [8, 9, 10]. The

most interesting point of the critical exponents is that they are used to group different physical systems into universality classes and they depend on a few parameters. For instance, in systems with short-range interactions, these parameters are related to the symmetries of the system. The dimensionality  $n$  of the order parameter (such as density, magnetization, *etc.*) and the dimension of the system  $d$  influence the critical exponents.

### 1.4.1 Critical Exponents of Equilibrium Systems

The well-known critical exponents of equilibrium systems and the scaling laws [11, 12, 8, 10, 13] are defined as (for a ferromagnetic system in an external field  $H$ ) for the zero-field specific heat  $C_H$ :

$$C_H \propto |t|^{-\alpha}; \quad (1.13)$$

for the zero-field magnetization  $M$ :

$$M \propto (-t)^\beta; \quad (\text{for } t < 0) \quad (1.14)$$

and also

$$M \propto H^{1/\delta}; \quad (\text{for } t = 0) \quad (1.15)$$

for the zero-field isothermal susceptibility  $\chi$ :

$$\chi \propto |t|^{-\gamma}; \quad (1.16)$$

for the correlation length  $\xi$ :

$$\xi \propto |t|^{-\nu}; \quad (1.17)$$

for the two-point correlation function  $G_c^{(2)}(r)$  at the critical temperature:

$$G_c^{(2)}(r) \propto r^{2-d-\eta}. \quad (1.18)$$

(Note that for  $t \neq 0$ ,  $G_c^{(2)}(r, t) \sim e^{-r/\xi(t)}$ .) Here, the reduced temperature  $t$  is given by  $t = (T - T_c)/T_c$ . These six critical exponents are not independent, and are related to one another through “scaling relations”.

## Scaling Theory of Kadanoff

According to the scaling theory of Kadanoff [14], which is based on the principle of reducing the effective number of degrees of freedom, the original system (let us consider the spin-1/2 Ising model with a nearest neighbor interaction  $J$  on a square lattice in an external field  $H$ ) is rescaled as  $N' = b^{-d}N$  where  $N$  and  $N'$  are the numbers of the particles of the original and the rescaled system, respectively. Here,  $b$  is an arbitrary variable and  $d$  is the dimension of the original system. If the original and the rescaled systems are regarded as thermodynamically equivalent, then it means that the free energies of these systems are equal to each other. Based on this inference, the partition functions of these systems are also conserved and given by

$$Z(t, H) = Z'(t', H'). \quad (1.19)$$

By using the conditions of the up-down symmetry and the property of scale invariance of the system, the scaling relations between the system parameters are defined as

$$t' = b^{y_t} t \quad \text{and} \quad H' = b^{y_H} H, \quad (1.20)$$

where  $y_t$  and  $y_H$  are the critical exponents of the corresponding scaling fields.

• **Generalized Homogeneous Function Forms of Some Quantities:**

• **Free Energy** Based on the conservation of the partition function and using  $f = \frac{1}{N} \ln Z$ , shown as equation 1.19, the relation between the free energies can be written as

$$Nf(t, H) = N'f(t', H') \Rightarrow Nf(t, H) = b^{-d}Nf(t', H'). \quad (1.21)$$

After some simplifications, the generalized homogeneous function form of the free energy is obtained as

$$f(t, H) = b^{-d}f(b^{y_t}t, b^{y_H}H). \quad (1.22)$$

• **Internal Energy** The homogeneous function behavior of the internal energy  $U(t, H)$  of the original system is

$$U(t, H) = \frac{1}{N} \frac{\partial}{\partial J} \ln Z(t, H), \quad (1.23)$$

where the redefined reduced temperature is  $t = \frac{J_c - J}{J_c}$ . Again, by using the conservation of the partition function and the scaling relations, we can rewrite this equation as

$$U(t, H) = \frac{1}{N} \left( \frac{-1}{J_c} \right) \frac{\partial}{\partial t} \ln Z = b^{y_t - d} \left[ \frac{1}{N'} \left( \frac{-1}{J_c} \right) \frac{\partial}{\partial t'} \ln Z' \right] = b^{y_t - d} U(t', H'). \quad (1.24)$$

Then, the generalized homogeneous function form of the free energy is

$$U(t, H) = b^{y_t - d} U(b^{y_t} t, b^{y_H} H). \quad (1.25)$$

• **Specific Heat** Specific heat is proportional to the second derivative of the free energy with respect to the temperature  $C_v \propto \frac{\partial^2 f}{\partial t^2}$ , then the generalized homogeneous function form of the specific heat is

$$C_H(t, H) = b^{2y_t - d} C_H(b^{y_t} t, b^{y_H} H). \quad (1.26)$$

As mentioned before,  $b$  is an arbitrary variable and it can be chosen as in the most beneficial way. Here, let us set  $b = t^{-1/y_t}$ , so this functional relation turns into

$$C_H(t, H) = t^{(d-2y_t)/y_t} C_H(1, t^{-y_H/y_t} H). \quad (1.27)$$

Note that scaling relations of this type imply that the thermodynamic quantity which is a function of two variables ( $t$  and  $H$  in this case) “collapses” into a single function when displayed in the form  $C_H(t, H)/t^{(d-2y_t)/y_t}$  as a function of  $Ht^{-y_H/y_t}$ . At zero external magnetic field, equation 1.27 is rewritten as

$$C_H(t, 0) = t^{(d-2y_t)/y_t} C_H(1, 0). \quad (1.28)$$

The  $\alpha$ -exponent can be obtained from equation 1.13 which indicates the behavior of the zero-field specific heat of a ferromagnetic system. From equations 1.13 and 1.27, the  $\alpha$ -exponent is obtained as

$$\alpha = \frac{2y_t - d}{y_t}. \quad (1.29)$$

• **Magnetization** Magnetization can be defined according to the following equation;

$$M(t, H) = \frac{1}{N} \frac{\partial}{\partial H} \ln Z(t, H). \quad (1.30)$$

The relation of the magnetization between the original and the rescaled systems are defined as

$$M(t, H) = \frac{1}{N} \frac{\partial}{\partial H} \ln Z = b^{y_H-d} \frac{1}{N'} \frac{\partial}{\partial H'} \ln Z' = b^{y_H-d} M(t', H'). \quad (1.31)$$

Then, the generalized homogeneous function form of the magnetization is

$$M(t, H) = b^{y_H-d} M(b^{y_t} t, b^{y_H} H). \quad (1.32)$$

Here, let us set  $b = t^{-1/y_t}$ , then equation 1.32 can be rewritten as

$$M(t, H) = t^{(d-y_H)/y_t} M(1, t^{-y_H/y_t} H), \quad (1.33)$$

and for the zero-external field, it is given by

$$M(t, 0) = t^{(d-y_H)/y_t} M(1, 0). \quad (1.34)$$

Equations 1.14 and 1.34 provides the  $\beta$ -exponent, defined as

$$\beta = \frac{(d - y_H)}{y_t}. \quad (1.35)$$

Similarly, if  $b$  is chosen as  $b = t^{-1/y_H}$ , the scaling form of the magnetization given by equation 1.32 is restated as

$$M(t, H) = t^{(d-y_H)/y_H} M(t^{-y_t/y_H} t, 1), \quad (1.36)$$

from equation 1.15, the  $\delta$ -exponent is given by

$$\delta = \frac{y_H}{(d - y_H)}. \quad (1.37)$$

• **Susceptibility** Susceptibility is proportional to the second derivative of the free energy with respect to the magnetic field  $\chi \propto \frac{\partial^2 f}{\partial H^2}$ , then the generalized homogeneous function form of the susceptibility is

$$\chi(t, H) = b^{2y_H-d} \chi(b^{y_t} t, b^{y_H} H). \quad (1.38)$$

For  $b = t^{-1/y_t}$ , the generalized homogeneous function form of the susceptibility becomes

$$\chi(t, H) = t^{(d-2y_H)/y_t} \chi(1, t^{-y_H/y_t} H), \quad (1.39)$$

and then at zero-magnetic field, the  $\gamma$ -exponent can be obtained from equations 1.16 and 1.39 as

$$\gamma = \frac{2y_H - 2}{y_t}. \quad (1.40)$$

• **Correlation Length** Generalized homogeneous function form of the correlation length is

$$\xi(t, H) = b\xi(b^{y_t}t, b^{y_H}H). \quad (1.41)$$

If we set  $b = t^{-1/y_t}$  at zero-external field (or  $b = t^{-1/y_H}$  at the critical temperature as  $t = 0$ ), then from equations 1.17 and 1.41, the  $\nu$ -exponent is given by

$$\nu_t = \frac{1}{y_t} \quad \text{and} \quad \nu_H = \frac{1}{y_H}. \quad (1.42)$$

• **Correlation Function** Correlation function measures the correlation between random variables of the system. Correlation function can be calculated by

$$G_c^{(2)}(r, t, H) = \frac{\partial}{\partial H_n} \frac{\partial}{\partial H_m} \ln Z = b^{2y_H - 2d} \frac{\partial}{\partial H'_n} \frac{\partial}{\partial H'_m} \ln Z', \quad (1.43)$$

so the generalized homogeneous function form of the correlation function is

$$G_c^{(2)}(r, t, H) = b^{2y_H - 2d} G_c^{(2)}\left(\frac{r}{b}, b^{y_t}t, b^{y_H}H\right). \quad (1.44)$$

To investigate the  $\eta$ -exponent, the generalized homogeneous function form of the correlation function is considered for  $b = r$ , then the  $\eta$ -exponent is given by

$$\eta = 2 + d - y_H. \quad (1.45)$$

The relations between these critical exponents are calculated from equations 1.29, 1.35, 1.37, 1.40, 1.42 and 1.45 as

$$\alpha + 2\beta + \gamma = 2 \quad (1.46)$$

$$\alpha + \beta(\delta + 1) = 2 \quad (1.47)$$

$$(2 - \eta)\nu = \gamma \quad (1.48)$$

$$\alpha + \nu d = 2 \quad (1.49)$$

## 1.4.2 Dynamic Critical Exponents

First investigations of the relaxational modes of equilibrium systems [4] and phase-ordering kinetics [15, 16], non-equilibrium dynamics were taken into consideration. Followed by this, the studies on the power-law time dependencies of the systems were studied [17]. More recently, considerable work has been carried out on systems which are driven to the non-equilibrium limits, for example, by contacting with different thermal baths or being under the effect of different dynamics, or external currents. In addition to the equilibrium critical exponents, new exponents are introduced for non-equilibrium dynamics. For instance, one of these additional critical exponents is the dynamical exponent  $z$  which relates the correlation length  $\xi$  and the divergences of the relaxation time  $\tau$  to each other by

$$\tau \propto \xi^z, \quad (1.50)$$

as can be obtained from a time dependent version of the scaling relation given by the equation 1.44

$$G(\mathbf{r}, t) = b^{2x} G\left(\frac{\mathbf{r}}{b}, b^z t\right), \quad (1.51)$$

where the scaling dimension is  $x = y - d$ . Here,  $\mathbf{r}$  and  $t$  describe the spatial and temporal coordinates. A number of other dynamic exponents may be defined in terms of  $z$ .

These additional exponents  $\theta_l$  and  $\theta_g$  associated with the probability of finding the (local  $\theta_l$  or global  $\theta_g$ ) order parameter of the system conserve its sign in time, were presented by Derida [18]. The corresponding exponents may be described as

$$P(t) \propto t^{-\theta}. \quad (1.52)$$

The general relation between the non-equilibrium critical exponents is given by [18]

$$z\theta_g = 1 - d + \lambda - \frac{\eta}{2}. \quad (1.53)$$

## 1.5 Universality: “Out of-Equilibrium” Classes

In this section, we will mainly focus on the out of-equilibrium systems with non-Hermitian Hamiltonian, namely dynamic Ising model, which violates the detailed balance condition and relaxes to a non-equilibrium state. As mentioned before, these systems are substantiated by the way of using different dynamics such as being in contact to heat baths at different temperatures, or being under the influence of external currents. The studies on systems which have non-conserved order parameter, (referred to as model-A [4, 5]) show that the critical behavior of the system remains stable despite the implementation of competing dynamics [19] and even if these dynamics break the symmetry of the system, the criticality is still unchanged [20]. In contrast, when the competing dynamics are applied to the model-B systems [4, 5] (with conserved order parameter) by an external field [21] or a local process which conserves the order parameter [2, 22, 23, 24], in the steady state angular dependence is observed in the obtained long-range correlations.

### 1.5.1 Dynamical Ising Classes

The well-known Ising model in equilibrium was presented by Lenz and Ising [25, 26] with a scaled Hamiltonian defined as

$$H = -J \sum_{i,j} s_i s_j - B \sum_i s_i, \quad (1.54)$$

where  $B$  is the external field and  $J$  is the energy interaction constant between the spins of the system. Here, spin variables  $s_i$  can take values  $\pm 1$ . Ising model with this Hamiltonian contains an up-down symmetry ( $Z_2$ ) of the spin variables. There is an exact solution of this model in one and two dimensions, introduced by Onsager [1]. This solution indicates that in one dimension, Ising model goes under a first-order phase transition at  $T = 0$  while a second-order phase transition occurs at  $\frac{k_B T_c}{J} = 2.269$  in two dimensions. In Table 1.1, the critical exponents are shown for different dimensions of the Ising model [3].

Critical Exponents	d=2	d=3	d=4 (Mean Field)
$\alpha$	0 (log divergence)	0.1097(6)	0
$\nu$	1	0.6301(2)	1/2
$\gamma$	7/4	1.3272(3)	1
$\beta$	1/8	0.3265(7)	1/2

Table 1.1: Equilibrium critical exponents of the Ising model for different dimensions  $d$

### 1.5.2 Kinetic Ising Model - Near Equilibrium

In the studies on the relaxational evolution of the systems near the equilibrium, kinetic Ising models which include the spin-flip (Glauber [27]) dynamics or the spin-exchange (Kawasaki [28]) dynamics were introduced. To satisfy the detailed balance condition and obtain the Gibbs state at the equilibrium limit, the transition rates  $\omega_{I \rightarrow J}$  and the probability distributions  $P(I)$  are chosen as to obey the detailed balance relation given as,

$$P(I) \omega_{I \rightarrow J} = P(J) \omega_{J \rightarrow I}. \quad (1.55)$$

As the system reaches its equilibrium, the probability distribution of the Gibbs state ( $P_{eq}(I) \propto \exp[-H(I)/k_B T]$ ) must be obtained from this condition. We then have

$$\frac{\omega_{I \rightarrow J}}{\omega_{J \rightarrow I}} = \exp[-\Delta H_{IJ}/k_B T]. \quad (1.56)$$

At this point, we would like to give detailed explanations on the principles of these dynamics.

The Glauber dynamics indicate a system in which the individual spins can change their states randomly with time under the effect of an external agency (e.g., a thermal bath). These are also known as spin-flip dynamics in literature as illustrated in Figure 1.2. The coupling between the spins of this Ising model system is assumed by considering that the transition probability  $w_I(s_i)$  of the particular spin depends on its neighboring spins, formulated by

$w_I(s_i) = 1 + s_i \tanh(\mathcal{J} \sum_{i'} s_{i'})$  where  $s_{i'}$  indicates the nearest neighbor spins of the particular  $s_i$  and  $\mathcal{J}$  is the energy interaction constant between these nearest neighbor spins [27]. By this assumption, the detailed balance condition in equilibrium was implemented to the system by

$$\frac{w_I(s_i)}{w_J(-s_i)} = \frac{1 - s_i \tanh(\mathcal{J} \sum_{i'} s_{i'})}{1 + s_i \tanh(\mathcal{J} \sum_{i'} s_{i'})}. \quad (1.57)$$

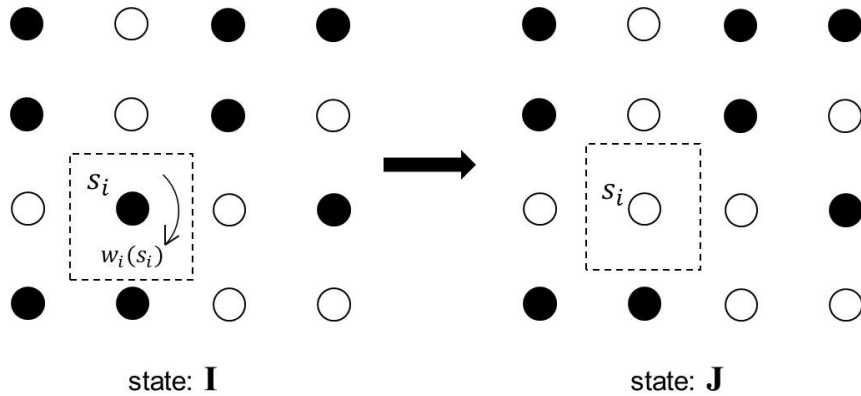


Figure 1.2: An illustration for Glauber dynamics. System evolution depends on the individual spins  $s_i$  which change their states randomly with a transition probability  $w_I(s_i)$ . Possible states of these spins are indicated by  $\bullet$  and  $\circ$ .

At first in literature, Kawasaki introduced a diffusive time-dependent Ising system in which spin exchanges occur with certain temperature-dependent transition probabilities  $w_{I \rightarrow J}$  [28]. The system in the corresponding study of Kawasaki is equivalent to the binary mixture systems with molecular diffusion when the quantum effect of the Heisenberg system is ignored. Being in contact with different thermal baths can trigger to obtain such diffusive dynamics in a system. Again in this study, certain transition probabilities of spin exchanges are used to determine the coupling between the spins of the system. In this isothermal process, the transition probabilities of that spin exchanges between  $s_i$  and  $s_j$  were defined as

$$w_{I \rightarrow J} = \frac{1}{2} \alpha \Pi_m (1 + \beta s_m s_j) \Pi_n (1 + \beta s_n s_i), \quad (1.58)$$

where  $\beta = \tanh(\mathcal{J}/k_B T)$  and  $s_n$  ( $s_m$ ) indicate the nearest neighbor spins of the particular  $s_i$  ( $s_j$ ), respectively. Please note that in these products, the terms of

$s_j s_i$  ( $s_i s_j$ ) are ignored. Here  $\alpha$  is the time scale constant and also independent of  $\{s_i\}$ . In equilibrium, system obeys the detailed balance condition by

$$\frac{w_{I \rightarrow J}}{w_{J \rightarrow I}} = \frac{\prod_m (\cosh K + s_j s_m \sinh K) \prod_n (\cosh K + s_i s_n \sinh K)}{\prod_m (\cosh K + s_i s_m \sinh K) \prod_n (\cosh K + s_j s_n \sinh K)}, \quad (1.59)$$

where  $K = \frac{\mathcal{J}}{k_B T}$ . Kawasaki (spin exchanges) dynamics in a lattice system are illustrated in Figure 1.3. Transformation obtained from the spin exchange dynamics is only considerable for the case of  $s_j = -s_i$ .

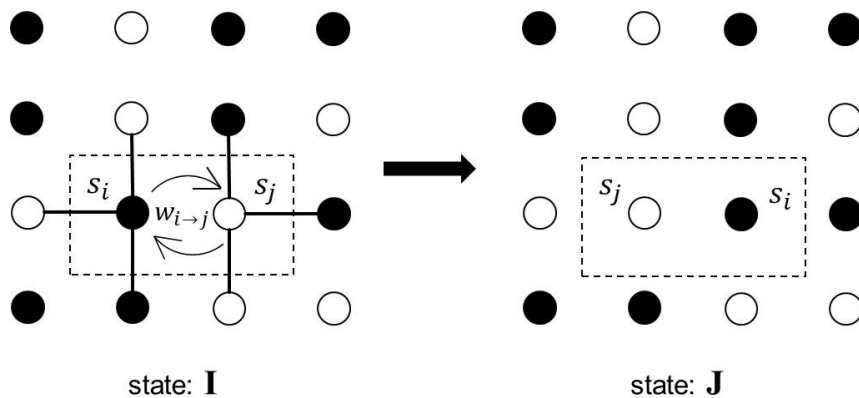


Figure 1.3: An illustration for Kawasaki dynamics. Based on an exchange between the spin pairs  $s_i$  and  $s_j$  with a transition rate  $w_{I \rightarrow J}$ , the energy of the system changes. Here,  $\bullet$  and  $\circ$  denote different states of the spins of the system. The energy interaction constants used in equation (1.58) are represented by solid lines.

For one dimensional  $d = 1$  kinetic Ising model with Glauber dynamics (model-A), a first order transition occurs at  $T = 0$ . The dynamic critical exponents of this system [27, 29] are determined as  $z_{Glauber}^{d=1} = 2$  and  $\theta_{g,Glauber}^{d=1} = 1/4$ . However for the same system with the Kawasaki dynamics (model-B), although phase transition is still observed at  $T_c = 0$ , Zwerger obtained a different dynamical exponent  $z_{Kawasaki}^{d=1} = 5$  [30]. These systems can be exactly solved and the obtained results indicate a new dynamic Ising universality class in which the static critical exponents are same while the dynamical ones are quite different. Research on different dimensions  $d = 1, 2, 3, 4$  of the kinetic Ising model [30, 31, 32, 33, 34, 35, 36] have resulted in various values for dynamical critical exponents of the system. The results of these studies are shown in Table 1.2 [3].

		$z$	$\lambda$	$\theta_g$
$d = 1$	A	2	1	1/4
	B	5		
$d = 2$	A	2.165(10)	0.737(1)	0.225(10)
	B	3.75	0.667(8)	
$d = 3$	A	2.032(4)	1.362(19)	0.41(2)
$d = 4$	A	2	4	1/2
	B	4		

Table 1.2: Dynamical critical exponents of the Ising model for different dimensions  $d$ . “A” and “B” denote the model-A and model-B [3]. Note that for the model-B in  $d = 2$ , the value of the dynamical critical exponent  $z$  is corrected with regard to the references [4, 5].

### 1.5.3 Kinetic Ising Model - Out of-Equilibrium

As mentioned before, kinetic Ising model relaxes to its non-equilibrium steady state as a result of competing dynamics of the system. Because of the fact that the dynamical Ising fixed point is stable in  $d = 4 - \epsilon$  dimensions as a result of the consistency of the spin inversion and the lattice symmetries, Grinstein claimed that the universality class of the kinetic Ising model should also include the stochastic systems (with Glauber dynamics) which have two states in each site and the  $Z_2$  symmetry [19]. There are numerous studies that confirm this theory such as Monte Carlo simulations [37, 38, 39, 40, 41] and theoretical analysis [42, 43, 44]. In particular, these studies are analyzed for the Ising model in contact with different heat baths, with Glauber dynamics [37, 42, 44, 45] or a combination of Glauber and Kawasaki dynamics [46] and the systems which hold majority rule [39, 41]. Note that in all of these studies model-A system is considered.

$\nu_{\perp}$	$\beta$	$\gamma$	$\eta$
0.62(3)	0.33(2)	1.16(6)	0.13(4)

Table 1.3: Critical exponents of the two-dimensional randomly driven lattice-gas [3]

The critical behavior of Model-B systems (in which order parameters, local and anisotropic, are conserved), are consistent with the kinetic Ising model with dipolar interaction. Præstgaard *et. al.* obtained the critical exponents of the two-dimensional models through simulations and field-theoretical results [47, 48]. Randomly driven lattice-gas system, the two-temperature model [49], the “Anisotropic Lattice Gas Automaton” (ALGA) model [50], and the infinitely fast driven lattice-gas model [51] belong to this universality class. The critical dimension is  $d_c = 3$ . The critical exponents of this universality class is indicated in Table1.3 [3]

The rest of the thesis is organized as follows:

The second chapter discusses the previous studies on the steady state phase transitions of the non-equilibrium systems with spin exchange or spin flip dynamics. A comprehensive literature review on the criticality properties of these non-equilibrium systems as they are in contact with thermal baths or driven by an external field will be presented in this chapter.

In chapter 3, we will introduce the global phase diagram of the two-finite temperature spin-1/2 Ising model on a square lattice with Kawasaki dynamics studied through the real space renormalization group method. General concepts of the renormalization group theory and the form of the transformation used will be explained. To compare the obtained results, the same analysis is carried out for this model near the equilibrium critical point with Glauber dynamics as shown in Appendix A. For the c-code used in this study the reader can review Appendix C.

In chapter 4 non-equilibrium phase transitions of the eight-vertex model with Kawasaki dynamics in contact with different heat baths (one of them at infinite temperature) will be analyzed through the Monte Carlo simulations. Universality property of this model for its non-equilibrium limits will be also investigated. The procedure used to obtain an error measure for the data collapse achieved by the finite size scaling is described in Appendix B. The c-codes of the Monte Carlo simulations and the finite-size scaling are presented in Appendices D and E, respectively.

Finally, the ongoing work related to the criticality of the two-finite temperature eight-vertex model near its equilibrium critical points is discussed in chapter 5.

## Chapter 2

# Literature Review

In recent years, a rich variety of knowledge about the general analytical framework for non-equilibrium systems have been acquired from the studies in the field of non-equilibrium critical phenomena [52]. To comprehend the nature of non-equilibrium phenomena is of paramount importance because non-equilibrium systems can be detected in many different areas of science. Due to this reason, non-equilibrium systems are taken into serious consideration in many studies from different domains such as physics, chemistry, biology [53, 54, 55]. Real systems in nature can be characterized by using simplified models. For instance the characterization of a ferromagnetic system in equilibrium is presented by Lenz and Ising through the well-known Ising model [25, 26]. Similarly, for non-equilibrium phenomena, Katz, Lebowitz and Spohn successfully analyzed the critical behaviors of fast ionic conductors [56] by introducing a driven lattice-gas model [57, 58].

Researchers of this field have shown extensive interest to the studies on the steady state phase transitions of non-equilibrium systems [17, 52]. Zia and Schmittmann proposed an approach of general classification of non-equilibrium steady states and their various properties for different limits and applications [17, 52, 59, 60]. Considerable understanding of the field of non-equilibrium steady state phase transitions is achieved by using the two temperature Ising model or (uniformly/nonuniformly) driven lattices. Firstly, a non-equilibrium model in an applied external field with particle-conserving hopping dynamics,

known as “driven lattice model” was introduced by Katz *et al.* [57, 58]. Starting with this work, the driven lattice models are regarded as a basis for different studies on non-equilibrium systems. To examine the characteristics of the corresponding model, there are many studies achieved by different methods such as Monte Carlo simulations (in two [57, 58, 61, 62, 63, 64, 65] and three [66] dimensions), mean-field solutions [67, 68] and field theoretic renormalization analysis [69, 70, 71].

In addition, research on systems with an anisotropic conserved dynamics indicates that these systems have distinct long-range correlations and different universality behaviors. For these models, long-range correlations are observed at all temperatures above the critical temperature ( $T > T_c$ ), and also the universality properties of these systems point out a new universality class other than the well-known Ising universality class. Studies on the long-range correlations with conserved anisotropic dynamics were carried out for driven lattices [49, 72, 73] and for the two temperature Ising model [48, 74]) by using field-theoretic analysis. Furthermore, the corresponding results of these studies were verified by Monte Carlo simulations as well (for driven lattices [72, 73] and for the two temperature Ising model [48, 74]).

The two temperature Ising model with conserved anisotropic dynamics has been widely used in the fields of non-equilibrium steady state phase transitions. Especially, there has been considerable interest in the two temperature Ising model with Kawasaki (exchange) dynamics, driven to non-equilibrium steady states by being coupled to two thermal baths (one of the baths has infinite temperature) [47, 48, 67, 68, 74, 75]. These studies show that the second-order phase transition of the corresponding model occurs at higher temperatures in comparison with the equilibrium critical temperature. This is another remarkable characteristic of these systems.

For the two temperature Ising model with anisotropic exchange dynamics, and in contact with two different thermal baths (one of them has infinite  $T$ ), Cheng *et al.* showed that the long-range correlations occur at  $T_c \approx 1.33T_o$  [74]. Here, the Onsager critical temperature is  $T_o \cong 2.2692J/k_B$ . Besides it is also found

by the Monte Carlo simulations that the critical temperature of this system is  $T_c \approx 1.36T_o$  [47, 76]. We would like to point out that for the driven lattice system, random spin exchanges along the field direction occur as the external field approaches to infinity. In this case, this system is equivalent to the two temperature Ising model with one of the temperatures infinite. Therefore at this limit, Monte Carlo simulations indicate that the critical temperatures of the driven lattice [76] and the two temperature Ising model [47] are equal to each other, as expected. The corresponding critical behavior of a non-equilibrium version of the time dependent Landau-Ginzburg model is also investigated by Præstgaard *et al.* through renormalization group (RG) analysis [48]. In their study, an  $\epsilon$ -expansion is obtained from field-theoretic approach. Based on their study and as well as numerous others, it is shown that non-equilibrium systems have new universality classes [3, 47, 48, 76].

Last but not least, distinct universality properties of non-equilibrium systems are also an interesting feature of the non-equilibrium phenomena, and these systems are categorized into different universality classes [3]. Although, in some cases, research on the criticality of the driven lattice-gas model (reviewed in detail by Schmittmann [77]) and the two temperature Ising model [3, 47, 48, 76] indicates a non-Ising critical behavior, numerous other studies have shown that the models with the Glauber spin-flip dynamics [27] or a spin exchange Kawasaki dynamics [28] are associated with the same universality class as their counterpart models in equilibrium [45, 46, 37, 65, 78, 79, 80, 81, 82, 83, 84, 85, 86, 87].

Non-equilibrium phase transitions were also analyzed for two coupled two-dimensional Ising models, each in contact with different heat baths, for several types of system dynamics. The critical behavior of this model with nearest neighbor interactions was investigated by using Monte Carlo simulations as the system is taken to be driven by spin flip dynamics [37, 85]. Blöte *et al.* observed an energy flux between the sublattices of the corresponding system [85]. In their subsequent work, Blöte *et al.* also considered a difference between the bond-strengths on the sublattices of this system [37]. In this mentioned study, the corresponding system is analogue of the model with inhomogeneous interactions and temperature. These studies indicated that the critical exponents of this model with

non-conserved (Glauber) dynamics were consistent with the universality class of the equilibrium Ising model.

In addition, the aforementioned system was also examined by Garrido *et al.* with competing dynamics through an analytical method and a numerical analysis (Monte Carlo simulations) [87]. In their study, each spin of the system was in contact with both thermal baths (with different spin dynamics) but with different probabilities. In other words, the probabilities of spin-flip and spin exchange attempts constitute the non-equilibrium dynamics of the system and also this model is equivalent to a system in contact with thermal heat baths with different temperatures. Based on this study, one can observe that still there is no observable deviation from the Ising universality class. Furthermore, there are other studies on this model achieved by introducing different combinations of the Glauber and Kawasaki dynamics [45, 49, 86]. The corresponding papers indicate that the criticality of the system shows an equilibrium Ising-like behavior for small values of the probability of the Kawasaki dynamics ( $p_{exchange} \leq 0.80$ ) and the second-order phase transition turns into first-order as the corresponding probability increases ( $p_{exchange} > 0.85$ ). As a result of this situation, a tricritical point is observed at  $p_{exchange} \simeq 0.83$ .

## Chapter 3

# Global Phase Diagram of the Two-Temperature Ising Model with Kawasaki Dynamics from Real Space Renormalization Group Theory

The two-finite temperature Ising model with conserved anisotropic dynamics on a square lattice is analyzed through a real space renormalization group (RSRG) transformation. Dynamics of the non-equilibrium system is characterized by different heat baths with finite temperatures  $T_x$  and  $T_y$  and also different time-scale constants  $\alpha_x$  and  $\alpha_y$  for spin exchanges in the  $x$  and  $y$  directions. For the first time in literature, global phase diagram and the critical surface of the two-temperature Ising model is obtained for all the critical points of the system, studied separately previously: the steady state, the equilibrium, and some certain limits at which one of the temperatures and/or exchange rates is infinite. This study was published in the European Physical Journal B, volume 85, 398 (2012).

### 3.1 The Model

We investigate the phase transitions of the spin-1/2 Ising model on a square lattice in contact with two-finite temperature thermal baths by means of a real-space renormalization group (RSRG) transformation. The energy of the system is defined as

$$E = - \sum_{\langle ij \rangle} J s_i s_j, \quad (3.1)$$

where  $J$  is the interaction energy constant, and  $\langle ij \rangle$  indicates a sum over nearest-neighbor pairs of sites. Spin variables  $s_i$  can take values  $\pm 1$ . Spin exchanges occur between the nearest-neighbor pairs in the  $x$  and  $y$  directions. In this process, as spin exchanges appear in different directions, the system is regarded as under the influence of different thermal baths; for the  $x$  (or  $y$ ) direction, the effective heat bath has the finite temperature  $T_x$  (or  $T_y$ ), respectively. Thus, the dynamics of a non-equilibrium system is carried out by this mechanism. We would like to point out that the system turns into its equilibrium state (for our system, the equilibrium of the spin-1/2 Ising model) as the corresponding temperatures are equal,  $T_x = T_y$ .

In this process, for two different neighboring spins, an exchange may arise in the  $x$  direction with the transition rate

$$w_x = \alpha_x [1 - \tanh(\Delta E / 2k_B T_x)], \quad (3.2)$$

and

$$w_y = \alpha_y [1 - \tanh(\Delta E / 2k_B T_y)], \quad (3.3)$$

in the  $y$  direction, where  $k_B$  is the Boltzmann constant. Here, the change in the energy of the system, observed because of the spin exchanges, is indicated by  $\Delta E$ . The unitless interaction constants between the nearest-neighbor spins  $K_x$  and  $K_y$  are used in place of  $T_x$  and  $T_y$ , defined as

$$K_x = \frac{J}{k_B T_x} \quad \text{and} \quad K_y = \frac{J}{k_B T_y}. \quad (3.4)$$

Here,  $\alpha_x$  and  $\alpha_y$  represent the timescale constants for exchanges along the  $x$  and  $y$  directions, respectively. Studied system with the corresponding parameters is shown schematically in Figure 3.1.

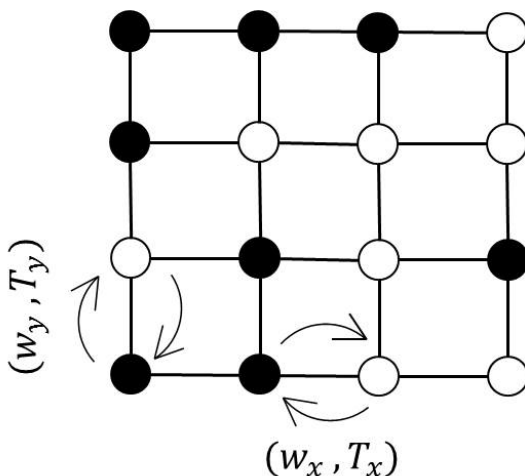


Figure 3.1: The original  $4 \times 4$  system is in contact with heat baths at different finite temperatures  $T_x$  and  $T_y$ . Up (down) spin variables are indicated by ● and ○, respectively. Spin exchanges occur along the  $x$  ( $y$ ) direction under the effect of the temperature  $T_x$  ( $T_y$ ) with the transition rate  $\omega_x$  ( $\omega_y$ ).

To observe the second-order phase transition of the system, the total magnetization of the system must be zero so the system is designed as the total numbers of the  $\pm 1$  spins are equal.

Our renormalization group (RG) method which is a tool for the transformation of a  $4 \times 4$  system with periodic boundary conditions and with zero magnetization to a scaled  $2 \times 2$  system again with a zero magnetization, will be explained in the next section with all its details.

## 3.2 The RG Transformation

### 3.2.1 The Concepts of Renormalization Group Theory

Renormalization group theory is established upon increasing the minimal length (in other words a change length scale) as  $a \rightarrow a' = ba$  such that  $\xi \rightarrow \xi' = \xi/b$  of the system, in order to reduce the number of degrees of freedom. RG approach

yields and explains the scaling laws, all the critical exponents, universality property and the determinants of the universality classes.

In the historical background of this theory, at first in 1966 an explanation for all the concepts of rescaling was presented by Kadanoff with a real understanding of the physical meaning of this technique [14]. Scaling laws of Kadanoff theory are described in chapter 1. However, this theory could not provide a way to calculate the critical points and the corresponding exponents. The second-order phase transitions of the investigated system could not be matched into the correct universality class of the model [9]. In addition, a valid recursion relation arising from the rescaling of the system, could not be derived in any way [9]. After that with the contributions of Kenneth G. Wilson in 1971, the missing concepts of this theory was completed. After this revolution, Kenneth G. Wilson was awarded the Nobel Prize in 1982 for his theory for critical phenomena in connection with the theory of phase transitions [88].

Again the scaling rules of the Kadanoff theory, as mentioned in chapter 1, are still valid for the RG formalization. Although the length scale of the system changes (so the number of the degrees of freedom of the system alters), at some points during the rescaling process, the criticality of the original system remains same. These points are called “fixed points”.

Association between the parameters of the original and the rescaled systems are given by recursion relations. For instance the relationship between the Hamiltonian of the original system  $H$  and the Hamiltonian of the rescaled system  $H'$  is given by the recursion relation as [8]

$$H' = \mathfrak{R}[H]. \quad (3.5)$$

The relation between the unitless energy coupling constants [8] is given by

$$\vec{K}' = \mathfrak{R}[\vec{K}]. \quad (3.6)$$

Here we denote the numerous parameters (the “coupling constants”) that define the scaled Hamiltonian with the vector  $\vec{K}$ . To calculate system parameters of the rescaled system numerically, the recursion relation is regarded as an iteration

function. As mentioned before, fixed points are described as the points at which the critical behaviors of the original and the rescaled systems remain invariant so that to calculate the fixed points, recursion relation function is iterated many times until an input (initial) point repeats itself as the outcome again and again. This situation can be described as [8]

$$\vec{K}^* = \mathfrak{R}[\vec{K}^*]. \quad (3.7)$$

Also, the new correlation length is found as

$$\xi' = \frac{\xi}{b}, \quad (3.8)$$

and at the critical points

$$\xi'(\vec{K}^*) = \frac{\xi(\vec{K}^*)}{b} \Rightarrow \xi(\vec{K}^*) = \begin{cases} 0 & T = 0 \text{ or } \infty \\ \infty & \text{critical fixed point} \end{cases} \quad (3.9)$$

A schematic RG strategy for a two dimensional system on a square lattice is presented by Figure 3.2.

As mentioned, this theory gives a method to obtain the critical points of the system in interest. Let us assume that the energy interaction coupling constant of the original system,  $K$  is close enough to the value of the critical point  $K_c$ . Then, repeated applications of the RG transformation will bring the coupling constants  $\vec{K}$  close to  $\vec{K}^*$ . In this case, the energy interaction coupling constant of the renormalized system,  $\vec{K}'$  obtained from the recursion relation equation 3.6, may be express in terms of a linearized recursion relation given by

$$\vec{K}' = \mathfrak{R}[\vec{K}] = \vec{K}^* + \frac{d\mathfrak{R}}{dK}(\vec{K} - \vec{K}^*) + \dots, \quad (3.10)$$

where  $\mathbf{M} \equiv \frac{d\mathfrak{R}}{dK}$  represents a linearization of the transformation through a matrix whose elements are  $\frac{dK'_i}{dK_j}|_{\vec{K}^*} = B_{ij}$ . Based on the eigenvalues and the eigenvectors of this matrix,  $\mathbf{M}U_i = \lambda_i U_i$ , the linear scaling fields  $U_i$  for  $i = 1, 2, \dots, n$  are obtained in terms of which the singular part of the free energy is expressed as

$$f_s(U_1, U_2, \dots, U_n) = b^{-d} f_s(b^{y_1} U_1, b^{y_2} U_2, \dots, b^{y_n} U_n). \quad (3.11)$$

This is the most general form of the free energy given by the equation (1.22). The eigenvalues of this matrix  $\lambda_i$  are related to the stability of the fixed point and are

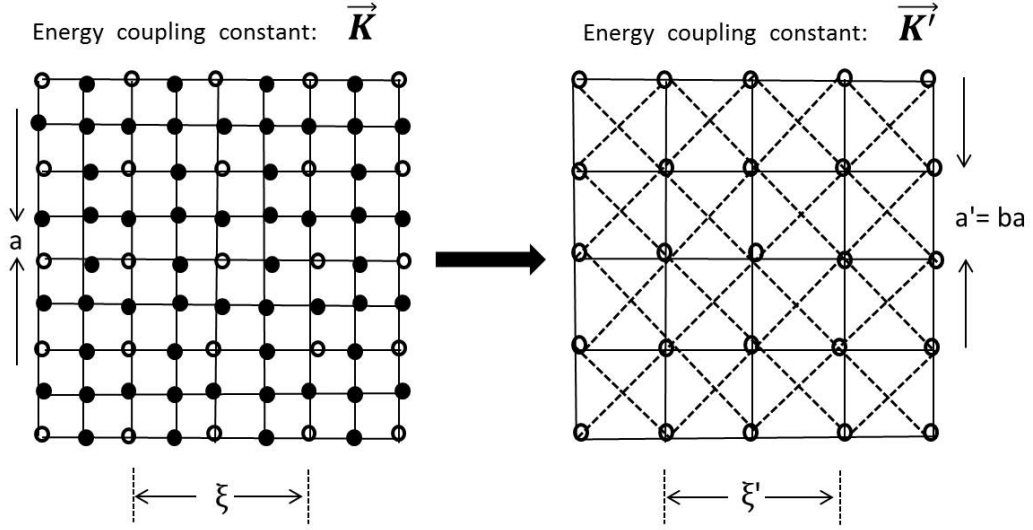


Figure 3.2: A  $b = 2$  renormalization scheme: The original lattice is split into two groups of spins denoted by  $\bullet$  and  $\circ$ . The dark circles  $\bullet$  indicate the spins that are eliminated by the transformation while the open circles  $\circ$  represent the remaining spins after the RG process. In the renormalized lattice, the remaining spins lie on square lattice with the nearest-neighbor distance increased by a factor of 2. The emergent next nearest neighbors links are denoted by dashed lines.

related to the critical exponents through  $\lambda_i = b^{y_i}$ . (Note that the composition law of the RG transformation ( $\lambda_i(b)\lambda_i(b) = \lambda_i(b^2)$ ) requires that  $\lambda_i = b^{y_i}$  with  $y_i$  independent of scaling factor  $b$  used in the transformation.) From the linearization of the recursion relation, relevant quantities such as the critical exponents can be obtained.

The behavior of  $U_i$  under the repeated action of the linear RG recursion relations is determined by the corresponding exponent  $y_i$ . The scaling field  $U_i$  of the system depends on the exponent  $y_i$  as

- if  $y_i > 0 \Rightarrow U_i$  is called **relevant**,
- if  $y_i = 0 \Rightarrow U_i$  is called **marginal**,
- if  $y_i < 0 \Rightarrow U_i$  is called **irrelevant**.

If the scaling field is relevant then the linear recursion relations will lead

the RG flows away from the critical point. On the other hand, for an irrelevant scaling field the RG flows extend toward the critical point. Consequently, one can not observe the relevant quantities in the second order phase transitions because they vanish. An illustration is presented in Figure 3.3 for the RG flows of a two-dimensional Ising model with different energy interaction constants  $J_x$  and  $J_y$  along the  $x$  and  $y$  directions, respectively.

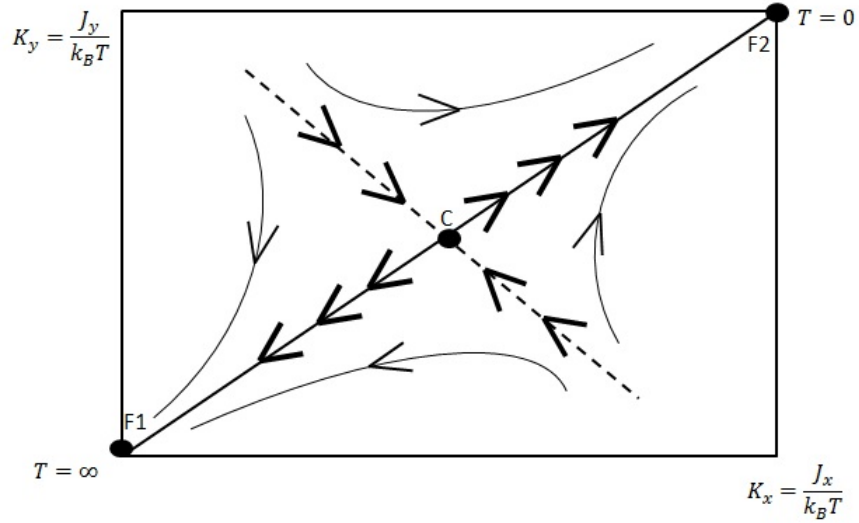


Figure 3.3: RG flows for the Ising model in high dimensional parameter space.  $C$  represents the unstable (relevant) critical fixed point while  $F1$  and  $F2$  indicate the stable (irrelevant) fixed points of the system.  $K_x$  and  $K_y$  are the unitless interaction constants along the the  $x$  and  $y$  directions, respectively. For the case of  $K_x = K_y$ , Onsager introduced an exact solution for this system [1]

### 3.2.2 General Remarks

In comparison to the field theoretical renormalization group theory, real space renormalization group (RSRG) transformation is much more convenient because of working directly on the lattice model of interest. However explicitly classifying of the systems according to their universality classes and being able to use the series expansion method for the critical exponents of the systems (although at

some dimensionality not too close to that of the studied system) are the main advantages of the field theoretical RG theory. In contrast, RSRG transformation is more functional for achieving the phase diagram of the system. In order to list the main disadvantages of the RSRG transformation, losing some the systematic nature of the approximation and the inaccuracies that normally need be introduced due to the truncations of the infinite lattice into finite, the uncorrelated pieces, and due to the truncations of the interaction energies at some level of complexity can be considered.

A “block spin transformation” which depends on the system parameters of the original lattice model, is introduced for the equilibrium RSRG transformation in order to construct a scaled version of the system. The equilibrium probabilities of the original system and the scaled (renormalized) system are associated with each other. In addition, these probabilities are produced from the renormalized versions of the interaction constants of the original system. In order to obtain a “fit” to the probabilities of the states of the renormalized system, new interaction constants may be needed to taken into account. In fact, for the more practical way it is important to truncate the number of interaction constants. The limitation in the number of renormalized interaction constants that may be used is also the result of the limited number of distinctly different probabilities of the states of the renormalized system.

### 3.2.3 Previous Work on RSRG Transformation

In this section, previous studies on the dynamical RSRG methods, that have been applied to systems mostly with Glauber dynamics in equilibrium are presented. In order to obtain the equilibrium dynamical critical exponent  $z$ , the dynamical version of the RSRG method was considered in different ways: in the first place, Monte Carlo simulations were used to obtain the parameters of the renormalized dynamical equations in position-space. Ma [89] presented a study on the dynamics of block spins constructed out of spins driven by a Monte Carlo simulation for Glauber dynamics. It was the first attempt to use this approach. After that, Swendsen [90] and Tobochnik *et al.* [91] considerably contributed to the Monte

Carlo approaches of the problem. In addition, it was argued by Yalabik and Gunton [92] that the parametrization of the renormalized state of the system may be accomplished by using the relaxation times of various types of correlations. Note that they investigated the two dimensional Ising model with Kawasaki dynamics in their work [92].

Additionally as an alternative to the Monte Carlo approach of the problem, another method was using a renormalization method which transforms the transition rates in the master equation of the original system to those of the rescaled system in a similar form of the original master equation. The dynamical critical exponent was also obtained from the ratio of the constants (that define the time scales at the fixed point) in these equations. This technique was used in many studies [93, 94, 95].

The most important characteristic point of these dynamical RG approaches is same: reducing the number of the dynamical degrees of freedom as well as the spatial correlations of the system. Block-spin transformation is a conventional method in which the blocks of  $n \times n$  spins of the original system can be substituted by single spins with the orientation prescribed by the majority rule. According to this rule, block spin up if the majority of the spins in the block is up, and vice versa. In general, for the block-spin transformation, the dynamics of the original system conserve in the block spins. Relaxation of the probability functions associated with the original system consists of the  $N$  time constants related to the eigenvalues of the  $N \times N$  Liouville operator. Due to the fact that the probabilities of the renormalized system are constituted from the linear combinations of those of the original system, the relaxation of the renormalized system occurs with the same time constants. Actually, the rate of change of block-spin probabilities to their higher order derivatives plays an important role to conserve the same eigenvalue structure. In this process, Markovian dynamics no longer exist because now the system has a “memory”: Based on the marginal majority rule, the probability of the transition of a block-spin per unit time becomes too large to let the system turns into its initial state. The transition rate of the state of the block-spin reduces to a smaller value as the corresponding state goes beyond this “infant-mortality” stage. As a result for the smaller time-scale dynamics one

can observe the non-Markovian effects. However for the larger time-constants dynamics contain the Markovian effects. Note that for the field-theoretic RG method, a similar approach is assumed for the separation of the time scales [48].

Detailed balance in the renormalized system cannot be declared because of the complexity of the probability flow among states. In some Monte Carlo RG studies, in which appropriate time dependent correlation functions in the original and scaled systems are to be obtained, the complexity of the dynamics of the system may be resumed to some degree [89, 92, 96, 97]. In general, research indicates that only the large time-constant modes in the scaled system is considered [92, 95, 98]. From the point of view of these studies, one can claim that a Markovian master equation for the renormalized system will be sufficient to describe its long-time behavior [92, 95, 98]. In particular Zheng [97] has pointed out that as the two dimensional Ising Model relaxes from a random initial state, short-time scaling in the exchange dynamics are no longer observed.

Studies on the scaling of the equilibrium critical dynamics do not constitute a comprehensive understanding for the steady state cases of this work.

Finally, studies on non-equilibrium systems, achieved by relaxation type of RG method, are also reported, for example systems with continuous growth mechanisms [99].

### 3.3 Our RG Transformation

Our transformation is based on a RSRG scheme to a non-equilibrium system at a steady state. The original system is regarded as a  $4 \times 4$  lattice with periodic boundary conditions in order to obtain its probabilities and relaxation rates. By choosing only the configurations with zero magnetization, the total number of the possible configurations of the system is reduced to  $N = 12870$  in our calculations. The original system is transferred into a  $2 \times 2$  lattice, again with periodic boundary conditions. In addition, we assume that for the possible states of the rescaled system, the total magnetization is also zero. So that this leads to 6

renormalized states with zero magnetization. Because of the fact that the block-spins are constituted from the spins of the original system, the probabilities of the possible states of these block variables are obtained from the steady state probabilities of the original variables. This condition is also valid for the equilibrium implementations. Accordingly, the interaction constants of the renormalized lattice are determined in such a way that these probabilities can be produced. The block-spin transformation used in the RSRG analysis is schematically shown in Figure 3.4.

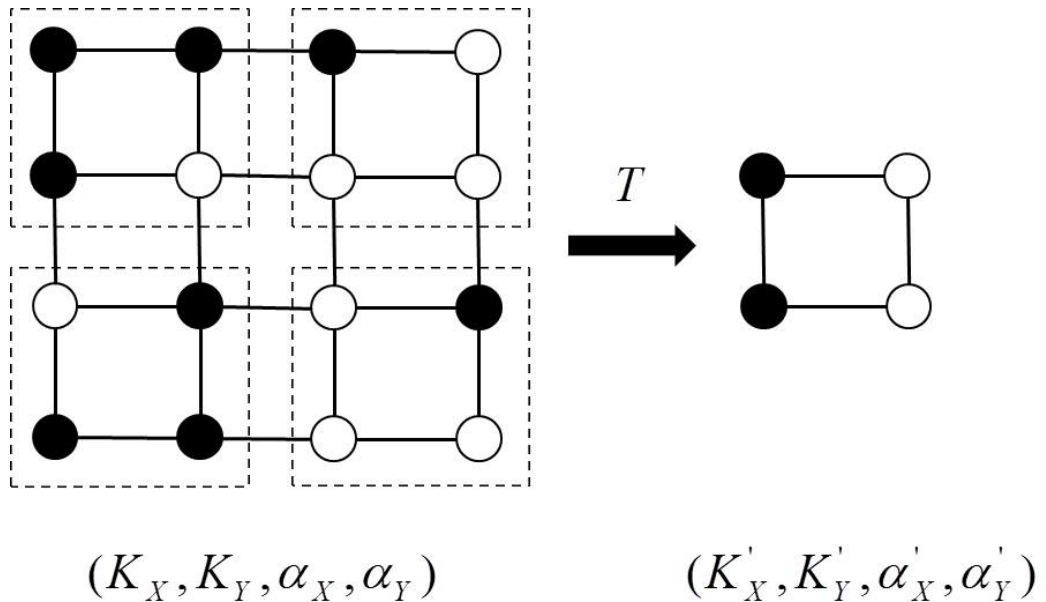


Figure 3.4: Block-spin transformation utilized in this study.  $\bullet$  and  $\circ$  indicate the  $\pm 1$  spins of the two dimensional spin-1/2 Ising model. The parameters of the original system are transformed into the ones of the rescaled system. Transfer matrix is denoted by  $T$ .

At this point, it is assumed that the renormalized system too obeys Markovian dynamics as the original one. As shown in Figure 3.5, based on the symmetry of the  $2 \times 2$  lattice in the presence of the  $x - y$  anisotropy, there are only 3 distinct steady-state probability values for the 6 renormalized states. Out of these 6 configurations of the rescaled system, only 4 distinct values are considered because of this symmetry. Note that although in the renormalized lattice there can be next-nearest neighbor and four spin coupling interactions, in our particular

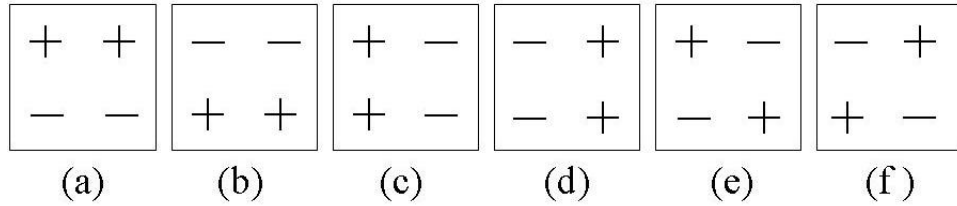


Figure 3.5: Possible 6 rescaled states of the renormalized  $2 \times 2$  system with  $M' = 0$ . Spin exchange can be accepted only for a single direction for the first four ordered states. The allowed exchange in (a) and (b) can occur along the  $y$  direction. Similarly, in (c) and (d) exchange can be seen along the  $x$  direction. However, spin exchange along both directions can be observed in (e) and (f). (Reproduced with kind permission of The European Physical Journal (EPJ) and Springer Science and Business Media) Copyright © Springer 2012

case the symmetries of the system do not allow for higher order interactions in a  $2 \times 2$  lattice. By means of the detailed balance condition, the form of the steady-state probabilities which is dependent on the ratio of a pair of such rates may be defined. Therefore it may be asserted that the renormalized system, together with the Markovian assumption, is equivalent to a system with exchange dynamics driven at two different temperatures (defined through detailed balance) in the two orthogonal directions with isotropic nearest neighbor coupling. As a result of the fact that the detailed balance condition may be achieved by a variety of spin-exchange rates, the coupling constants are determined with some arbitrariness in spite of all the assumptions carried on this procedure. However, one of the argument on the set of coupling constants obtained by this method is that it can be considered that the set of coupling constants obtained by this method corresponds to the result of the re-parametrization of the spin-exchange rates in terms of the two coupling constants. By using time-constants of the two slowest decaying modes of the system, the constants that define the time-scales of the renormalized dynamics are calculated. As a result, some justification is added to the assumption of Markovian dynamics.

If the corresponding assumptions are omitted and non-Markovian dynamics

and/or more complicated spin-exchange processes for the block-spins are considered, then there will be more parameters to the dynamics of the system. However this is the main condition on the detailed balance if one decides to ignore the detailed balance assumption for the renormalized dynamics. Actually, two more independent coupling constants and an additional time scale to the dynamics would also be needed for the designation of additional of eigenvectors (and corresponding eigenvalues) of the original system. In order to obtain the recursion relations between the original and the renormalized systems, this dynamics must be considered for the original system. However, our studies indicate that these additional parameters in the dynamics of the system cause a more complex model and they do not entail any important corrections in our results. It would be difficult to calculate the faster processes in the original and the scaled systems and identify the corresponding modes in the those systems. In addition, Zheng indicates that for conserved dynamics in equilibrium, shorter time-scale processes may best be treated separately for dynamical scaling[97]. In any case, by the assumption that the form displayed in equations 3.2 and 3.3 are valid for the renormalized system as well, the complexity in the dynamics is truncated.

### **RSRG procedure:**

First of all, in order to carry out the block spin transformation, a transformation matrix  $T$  with a size  $6 \times 12870$  is constructed. The probabilities of the states of the original system turns into those of the rescaled system by using the transfer matrix as

$$P'(i) = \sum_j T_{ij} P(j). \quad (3.12)$$

The original square lattice of  $4 \times 4$  sites is divided into 4 individual blocks. The new spin on a site of the rescaled square lattice is produced from each block. The possible states of the rescaled spins are determined by the sign of the sum of spins in their conjugated block. In case the sum is equal to zero, the sign of the rescaled spin is determined based on the constraint that the total magnetization of the rescaled system is zero. In case of having more than one such possibility, equal

distribution of the corresponding probability is considered between these possible states. (This transformation is only valid for the value of the energy coupling constant  $J$  is positive, otherwise this leads to an antiferromagnetic system so the symmetry of the ordered states cannot be protected.) Conservation of the probability implies

$$\sum_i T_{ij} = 1, \quad (3.13)$$

for all  $j$ . On the other hand, it is expected that a totally random original system (with equal probabilities  $P(i)$ ) should map to a totally random renormalized state. As a result of this situation,  $\sum_j T_{ij}$  should be independent of  $i$ . This is the second condition on the constructed transfer matrix. Although in our procedure the constituted transfer matrix exactly provides the first condition given in the equation (3.13), the second condition is satisfied approximately, within 0.5%.

The scaled interaction constants,  $K'_x$  and  $K'_y$  and the scaled transition rates  $\alpha'_x$  and  $\alpha'_y$  are obtained from the transformation process between the original system to the rescaled system, in terms of the original values  $K_x$ ,  $K_y$ ,  $\alpha_x$  and  $\alpha_y$ .

The  $2 \times 2$  renormalized system can be calculated easily because of its simple dynamics. By using the sequence of the states as shown in Figure 3.5, the Liouville matrix of the renormalized system is defined as

$$E' = \begin{pmatrix} -2\Omega_y & 0 & 0 & 0 & \omega_y & \omega_y \\ 0 & -2\Omega_y & 0 & 0 & \omega_y & \omega_y \\ 0 & 0 & -2\Omega_x & 0 & \omega_x & \omega_x \\ 0 & 0 & 0 & -2\Omega_x & \omega_x & \omega_x \\ \Omega_y & \Omega_y & \Omega_x & \Omega_x & -2(\omega_x + \omega_y) & 0 \\ \Omega_y & \Omega_y & \Omega_x & \Omega_x & 0 & -2(\omega_x + \omega_y) \end{pmatrix} \quad (3.14)$$

where the transition rates may be described in terms of the detailed-balance condition:

$$\frac{\omega_x}{\Omega_x} = \exp(8K'_x) \quad \text{and} \quad \frac{\omega_y}{\Omega_y} = \exp(8K'_y). \quad (3.15)$$

Here the assumption of the periodic boundary conditions in both directions results in the factor 8.

In order to achieve the scaled interaction constants,  $K'_x$  and  $K'_y$ , and the ratio of the scaled transition rates  $\alpha'_x/\alpha'_y$ , it is needed to calculate the three largest eigenvalues and corresponding eigenvectors of the Liouville matrix. The steady state is determined by the largest eigenvalue  $\lambda_{\max} = 0$ . It is possible to obtain the corresponding eigenvector from the steady state probabilities. The form of this eigenvector is consistent with the symmetries of the system and defined as

$$\Psi^{(0)} = \begin{pmatrix} a \\ a \\ b \\ b \\ c \\ c \end{pmatrix} \quad (3.16)$$

with

$$\begin{pmatrix} b \\ c \end{pmatrix} = \begin{pmatrix} \omega_x \\ \Omega_x \end{pmatrix} = \exp(8K'_x) \quad (3.17)$$

and

$$\begin{pmatrix} a \\ c \end{pmatrix} = \begin{pmatrix} \omega_y \\ \Omega_y \end{pmatrix} = \exp(8K'_y). \quad (3.18)$$

In addition, below the eigenvalues and the eigenvectors corresponding to slowest relaxation with the same symmetry are defined:

$$\lambda_1 = -2\Omega_y \quad \text{with} \quad \Psi^{(1)} = \begin{pmatrix} 1 \\ -1 \\ 0 \\ 0 \\ 0 \\ 0 \end{pmatrix} \quad (3.19)$$

and

$$\lambda_2 = -2\Omega_x \quad \text{with} \quad \Psi^{(2)} = \begin{pmatrix} 0 \\ 0 \\ 1 \\ -1 \\ 0 \\ 0 \end{pmatrix} \quad (3.20)$$

Relaxation of magnetization waves in  $y$  and  $x$  directions are associated with  $\Psi^{(1)}$  and  $\Psi^{(2)}$ , respectively. By assuming that the transition rates of the rescaled system obey the form given by equations (3.2) and (3.3), the rescaled parameters can be calculated from the steady state probabilities and relaxation time which are to be obtained from the scaling of the  $4 \times 4$  system. Then the rescaled parameters are defined

$$K'_x = \frac{1}{8} \ln \left( \frac{b}{c} \right) \quad (3.21)$$

$$K'_y = \frac{1}{8} \ln \left( \frac{a}{c} \right) \quad (3.22)$$

$$\alpha'_x = -\frac{\lambda_2}{4} \left( \frac{b}{c} + 1 \right) \quad (3.23)$$

$$\alpha'_y = -\frac{\lambda_1}{4} \left( \frac{a}{c} + 1 \right). \quad (3.24)$$

Our RG procedure is then as follows: At first the  $12870 \times 12870$  Liouville operator  $L$  is constructed for the  $4 \times 4$  original system. The eigenvalues  $\lambda$  and the corresponding eigenvectors  $\Phi$  of the original system can be computed as

$$L\Phi^{(i)} = \lambda_i \Phi^{(i)}. \quad (3.25)$$

Only three of the eigenmodes (the one corresponding to the steady state probabilities,  $\Phi^{(0)}$ , and those corresponding to the slowest relaxation of the system with symmetries given in equations (3.19) and (3.20),  $\Phi^{(1)}$  and  $\Phi^{(2)}$ ) are need to be calculated. The transfer matrix,  $T$  converts the eigenvectors of the original system to the ones of the rescaled system as the 12870 states of the original system transforms into the 6 possible states of the renormalized system. The relation which converts the steady state probabilities to their rescaled version is given by

$$\Psi_i^{(0)} = \sum_j T_{ij} \Phi_j^{(0)}. \quad (3.26)$$

Note that the parameters used in equations (3.23) and (3.24) include the eigenvalues  $\lambda_1$  and  $\lambda_2$ . All the necessary quantities to get the rescaled parameters as in equations (3.21)- (3.24) are obtained by this formulation.

### 3.4 Results and Conclusion

The critical behavior of the two-temperature spin-1/2 Ising model on a square lattice is obtained through the RG flows in the space of interaction parameters. RG flows occurs when the parameters of the original system transform into those of the renormalized system. RG flows drift into the critical fixed points so the critical surface is analyzed through the RG flows of the system.

The critical surface and the critical points obtained from the RG flows are schematically presented in Figure 3.6. The critical surface is designed as a function of the parameters  $K_x$ ,  $K_y$ , and  $r$ , where  $r = (\alpha_x - \alpha_y)/(\alpha_x + \alpha_y)$ . Note that in order to determine the steady states of the system, the ratio  $\alpha_x/\alpha_y$  must be considered because time can be scaled arbitrarily. By choosing these parameter space, one obtains a symmetric system with respect to the simultaneous transformation  $K_x \longleftrightarrow K_y$  and  $r \longleftrightarrow -r$ . In Figure 3.6, only one side of the critical surface in which the relation between the energy interaction constants are defined as  $K_x > K_y$ , with the corresponding RG flows are shown. Special case  $r = \pm 1$ : If one of the rates  $\alpha$  equals to zero, spin exchanges in the corresponding direction are obstructed. It means that the total magnetization along the other direction is conserved. Furthermore in this case, the steady state properties become dependent on the initial condition. At this point, it is assumed that this case may be substantiated while spin exchanges in both directions occur with finite transition rates, and while one of them becomes very large, the other stays finite. In this way, one can avoid the ergodicity problems.

At this limit, there are two interesting special cases:

1<sup>st</sup> case:  $((T_i = \infty, \alpha_i = \infty)$  while  $(T_j = \text{finite}, \alpha_j = \text{finite}))$  Having an infinite temperature associated with the infinitely fast process of spin exchange in one direction as spin exchanges occur at finite values of the transition rate under the effect of a finite temperature in the other direction.

In this case, effective random spin exchanges along the corresponding column or row appear. Consequently, the system can be exactly solved for the finite exchange rate in the other direction [68, 67, 75]. In addition, for this condition

mean-field like critical behavior is expected. This case is indicated as  $R_1$  in Figure 3.6.

*2<sup>nd</sup> case:*  $((T_i = \text{finite}, \alpha_i = \infty)$  while  $(T_j = \infty, \alpha_j = \text{finite}))$  Having a finite temperature related to the infinitely fast process while in the other direction there is an infinite temperature associated with the finite process of the spin exchanges.

As a result of this case, the dynamics of the system leads to the well-known equilibrium Ising model. The slow process acts to randomize the magnetization of the fast columns or rows. Note that due to the fact that the equilibrium condition is associated with equal magnetization of rows and columns, this posture is also obtained in the corresponding random process. Consequently at this limit equilibrium type behavior appears. The critical point for this case is shown as  $R_2$  in Figure 3.6. Note that the RG flow from  $R_2$  is conjectured to extend into the equilibrium fixed point.

According to the limitations of our numerical calculations, the RG transformation cannot be carried out for very small or very large values of  $\alpha$ . However for the  $r = \pm 1$  cases, extrapolation method is used for the calculations at  $r \approx \pm 0.82$ , for which  $(\alpha_x/\alpha_y)^{\pm 1} = 0.1$ .

Before all else, we would like to present the known or previously studied points about this system. As mentioned, at the limit where the two temperatures  $T_x$  and  $T_y$  are equal, system turns into the equilibrium Ising model. Again for this limit, the critical behavior is independent of  $\alpha_x$  and  $\alpha_y$ . The critical coupling constant of the two-dimensional Ising model in equilibrium was exactly obtained by Onsager as  $K_o = J/k_B T_o = 0.4407\dots$  [1].

In addition Præstgaard *et al.* analyzed this system in the case of  $\alpha_x = \alpha_y$  and  $K_x = 0$ ; as a function of  $K_y$  [48]. Their study indicates that the corresponding critical point of this situation, shown as  $K_P$  in Figure 3.6, was determined by  $K_P = 0.322 = 0.732K_o$ .

Moreover Krug *et al.* investigated this system at the limit in which  $\alpha_x/\alpha_y = 0$

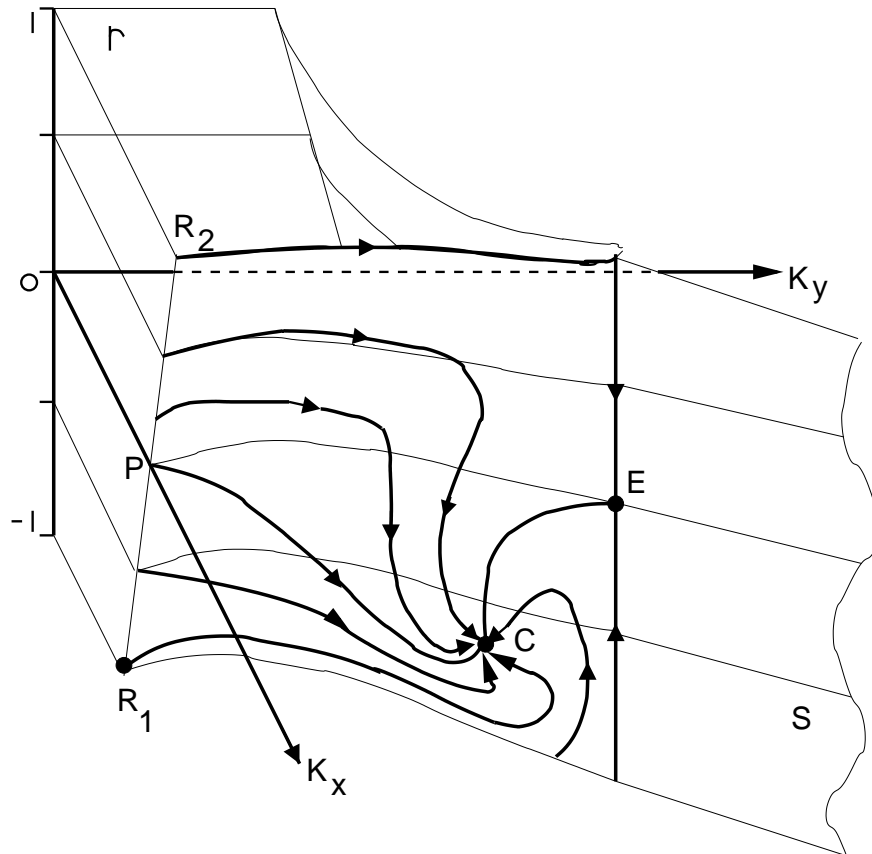


Figure 3.6: A schematic drawing of the critical surface of the system.  $C$  and  $E$  indicate the fixed points for the steady-state and the equilibrium, respectively.  $R_1$ ,  $R_2$  and  $P$  denote the critical points for certain limits. Thick lines indicate the RG flows. Thin lines refer to the cross sections at certain values of the variable  $r$ . Surface  $S$  (at  $K_x = K_y$ ) corresponds to the first-order phase transition between the ordered states at low temperatures. (Reproduced with kind permission of The European Physical Journal (EPJ) and Springer Science and Business Media) Copyright © Springer 2012

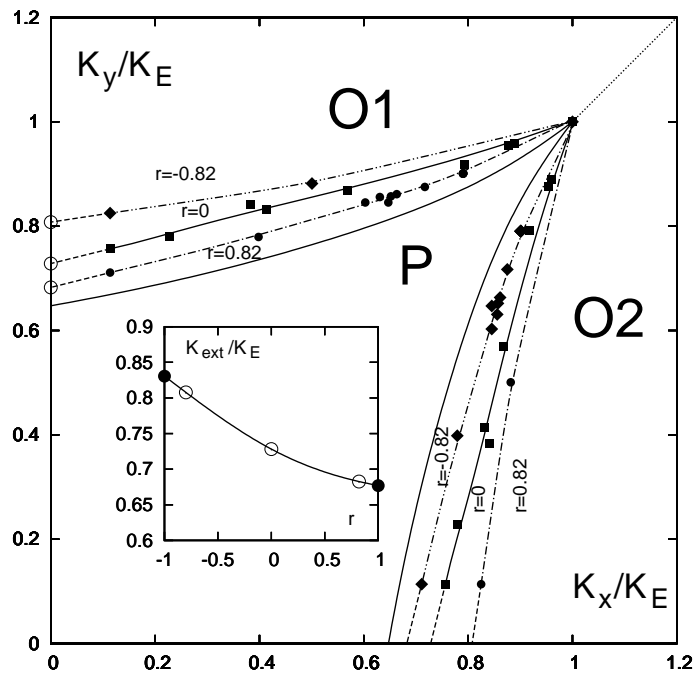


Figure 3.7: The phase diagram for various values of the parameter  $r$ .  $P$  represents the disordered paramagnetic phase, while  $O1$  and  $O2$  are the two symmetric ordered phases separated from one another by the first order transition line at the upper right corner. The inner most phase boundary is the result of Monte Carlo work reported [2] for  $r = 0$ . The diagram and the inset are further explained in the text. (Reproduced with kind permission of The European Physical Journal (EPJ) and Springer Science and Business Media) Copyright © Springer 2012

and  $K_y = 0$  [68]. Based on this search, for the type of exchange we are using, the exact value of the critical coupling, defined as  $K_{R1}$  in Figure 3.6, is reported by Sanli as  $K_{R1} = 0.59K_o$  [75].

As described in detail above, when  $K_y = 0$  and  $r = 1$ , for  $K_x$ , the critical coupling value, indicated as  $K_{R2}$  in Figure 3.6, is expected to be equal to the Onsager critical point  $K_o$ .

We would like to remind that our transformation depends on the three largest eigenvalues and the corresponding eigenvectors of the Liouville matrix. By using the calculations in the long time scaling regime, the dynamical critical exponent of the system is obtained in this regime. While the field theoretic RG method using the  $\epsilon$ -expansion yields the critical exponents  $\eta = (4/243)\epsilon^2$ ,  $\nu = (1/2) + (1/12)\epsilon + O(\epsilon^2)$ , dynamical scaling relations imply  $z = 4 - \eta$  for the steady state fixed point [48]. Furthermore according to a study on the two temperature lattice gas using Monte Carlo simulation, the findings are consistent with these theoretical results and the critical exponents are given as  $\nu = 0.60(5)$ ,  $\eta = 0.20(8)$ ,  $\beta = 0.33(6)$  and  $\gamma = 1.08(8)$  [47]. This suggests that the dynamical critical exponent is approximately  $z \approx 3.80$ .

We will now presents the results of our calculations: The equilibrium critical point indicated by  $E$  in Figure 3.6 has a value of  $K_E = 0.8789$ . The reason of this high value is analyzed and it is found that the conserved order parameter dynamics cause strong finite size effects. Apart from that, the values of the other critical points are calculated as  $K_P = 0.73K_E$ ,  $K_{R1} = 0.68K_E$  and  $K_{R2} = 0.83K_E$ .

An illustration of the full RG flow is presented in Figure 3.6. As mentioned in detail above, the flow has the symmetry ( $K_x \longleftrightarrow K_y$  and  $r \longleftrightarrow -r$ ). Although at the limit in which  $\alpha_x/\alpha_y = 1$ , system reaches its equilibrium state at the point  $K_x = K_y = K_E$ , RG flows extend into the steady state fixed point of the system from the equilibrium state for the  $\alpha_x/\alpha_y \neq 1$  limits. The corresponding steady state fixed point of the non-equilibrium phase transition is indicated as  $C$  in Figure 3.6 with  $r_C = 0.099$ ,  $K_{Cx} = 0.791$ ,  $K_{Cy} = 0.693$ . The new universality class of the non-equilibrium transition of the system is a result of this fixed point. There is a certain difference between this unfamiliar universality class and the

equilibrium universality class associated with fixed point  $E$ . The values of the correlation length exponent  $\nu$  is obtained from the eigenvalues of the linearized transformation around the fixed points for both universality classes. It is also reported in this study that the values of the exponent  $\lambda_c$  corresponding to the critical crossover from the equilibrium to the steady state and the time-scale exponent  $z = \log_2(\alpha/\alpha')$  for these fixed points.

The phase diagram for different values of  $r$  are presented in Figure 3.7. We would like to point out that in Figure 3.7 the coupling constants have been scaled by the equilibrium critical coupling. The filled points indicate the intersections of the critical RG trajectories and the planes of the critical surface for a particular  $r$ . (Because of the inaccuracies in estimating the path of the trajectory from recursion points, there are few irregularities at point positions.) The Bezier smoothed fits to these points are denoted by the corresponding lines. Extrapolations to values on the axes are given by the dashed extensions to the lines indicated as the open circles. The inset in Figure 3.7 shows these extrapolated values on the  $K_y$  axis. Estimated critical values of  $K_y$  when  $K_x = 0$  at  $r = -1$  and  $r = +1$  are obtained from this plot and reported in Table 3.1. There is a slight variation in the phase diagram with respect to the relative exchange time scales in the  $x$  and  $y$  directions.

If the results of our method are analyzed, most important flaw will be considered as the large values of the obtained equilibrium critical point  $K_E$  and the corresponding correlation length exponent  $\nu$ . As mentioned, due to the very strong finite-size effects associated with conserved dynamics in the original and the scaled lattices, this flaw occurs. (Especially one can observe the effects of the conserved dynamics for a  $4 \times 4$  system by calculating the point at which specific heat forms a peak. The exact solution of such a calculation shows that for the system with conserved order parameter, the peak of the specific heat occurs at approximately  $K = 2.6$  whereas it appears at approximately  $K = 1.5$  for the non-conserved system.) It is understood that the dynamical critical exponents, which are obtained from the ratios of the time scales associated with the original

Table 3.1: Quantitative results for various phase transition points studied in this work. Results from other studies are also included for comparison. Critical points  $P$ ,  $R_1$ , and  $R_2$  belong to steady state, mean-field, and equilibrium universality classes respectively. (Reproduced with kind permission of The European Physical Journal (EPJ) and Springer Science and Business Media) Copyright © Springer 2012

Phase Point ( $K_x, K_y, r$ )	Quantity	This work	Previous Studies
Steady state $C:(0.791, 0.693, 0.099)$	$\nu$	0.65	0.60(5) [47]
	$z$	3.1	$\approx 3.80$ [48, 47]
Equilibrium $E:(K_E, K_E, 1)$	$K_E$	0.8789	$K_o = 0.4407..$ [1]
	$\nu$	1.74	1 (exact)
	$z$	3.72	3.75 [4, 5]
	$\lambda_c$	0.36	—
$P (K_P, 0, 0)$	$K_P$	$0.73K_E$	$0.732K_o$ [48]
$R_1 (K_{R1}, 0, -1)$	$K_{R1}$	$0.68K_E$	$0.59K_o$ [75]
$R_2 (K_{R2}, 0, 1)$	$K_{R2}$	$0.83K_E$	$K_o$ (our conjecture)

and renormalized lattices, is considerably accurate. The reason for this situation is the fact that these time scales change very slowly for each of the lattices, and that the ratio is relatively insensitive to the precise value of the fixed point parameters. The finite size effects in our calculations can be regarded as a systematic inaccuracy because the very atypical phase diagram of the system in Figure 3.7, obtained when all interactions are scaled by the critical equilibrium coupling, is a strong evidence of this argument. One can also notice that our results in Figure 3.7 are very consistent with previous Monte Carlo studies.

In conclusion, global phase diagram of the system is reported with a variety of the critical points of the system. In addition, the obtained values of these critical points are presented with the corresponding values of the interrelated previous studies. It is observed that the crossover of critical behavior from equilibrium to steady state appears for the values of the temperatures  $T_x$  and  $T_y$  close to each other. The value of  $\lambda_c$  we report can be compared with the ones might be obtained from Monte Carlo studies in this regime.

Note that in the Appendix A, comparable results of the same system, this time with non-conserved dynamics, are presented.

### 3.5 Discussion on the Suitability of Proposed Transformation

Since this study is the first work on the full phase diagram of the two-finite temperature Ising model with conserved order parameter and also the first attempt to use a real space renormalization group transformation for this anisotropic model, we would like to discuss at this point the validity of the suggested procedure. In general, it is suitable to use a RSRG method for the isotropic systems. To understand the nature of using a RSRG method for the non-equilibrium systems of which the characteristic length scales in the  $x$  and  $y$  directions scale with different exponents, a brief discussion of the availability of this technique is presented.

In our transformations, new block-spins which have a distance a factor  $b = 2$  larger than the distance between the original spins are constructed. Furthermore the probabilities of the possible states of the rescaled system is also determined in accordance with the steady state probabilities of the original spin configurations. Consequently, the new system precisely harmonizes to one in which the characteristic distances (such as the correlation lengths) have been reduced by a factor  $b = 2$ . Especially, infinite (or zero) correlation length systems turn again into infinite (or zero) correlation length systems. It is eventually observed that the critical points certainly flow into fixed points. So that the phase diagram of the system can be determined by this method as usual.

However, one can encounter a limitation for the determination of the correlation length exponent. As mentioned in Chapter 1, the scaling relation for correlation length is defined as  $\xi(t)/b = \xi(tb^{\lambda_t})$  and its behavior at the critical point is given by  $\xi(t) \sim t^{-\nu}$ . As a result of these scaling laws, a unique correlation length exponent is obtained as  $\nu = 1/\lambda_t$ . Here, the variable  $t$  indicates the small deviation from criticality. This exponent is independent of the direction. Because of this limitation of our method, we cannot report any anisotropy in this exponent. In our study, the value corresponding to  $1/\lambda_t$  is presented. In addition, in spite of using the linearization of the RG transformation, the dynamical critical exponent  $z$  is obtained from the comparison of the time scales of the original and

renormalized systems at a fixed point.

Keeping a certain aspect ratio for finite lattices may be necessary for data collapse in studies of finite size scaling, where one is explicitly studying the interplay between the correlation length and the system size. The RG procedure, on the other hand, uses block sizes which are explicitly less than the correlation length, especially near critical points where the theory is so successful.

It is true that the fixed point (isotropic or anisotropic) is scale invariant, but this does not mean that the anisotropic system cannot be analyzed by an RG transformation that has equal scaling factors for the two directions. Quantitatively, for a symmetric transformation such as ours, one has for the correlation function:

$$G\left(\frac{x}{L_x}, \frac{y}{L_y}\right) \text{ transforms to } G\left(\frac{x}{L_x/b}, \frac{y}{L_y/b}\right),$$

with  $L_x$  and  $L_y$  correlation lengths and  $b$  the scaling factor. Quite obviously, infinite (zero) correlation lengths will scale into infinite (zero) correlation lengths and therefore critical couplings will transform into critical couplings. The RG flow on the critical surface will be different from a transformation that would use unequal scaling factors, but that is to be expected. As long as critical couplings transform into other critical couplings, the phase diagram may be obtained, and that is what we claim to do. The anisotropic fixed points are (admittedly important) special points on the phase diagram, which we discuss below, but the production of the phase diagram depends solely on the property that critical couplings transform into critical couplings.

Now, near a fixed point, the correlation lengths scale as

$$\frac{L_x(t)}{b} \sim L_x(b^{\lambda_x}t) \quad \text{and} \quad L_y/b \sim L_y(b^{\lambda_y}t),$$

equal to

$$\frac{1}{bt^{\varepsilon_x}} \sim \frac{1}{(tb^{\lambda_x})^{\varepsilon_x}} \quad \text{and} \quad \frac{1}{bt^{\varepsilon_y}} \sim \frac{1}{(tb^{\lambda_y})^{\varepsilon_y}},$$

for a small deviation  $t$  (of the relevant variable) from the fixed point;  $\lambda_x$  and  $\lambda_y$  are the corresponding eigenvalues, with  $\varepsilon_x$  and  $\varepsilon_y$  the unequal, anisotropic exponents (equal to minus the correlation length exponent “ $\nu$ ”). To preserve the

scaling form one needs to have

$$\varepsilon_x = -\frac{1}{\lambda_x} \quad \text{and} \quad \varepsilon_y = -\frac{1}{\lambda_y}.$$

Since the transformation in the  $x$  and  $y$  directions is coupled, one cannot determine the exponents  $\lambda_x$  and  $\lambda_y$ , so that the anisotropic correlation length exponents  $\varepsilon_x$  and  $\varepsilon_y$  cannot be determined.

In addition, one may suggest a transformation which accomplishes

$$L_x, L_y \quad \text{transforms to} \quad \frac{L_x}{b}, \frac{L_y}{b^D},$$

with  $D$  chosen such that

$$\frac{L_x(t)}{b} \sim L_x(b^{\lambda_x}t) \quad \text{as before, but} \quad \frac{L_y(t)}{b^D} \sim L_x(b^{\lambda_x}t)$$

equal to

$$\frac{1}{t^{\varepsilon_x}b} \sim \frac{1}{(b^{\lambda_x}t)^{\varepsilon_x}} \quad \text{as before, and} \quad \frac{1}{(b^D t^{\varepsilon_y})} \sim \frac{1}{(b^{\lambda_x}t)^{\varepsilon_y}}.$$

This leads to  $D = \lambda_x/\lambda_y$ , as well as  $\varepsilon_x = -1/\lambda_x$  and  $\varepsilon_y = -1/\lambda_y$  as before. This is formally an equivalent, another form of scaling. The eigenvalues  $\lambda_x$  and  $\lambda_y$  are still not accessible, so neither is  $D$ , and the procedure cannot be carried out. This form of scaling may be favored because it leads to single relevant scaling ( $b^{\lambda_x}t$ ) in both  $x$  and  $y$  directions. The question is whether this is a requirement. Our ability to scale the relevant variable by different values ( $b_x^\lambda$  in the  $x$  direction and  $b_y^\lambda$  in the  $y$  direction) is a consequence of the group property of scaling an anisotropic system. Indeed the suggested scaling is also consistent with this property:

- Suggested form:

$$\frac{L_x(t)}{b}, \frac{L_y(t)}{b^D} \Rightarrow L_x(b^{\lambda_x}t), L_y(b^{\lambda_y}t),$$

equivalently this form corresponds to

$$\frac{L_x(t)}{b^{1/D}}, \frac{L_y(t)}{b} \Rightarrow L_x(b^{\lambda_y}t), L_y(b^{\lambda_x}t).$$

scaling only in  $x$  direction:

$$\frac{L_x(t)}{b}, \frac{L_y(t)}{b^0} \Rightarrow L_x(b^{\lambda_x}t), L_y(b^0t).$$

- Our scaling:

$$\frac{L_x(t)}{b}, \frac{L_y(t)}{b} \Rightarrow L_x(b^{\lambda_x t}), L_y(b^{\lambda_y t}).$$

- General group property:

$$\frac{L_x(t)}{b^p}, \frac{L_y(t)}{b^q} \Rightarrow L_x(b^{p\lambda_x t}), L_y(b^{q\lambda_y t}).$$

So formally, all of these forms of scaling are valid.

We further point out that it should in principle be possible to construct a position space RG transformation so that the length scaling is carried out first in one direction, and then in the other, so that the effects of scaling in different directions would be apparent. In particular, the linearization of the transformation near a fixed point would be the successive application of two linear operations, each corresponding to the scaling operations in different directions. Eigenvalues of these operators would then lead to different scaling exponents for the correlations in different directions.

Briefly, an RG transformation with equal scaling factors in both directions could even yield the anisotropic correlation function eigenvalues  $\varepsilon_x$  and  $\varepsilon_y$ , if scaling in the  $x$  and  $y$  directions could be uncoupled. Consider the following RG scheme:

- We first scale in the  $x$  direction by a factor  $b$ :

$$(K_x, K_y) \text{ transforms to } (R(K_x, K_y), K_y),$$

(Note that  $L_x$  transforms to  $L_x/b$ ,  $L_y$  is unchanged.)

- Then scale in the  $y$  direction by the same factor  $b$ :

$$(K'_x, K_y) \text{ transforms to } (K'_x, R(K_y, K'_x)),$$

(Note that this time  $L_x$  is unchanged,  $L_y$  transforms to  $L_y/b$ .)

This pair is then equivalent to our transformation. Now one can, in principle, find the exponents  $\varepsilon_x$  and  $\varepsilon_y$  because  $\lambda_x$  can be obtained from a linearization of the first transformation at the fixed point, and  $\lambda_y$  from the second. So, isotropic

scaling can, in principle, provide even the anisotropic exponents! Our transformation, being equivalent to the combination of the above transformations, would yield upon linearization, the sum of the linearized versions of the above transformations.

In other words, our transformation corresponds to the product of these two operations, and our eigenvalues are those of the sum of the above two linearized operators. Therefore, we cannot extract the eigenvalues corresponding to the anisotropic exponents. Our RG trajectories nevertheless, follow those of the combined scaling transformation. Although this two-step RG procedure would be possible in principle, we feel that the errors that would be introduced through various approximations in such a procedure might be prohibitive in practice.

## Chapter 4

# A Monte Carlo Study on the Steady State Phase Transitions of the Eight-Vertex Model with Conserved Order Dynamics

Non-equilibrium phase transitions of the eight-vertex model is studied through Monte Carlo simulations. The non-equilibrium eight-vertex model is treated as a two interlacing two-dimensional spin-1/2 Ising models on square lattices. The dynamics of the system is taken to be driven by spin exchanges within the sublattices, each in contact with a different thermal bath. In this study, thermal baths are considered as one of them with infinite temperature while the other has a finite value. By the means of four independent Monte Carlo simulations, each with  $60 \times 10^6$  Monte Carlo steps, the critical behavior of this non-equilibrium system is investigated.

We would like to point out that it is observed in many studies on the critical behavior of the non-equilibrium systems with conserved anisotropic dynamics (for driven lattices [49, 72, 73, 76] and two-temperature Ising model [47, 48, 67, 68, 74]) that for the finite-size scaling, the anisotropic scaling is an important condition.

In addition, in the first study of this thesis (chapter 4), it is also understood that this scaling condition plays an essential role on the analysis of a non-equilibrium system. To avoid the complication related to this condition, it is proposed that one can consider to choose different dynamics not in different directions but on different sublattices. For this purpose, one may suggest to choose the eight-vertex model which is non-universal in equilibrium.

At 1971, R.J. Baxter first introduced the exact solution of the “zero-field” eight vertex model in equilibrium [100]. This was a very important study in the field of phase transitions because with this study, the concept of the universality is considered to gain a completely new perceptive for the critical phenomena. It is understood by the exact calculations of the free energy of this model that static critical phenomena does not have universality property [100]. It is observed that the critical exponents depend on the energy interactions of the system.

It is therefore of interest to investigate the criticality (and hence the universality) of the non-equilibrium properties of the eight-vertex model near its non-universal equilibrium critical points.

## 4.1 The Model

The Hamiltonian of the eight-vertex model on a square lattice with periodic boundary conditions in equilibrium is defined as

$$\mathcal{H} = -\frac{H}{k_B T} = \sum_{i=1}^L \sum_{j=1}^L [K(s_{i,j}s_{i+1,j+1} + s_{i+1,j}s_{i,j+1}) + Q(s_{i,j}s_{i+1,j}s_{i,j+1}s_{i+1,j+1})], \quad (4.1)$$

where the next-nearest coupling constant and the four-spin coupling constant is denoted by the energy coefficients  $K$  and  $Q$ , respectively. Here, spin variables  $s_{i,j}$  can take values  $\pm 1$  and  $k_B$  is the Boltzmann constant. If the four spin coupling  $Q$  connects the Ising lattices to each other is zero, then the corresponding Ising lattices of the system separate and become two independent Ising models. The critical line on the  $K - Q$  plane introduced by R. J. Baxter in order to obtain

the phase transitions of this system defined by

$$K_c = B(Q) = \frac{1}{2} \ln[e^{-2Q} + \sqrt{1 + e^{-4Q}}]. \quad (4.2)$$

The non-universal static critical exponents  $\nu$  and  $\beta$  are defined as a function of  $Q$ ,

$$\nu = \frac{\pi}{2\mu} \quad \text{and} \quad \beta = \frac{\pi}{16\mu} \quad \text{where} \quad \cos \mu = \tanh 2Q. \quad (4.3)$$

In addition, the critical exponent  $\alpha$  is associated with the four spin coupling constant  $Q$  as

$$\sin \frac{\pi\alpha}{4(1 - \frac{\alpha}{2})} = \tanh 2Q. \quad (4.4)$$

In this study, the non-equilibrium critical dynamics of the eight-vertex model with Kawasaki dynamics is investigated by Monte Carlo simulations. Periodic boundary conditions were assumed for the system. In general the studied system is constructed by two interpenetrating spin-1/2 Ising models on square lattices, each in contact with a heat bath at a different temperature, which are interacting through an inter-sublattice coupling. Spin exchanges within the sublattices define the dynamics of the non-equilibrium system. To observe a second order phase transition, the magnetization of both sublattices are set to zero. Two different effective temperatures (one of them infinite;  $T_2 = \infty$ ) on the system are imposed to define the dynamics of the system. When a spin exchange occurs in one of the sublattices, this take place with a dynamics associated with the temperature related to the corresponding sublattice.

Implementation of the detailed balance for exchanges in each sublattice is achieved by using

$$\mathcal{H}_1 = -\frac{H}{k_B T_1} = K_1 \sum_{\langle ij \rangle} s_i s_j + Q_1 \sum_{\langle ijmn \rangle} s_i s_j s_m s_n, \quad (4.5)$$

for exchanges in the sublattice-1, and

$$\mathcal{H}_2 = -\frac{H}{k_B T_2} = K_2 \sum_{\langle ij \rangle} \sigma_i \sigma_j + Q_2 \sum_{\langle ijmn \rangle} s_i s_j s_m s_n, \quad (4.6)$$

for exchanges in the sublattice-2, where  $\langle ij \rangle$  and  $\langle mn \rangle$  indicate sums over nearest neighbor pairs of sites in the two sublattices and  $\langle ijmn \rangle$  denotes sum over all

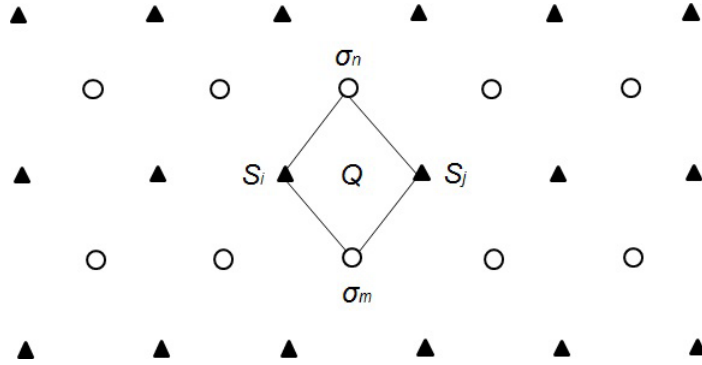


Figure 4.1: An illustration for the two spin-1/2 Ising model sublattices connected to each other with a four spin coupling constant  $Q$  shown in the plaquette. The spin sites denoted by  $\blacktriangle$  and  $\circ$  belong to the two sublattices.

spin quads on a plaquette as indicated in Figure 4.1. Here, variables  $s_i$  and  $\sigma_m$  represent the spins in the first and second sublattices respectively. The values of these variables can be  $\pm 1$ . In addition  $k_B$  is the Boltzmann constant. The nearest neighbor and the four spin coupling constants are denoted by the coefficients  $K_i$  and  $Q_i$ . These constants are dependent on the temperature of the heat bath in contact with that sublattice:

$$K_i = \frac{J}{k_B T_i} \quad \text{and} \quad Q_i = \frac{J_q}{k_B T_i} \quad (4.7)$$

where  $J_q$  indicates the inter-sublattice coupling constant and  $J$  is the sublattice nearest neighbor energy interaction constant.

When the effective temperatures of the two sublattices are equal, *i.e.*,  $T_1 = T_2$ , this leads the coupling constants to be equal,  $K = K_1 = K_2$  and  $Q = Q_1 = Q_2$ . Therefore, at this ‘‘Baxter’’ limit, system is in equilibrium and the exact solution is known [100]. Besides, to consider the value of the temperature  $T_2$  as infinite, indicates that the values of the nearest neighbor coupling constant  $K_2$  and the four spin coupling constant  $Q_2$  are zero as well. As a result of this, spin exchanges occur randomly on the second sublattice.

## 4.2 Monte Carlo Simulations

In this study, the system has been investigated for spin exchanges by using the standard Monte Carlo (MC) simulations (Metropolis [101]) for spin exchanges. To perform this procedure, a configuration change at a randomly selected site consistent with the assumed dynamics of the system is chosen. The corresponding spin exchange is carried out directly if the final configuration of the system has a lower energy than its initial state ( $\Delta\mathcal{H}_i > 0$ ). Contrarily, this exchange depends on a probability  $\exp[-\Delta\mathcal{H}_i]$  (Metropolis [101]) where  $\Delta\mathcal{H}_i$  is the increase in the appropriate quantity given in the equations (4.5) or (4.6). Time parameter is measured by Monte Carlo steps (MCS).  $N^2$  spin exchange attempts define one MCS, so that the time parameter does not depend on the system size  $N$ .

To construct the system, the two  $N \times N$  size sublattices with randomly distributed spins and zero magnetization are used. The probabilities of the spin exchanges within the two sublattices are equal ( $P_1 = P_2 = 0.5$ ). In addition, as mentioned before, to observe a second order phase transition, the total magnetization of these sublattices are set at zero,  $m_1 = m_2 = 0$ . This leads to equal number of spins in these sublattices,  $N_1 = N_2$ .

We repeat this procedure for  $60 \times 10^6$  MCS in each independent 4 runs. The energies  $E_1$  and  $E_2$  of the two sublattices are accumulated and recorded every 10 MCS after the first 100 MCS. Note that the reason of the 4 independent runs is to control the system for the possibility of reaching a frozen state. Then, the “energy” fluctuation per spin corresponds to

$$\frac{C_v}{k_B} = (\langle E^2 \rangle - (\langle E \rangle)^2) / N^2. \quad (4.8)$$

where  $E$  is the spin product  $\sum_{\langle ij \rangle} s_i s_j$  for the sublattice-1 at finite temperature. We would like to point out that the sums that involve the spins  $\sigma$  (which exchange randomly due to their contact with the infinite temperature heat bath) lead to correlations consistent with totally random variables. We will adopt the terminology “specific heat” to indicate this fluctuation although this term is mainly used in equilibrium systems. For different system sizes ( $N = 32, 40, 80, 100$ ), these energy fluctuations are measured. In order to investigate the critical exponent

associated with the correlation length exponent  $\nu$ , the standard procedure of finite size scaling (FSS), formulated by Fisher [102, 103, 104], is applied. This procedure produces a relation given in the equation 1.26 for energy fluctuations

$$\widetilde{C}_v(t, N) = b^{2\lambda-d} \widetilde{C}_v(b^\lambda t, \frac{N}{b}), \quad (4.9)$$

where the reduced temperature  $t$  is defined as  $t = (K - K_c)/K_c$  and  $\lambda = 1/\nu = 1/y_t$ . Here, for  $b = N$  the associated collapse of this scaling relation is determined by

$$\frac{\widetilde{C}_v(t, N)}{N^{2\lambda-d}} \sim \widetilde{C}_v(N^\lambda t, 1). \quad (4.10)$$

For this system, the dimension  $d$  is equal to 2. In order to calculate the singular part of the specific heat  $\widetilde{C}_v$  in the equation (4.9), a constant term “ $g$ ” need to be subtracted from  $C_v$  in the equation (4.8). In principle, one expects to observe a collapse of all data on a single curve near the critical point in a plot of  $\widetilde{C}_v/N^{2\lambda-d}$  versus  $N^\lambda t$  based on the scaling form given the equation (4.10). It is to say that this functional relation of the scaling must be independent of system size.

$J_q$	0	0.1	0.2	0.3	0.4	0.5
$K_c$	0.44	0.45	0.46	0.49	0.53	0.59

Table 4.1: Critical temperature  $K_c$  values for different  $J_q$  values.

Second order phase transitions correspond to the peak points of the specific heat on scaling plots. Collapse of data on these plots are evidence of divergence of fluctuations as  $N \rightarrow \infty$ . This leads to the identification of critical points and exponents through MC simulations. The corresponding data collapses of our MC simulations for different values of the inter-sublattice coupling constant  $J_q$  of the system are shown in Figure 4.2. These best collapses correspond to a value of the critical exponent equal to  $\lambda = 1.00 \pm 0.03$ . In Table 4.1, the corresponding critical points are reported with the related inter-sublattice constants. In this work, contrary to the model studied by Præstgaard *et al.* [48], an increase in  $T_c$  is not observed as coupling to the  $T = \infty$  lattice becomes stronger.

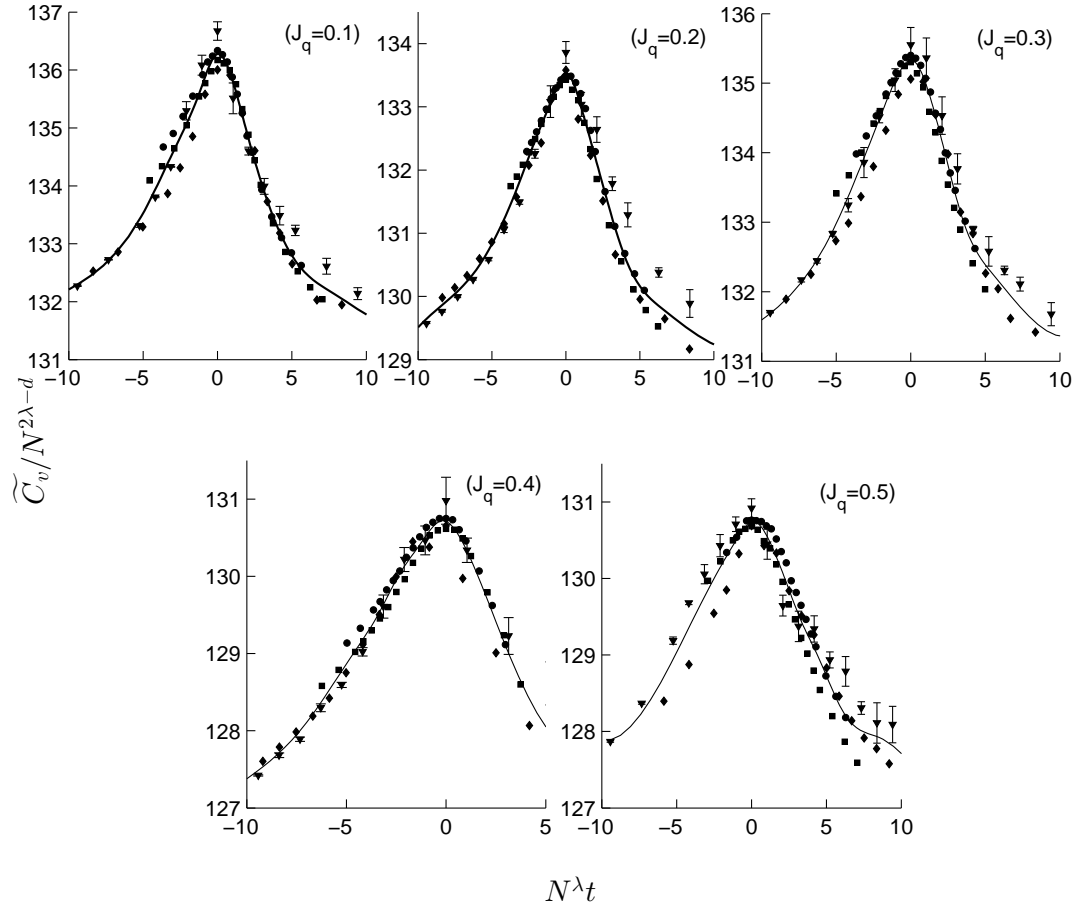


Figure 4.2: Finite-size scaling plot of  $\widetilde{C}_v/N^{2\lambda-d}$  versus  $N^\lambda t$  for different values of  $J_q$ . The best collapse obtained from the adjustable parameters  $K_c, \lambda$  and  $g$  are indicated by the solid lines. Symbols are as follows:  $N = 32(\bullet), 40(\blacksquare), 80(\blacklozenge), 100(\blacktriangledown)$ .

### 4.3 Data Collapse

In order to investigate the critical properties of the non-equilibrium eight vertex model, the obtained data from MC simulations is analyzed through finite-size scaling. After the FSS process near the critical point one can observe that the plot of the specific heat shows a data collapse independent of the system size. Therefore, the critical exponent  $\lambda$  can be determined from the divergence behavior of this rescaled data. As mentioned, there are three adjustable parameters  $(K_c, \lambda, g)$  for the best collapse of our data. Various collapses can be achieved by using different values of these parameters. To obtain the best fit of our data, our procedure is as described below:

- **STEP-1: Monte Carlo Simulations:**

As mentioned in the previous section, for a particular value of  $J_q$ , MC simulations are carried out for different values of the coupling constant  $K_1$  of the sublattice-1 while  $K_2 = 0$ . The specific heat  $\widetilde{C}_v$  of the system with a particular value of  $J_q$  is obtained as function of the coupling constant  $K_1$  for different system sizes such as  $N = 32, 40, 80, 100$ . (In each plot of the specific heat there are 20 data points from different values of  $K_1$ .)

- **STEP-2: Error Analysis:**

- In order to calculate the possible error of a MC simulation, independent samples of the quantity we are calculating ( $\widetilde{C}_v$ ) are accumulated from the corresponding Monte Carlo process. The particular MC simulation is divided into the independent samples of the data sets by using a time scale much larger than the correlation time of the system ( $t \gg \tau$ ). Note that the total number of the independent samples increases by a factor of 4 since for every value of the coupling constants, 4 independent runs were carried out in this work. The number of independent samples that can be obtained from the MC simulations depend on the temperature. For different values of the coupling constant  $K_1$  in the plot of  $\widetilde{C}_v$ , the correlation times vary from 6000MCS

to 10000 MCS for higher temperatures (the disordered phase). In contrast, for the lowest temperatures in our simulations, our run time of  $60 \times 10^6$  MCS barely covers the corresponding correlation times. As a result, there are only 4 independent measurements for the lowest temperatures. This is a result of the slowing down of the system.

- After the determination of the correlation time of the specific heat  $\widetilde{C}_v$  for each value of  $K_1$ , numbers of independent samples are obtained as  $m = T/t$  where  $T = 60 \times 10^6$  MCS and  $t \gg \tau$ .
- The error bars of the obtained data points are calculated by dividing the standard deviation of the corresponding independent samples to the square root of the total number of those samples, as  $\frac{\Delta \widetilde{C}_v}{\sqrt{m}}$ . In each graph of Figure 4.2, error bars obtained from this analysis are only presented for  $N = 100$  system size. The error bars for  $N < 100$  lattices are smaller than the sizes of the points in Figure 4.2.

- **STEP-3: Spline Interpolation:**

An error measurement  $\varepsilon$  is needed to evaluate the goodness of the data collapse obtained from the adjustable parameters  $(K_c, \lambda, g)$  in the FSS process. For this purpose, spline fitting is used to get the corresponding error measurement  $\varepsilon$  to determine the best set of these parameters which provide the minimum error. The spline curve fitted to all scaled data points is also drawn in Figure 4.2. Appendix B presents all the details of the spline interpolation procedure.

In this study, 80 data points (20 spots from each plot of the specific heat for a particular system size) are obtained from the FSS process. These data are partitioned into 10 intervals so that there will be 8 data points in each of them. Due to the fact that the goodness of the finite size scaling depends on the values near the critical point, out of the 80 data points of the specific heat only the central 40 of them (contained in the 5 central intervals) are taken into account.

To calculate the error  $\varepsilon$  of the FSS process, the mean squared deviation between the rescaled data-set and the created curve spline is considered. In

order to obtain the minimum error for each particular value of the parameter  $\lambda$ , optimum values of the parameter  $g$  are analyzed. These values are presented in Table 4.2.

It is observed that the scaling  $C_v/N^{2\lambda-d}$  shows logarithmic behavior (even though through a non-uniform limit) as  $C_v/\ln N$  as  $\lambda$  approaches 1. The change in parameter  $g$  is also consistent with the corresponding behavior as  $\lambda \rightarrow 1$ , as shown in Table 4.2. Due to this reason, when a logarithmic scaling is used the corresponding  $g$  value is quite different from the limiting forms when  $\lambda \neq 1$ . This situation can be seen in Figure 4.3. Minimum errors corresponding to values of  $\lambda$  in Table 4.2 reach minimal values at  $\lambda = 1$ , as indicated in Figure 4.4. The obtained trend line equations for ( $\lambda < 1$ ) and ( $\lambda > 1$ ) cases, and the intersection points of these lines are given in Table 4.3. The possible variation in  $\lambda$ -coordinate of intersection of the trend lines as shown in Figure 4.4 results in an uncertainty in our calculation of  $\lambda$ . This uncertainty is relatively small. The estimated value of the critical exponent  $\lambda$  is  $1.00 \pm 0.03$ .

## 4.4 Results and Conclusion

This study indicates that for all values of  $J_q$ , as a result of the finite-size scaling, the best fit of specific heat curves of the system arises at  $\lambda = 1.00 \pm 0.03$ . The resulting curves are presented in Figure 4.2. In addition, a second order phase transition occurs at lower temperatures as the sublattices of the system are coupled to each other by a larger inter-sublattice coupling  $J_q$ , as presented in Table 4.1.

However while the phase transitions for different values of  $J_q$  occur at different critical temperatures, the corresponding critical exponents are the same. These results for the non-equilibrium eight-vertex model with Kawasaki dynamics in contact with different heat baths (one of them at infinite temperature) are consistent with the equilibrium Ising universality class.

In conclusion, to the best of our knowledge, this is the first study that indicates

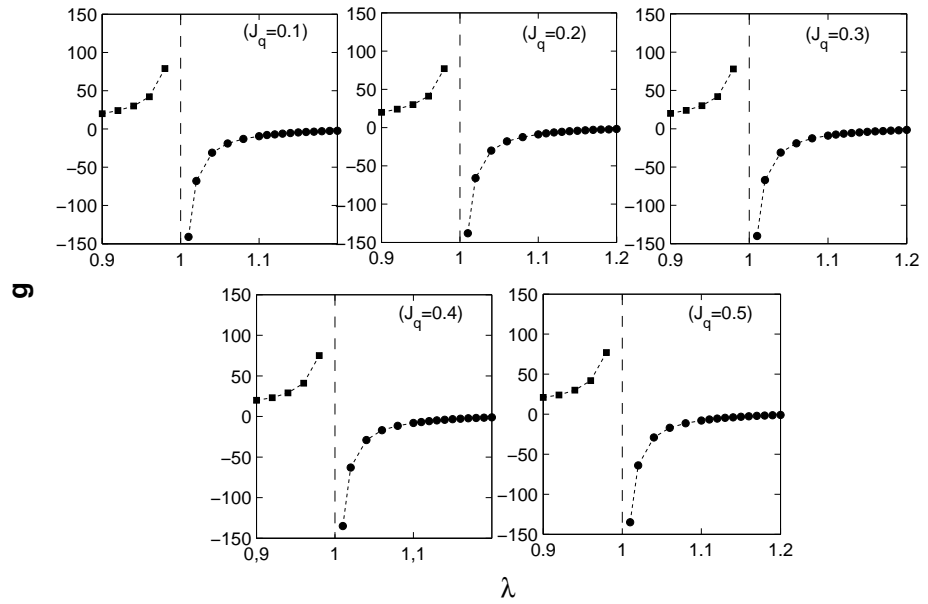


Figure 4.3: Plot of  $g$  versus  $\lambda$  for different values of  $J_q$ . Here, dotted points denote all data points, presented in Table 4.2 and the dashed line indicates the existence of the singularity at  $\lambda = 1$  between the curves.

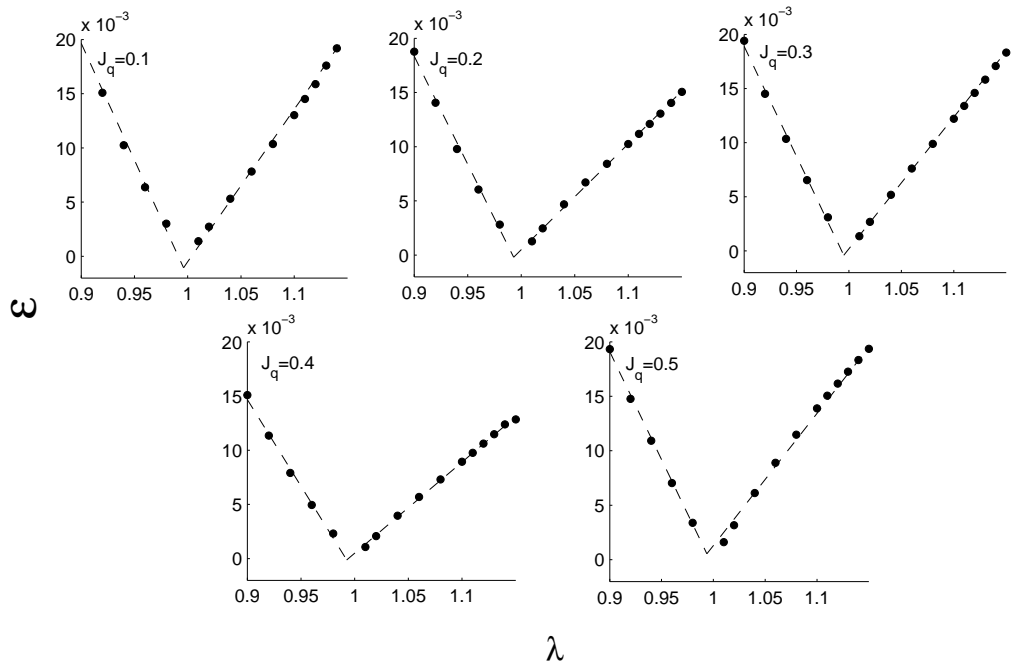


Figure 4.4: Plot of  $\varepsilon$  versus  $\lambda$  for different values of  $J_q$ . Here, dotted points denote all data points, presented in Table 4.2 and the dashed line indicates the interpolated lines.

$J_q = 0.1$			$J_q = 0.2$			$J_q = 0.3$			$J_q = 0.4$			$J_q = 0.5$		
$\lambda$	$g$	$\varepsilon$	$\lambda$	$g$	$\varepsilon$	$\lambda$	$g$	$\varepsilon$	$\lambda$	$g$	$\varepsilon$	$\lambda$	$g$	$\varepsilon$
0.9	20	0.0202	0.9	20	0.0188	0.9	20	0.0194	0.9	20	0.0151	0.9	21	0.0193
0.92	24	0.0151	0.92	24	0.0141	0.92	24	0.0145	0.92	24	0.0145	0.92	23	0.0148
0.94	30	0.0103	0.94	30	0.0098	0.94	30	0.0103	0.94	30	0.0079	0.94	30	0.0109
0.96	42	0.0064	0.96	41	0.0060	0.96	42	0.0065	0.96	41	0.0049	0.96	42	0.0070
0.98	79	0.0030	0.98	77	0.0028	0.98	78	0.0031	0.98	75	0.0023	0.98	77	0.0034
1.01	-141	0.0014	1.01	-138	0.0013	1.01	-140	0.0014	1.01	-135	0.0011	1.01	-135	0.0016
1.02	-68	0.0027	1.02	-66	0.0025	1.02	-67	0.0027	1.02	-63	0.0021	1.02	-64	0.0032
1.04	-31	0.0053	1.04	-30	0.0047	1.04	-31	0.0052	1.04	-29	0.0040	1.04	-29	0.0061
1.06	-19	0.0078	1.06	-18	0.0067	1.06	-19	0.0076	1.06	-17	0.0057	1.06	-17	0.0089
1.08	-13.1	0.0104	1.08	-12.4	0.0084	1.08	-12.5	0.0099	1.08	-11.5	0.0073	1.08	-11.4	0.0115
1.1	-9.5	0.0130	1.1	-8.8	0.0102	1.1	-8.9	0.0122	1.1	-8	0.0089	1.1	-7.9	0.0139
1.11	-7.9	0.0145	1.11	-7.6	0.0112	1.11	-7.6	0.0134	1.11	-6.8	0.0098	1.11	-6.6	0.0150
1.12	-7.1	0.0159	1.12	-6.4	0.0121	1.12	-6.5	0.0146	1.12	-5.8	0.0106	1.12	-5.5	0.0162
1.13	-6.1	0.0176	1.13	-5.5	0.0131	1.13	-5.6	0.0158	1.13	-4.9	0.0115	1.13	-4.6	0.0173
1.14	-5.3	0.0192	1.14	-4.7	0.0140	1.14	-4.8	0.0171	1.14	-4.1	0.0124	1.14	-3.9	0.0183
1.15	-4.5	0.0206	1.15	-4.1	0.0151	1.15	-4.1	0.0183	1.15	-3.4	0.0128	1.15	-3.2	0.0194
1.16	-4	0.0221	1.16	-3.5	0.0161	1.16	-3.5	0.0196	1.16	-2.8	0.0137	1.16	-2.6	0.0204
1.17	-3.5	0.0238	1.17	-3	0.0172	1.17	-3	0.0210	1.17	-2.3	0.0147	1.17	-2.1	0.0214
1.18	-3	0.0256	1.18	-2.5	0.0184	1.18	-2.5	0.0224	1.18	-1.9	0.0157	1.18	-1.7	0.0223
1.19	-2.6	0.0274	1.19	-2.4	0.0185	1.19	-2.1	0.0239	1.19	-1.5	0.0167	1.19	-1.3	0.0233
1.2	-2.3	0.0293	1.2	-1.8	0.0209	1.2	-1.5	0.0209	1.2	-1.2	0.0192	1.2	-1	0.0246

Table 4.2: Quantitative results for the critical exponent  $\lambda$  with the minimum errors of the finite size scaling of the specific heat for different  $J_q$  values.

$J_q$	$\lambda < 1$		$\lambda > 1$		$IntersectionPoint (y_1 = y_2)$	
	$Errorparameter : \varepsilon_1(\lambda)$	$R^2$	$Errorparameter : \varepsilon_2(\lambda)$	$R^2$	$\lambda$	
0.1	$y_1 = -0.2155\lambda + 0.2136$	0.9923	$y_2 = 0.1513\lambda - 0.1527$	0.9909	0.9986	
0.2	$y_1 = -0.1995\lambda + 0.1979$	0.9946	$y_2 = 0.0897\lambda - 0.0884$	0.9692	1.0020	
0.3	$y_1 = -0.2029\lambda + 0.2015$	0.9953	$y_2 = 0.1123\lambda - 0.1113$	0.9819	0.9924	
0.4	$y_1 = -0.1597\lambda + 0.1584$	0.9949	$y_2 = 0.0874\lambda - 0.0872$	0.9922	0.9939	
0.5	$y_1 = -0.1979\lambda + 0.1972$	0.9983	$y_2 = 0.1186\lambda - 0.1171$	0.9947	0.9931	

Table 4.3: The interpolated line equations  $y_1$  and  $y_2$  are obtained from the data pairs  $(\lambda, error)$ , shown in Table 4.2, for  $(\lambda < 1)$  and  $(\lambda > 1)$  cases respectively.  $R^2$  defines the goodness of this interpolation.

a strong evidence of the existence of the universality in the two-temperature eight vertex model with one temperature is infinite.

## Chapter 5

# Further Considerations: Full Phase Diagram of the Non-Equilibrium Eight-Vertex Model with Conserved Order Dynamics

Our study of the non-equilibrium transitions described in the previous chapter considered a system in which one of the heat bath temperatures was infinitely large. This case therefore corresponds to a system quite far from equilibrium.

In this chapter, ongoing research on systems which have small deviations from the equilibrium Baxter critical points. Since these critical points do not display universality in exponents, it is an important question whether this non-universality survives into the nearby non-equilibrium regime. Some of the basic points mentioned in the previous chapter will be repeated to make this section self-contained.

Two different non-equilibrium regions around the critical Baxter line were probed:

**First Case:** Changing only the temperature  $T_2$  in contact with sublattice-2, while the other temperature is kept fixed at a Baxter critical value. (Hereafter referred to as “*single temperature variation*”.)

**Second Case:** Changing the temperatures  $T_1$  and  $T_2$  of both thermal baths symmetrically with respect to a Baxter critical temperature. (Hereafter referred to as “*two temperature variation*”.)

## 5.1 The Model

Again, non-equilibrium properties of the eight-vertex model, constructed by connecting two different Ising lattices with a four spin interaction, are investigated with Monte Carlo simulations. The system is driven to non-equilibrium steady states by putting the Ising lattices in contact with two different heat baths. Phase transitions and the critical exponents are obtained for different temperature limits. Spin exchanges within sublattices occur at different finite temperatures  $T_1$  and  $T_2$  in the non-equilibrium system. To examine the phase transitions, total magnetization in each sublattice is taken as zero.

The Hamiltonian of the system is defined as

$$H = J \sum_{\langle ij \rangle} s_i s_j + J \sum_{\langle i'j' \rangle} \sigma_{i'} \sigma_{j'} + J_q \sum_{\langle ij'i'j' \rangle} s_i s_j \sigma_{i'} \sigma_{j'}, \quad (5.1)$$

where  $\langle ij \rangle$  and  $\langle i'j' \rangle$  denote sums over nearest neighbor pairs of sites in the two sublattices and  $\langle ij'i'j' \rangle$  indicates sum over all spin quads on a unit square as indicated in the Figure 4.1. Here,  $k_B$  is the Boltzmann constant and variables  $s_i$  and  $\sigma_i$  denote the spins in sublattices 1 and 2 respectively. In this equation,  $J$  is the sublattice energy interaction constant between the nearest neighbors and  $J_q$  is the inter-sublattice coupling constant. Then, the unitless energy parameter can be written as

$$\tilde{E} = \frac{\langle E \rangle}{J} = \sum_{\langle ij \rangle} s_i s_j + \sum_{\langle i'j' \rangle} \sigma_{i'} \sigma_{j'} + \left(\frac{J_q}{J}\right) \sum_{\langle ij'i'j' \rangle} s_i s_j \sigma_{i'} \sigma_{j'}. \quad (5.2)$$

The nearest neighbor and four spin coupling constants of the system are introduced as

$$K_i = \frac{J}{k_B T_i} \quad \text{and} \quad Q_i = \frac{J_q}{k_B T_i} \quad (5.3)$$

where  $i$  denotes the corresponding sublattice. In order to decrease the number of parameters of the system, we need to define a parameter “ $\alpha$ ” between the effective temperatures  $T_1$  and  $T_2$  using

$$\alpha = \frac{T_1}{T_2}, \quad (5.4)$$

so that the relations between the coefficients of the system are defined as

$$K_2 = \alpha K_1 \quad \text{and} \quad Q_2 = \alpha Q_1. \quad (5.5)$$

According to these relations,  $K_1, Q_1$  and  $\alpha$  are the parameters of the phase space of the system.

Again, the fluctuations of the unitless energy parameter  $\tilde{E}$  are considered:

$$\tilde{C} = (\langle \tilde{E}^2 \rangle - \langle \tilde{E} \rangle^2). \quad (5.6)$$

For an equilibrium system the specific heat would be given by  $C_v = \frac{J^2}{(k_B T^2)} \tilde{C}$ .

As in mentioned in the previous section, energy fluctuations of the system are obtained by Monte Carlo simulations with the same procedure.

We consider two cases corresponding to possible values of the parameters. Note that the system is in equilibrium ( $T_1 = T_2$ ) at  $\alpha = 1$  and for this limit, R.J. Baxter [100] determined a critical line as a function of four spin coupling constant, shown in equation (4.2). We examine the phase space ( $K_1, Q_1, \alpha$ ) of the system for certain conditions.

- **Single Temperature Variation:** A point is chosen on the critical Baxter line. The values of the parameters of four spin coupling constant  $Q_1$  and energy interaction constant  $K_1$  are determined as  $Q_1 = Q_c$  and  $K_1 = K_c = B(Q_1)$  where  $B$  is the function of the critical Baxter line, given in equation (4.2). Here,  $K_c$  and  $Q_c$  are the chosen critical point of equilibrium eight-vertex model. Then, the phase transitions for  $0 < \alpha < 2$  are investigated as shown in the Figure 5.1. It

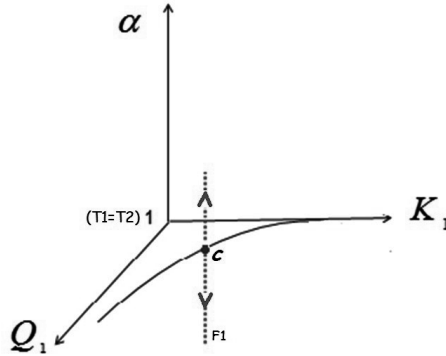


Figure 5.1: An illustration of the phase space of the non-equilibrium eight-vertex model. In the first case of our study, phase transitions are examined along the direction of the dotted line  $F_1$ . The solid line represents the critical Baxter line ( $K_1 = B(Q_1)$ ) in equilibrium and “ $c$ ” denotes a critical point on this line.

should be remembered that the energy constants  $K_2$  and  $Q_2$  of the other sublattice are functions of  $K_1$ ,  $Q_1$  and  $\alpha$ .

- **Two Temperature Variation:** In this case, two different points proportional to a critical point on the critical Baxter line are assigned as shown in the Figure 5.2. Spin exchanges occur at sublattice-1 with energy constants  $K_1 = \delta B(Q_c)$  and  $Q_1 = \delta Q_c$ . Similarly for sublattice-2, dynamics of the system change with energy constants  $K_2 = B(Q_c)/\delta$  and  $Q_2 = Q_c/\delta$ . This leads to  $K_2 = K_1/\delta^2$  and  $Q_2 = Q_1/\delta^2$ . Here, the ratio parameter  $\delta$  is defined as  $\delta = \sqrt{1/\alpha} = \sqrt{T_2/T_1}$ .

Results of our calculations seem to imply that line  $F_1$  is part of the critical surface, and  $F_2$  is perpendicular to it, as shown in Figures 5.1 and 5.2.

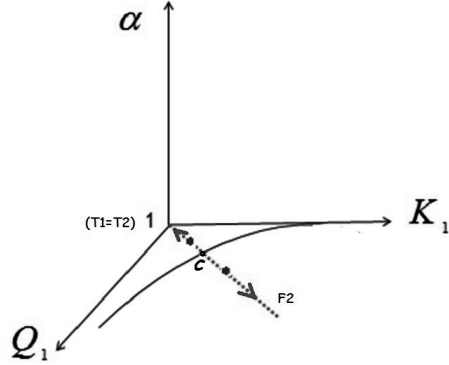


Figure 5.2: An illustration for the second case of our study, phase transitions are examined along the direction of the dotted line  $F_2$ , which does not lie on the  $\alpha = 1$  surface, but crosses it at point “ $c$ ”. The solid line represents the critical Baxter line in equilibrium and “ $c$ ” denotes a critical point on this line.

## 5.2 Preliminary Results

### 5.2.1 Single Temperature Variation:

$$(Q_1 = Q_c, K_1 = B(Q_1)) \text{ and } (Q_2 = \alpha Q_1, K_2 = \alpha K_1)$$

As discussed in the previous section, the energy interaction constant  $K_1$  is determined as  $K_1 = B(Q_1)$  where the corresponding four spin coupling constant  $Q_1$  is equal to  $Q_c$ . Hence, a particular critical point on the equilibrium Baxter critical line is chosen. Other parameters ( $K_2$  and  $Q_2$ ) can be obtained from the value of the temperature ratio  $\alpha$ . It is shown in Figure 5.3 that the singularity in the energy fluctuations of the system occurs at non-equilibrium limits ( $\alpha \neq 1$ ) for different system sizes. The solid line in each graph denotes the equilibrium condition ( $T_1 = T_2$ ) of the system.

To investigate the criticality of the system, correction to scaling defined from the concept of the renormalization group theory is carried out as

$$C_v(N) \approx aN^\lambda \left[ 1 + \frac{b}{N} \right]. \quad (5.7)$$

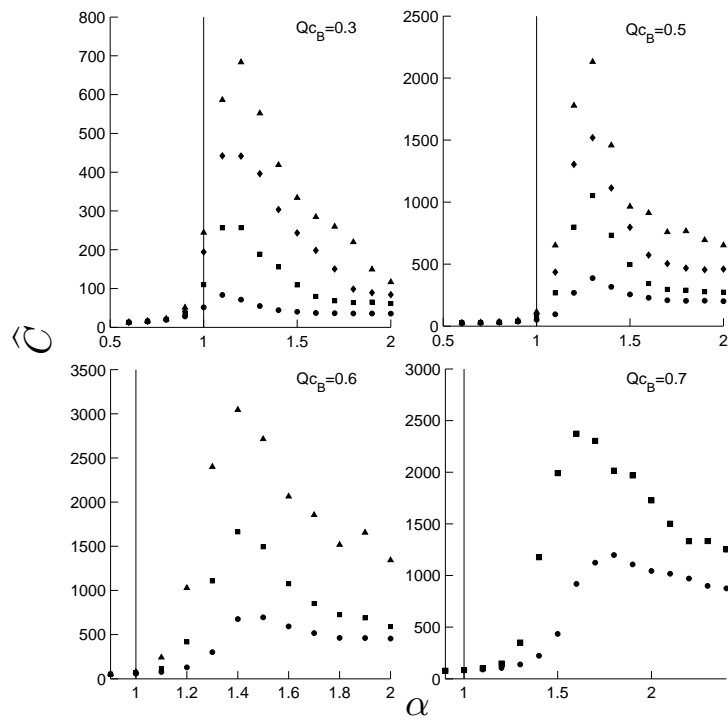


Figure 5.3: Plot of  $\hat{C}$  versus  $\alpha$  for different four spin coupling constant  $Q_1 = Q_{c_B}$ . Symbols are as follows:  $N = 32(\bullet)$ ,  $64(\blacksquare)$ ,  $96(\blacklozenge)$ ,  $128(\blacktriangle)$ . Along the solid line, equilibrium phase transitions occur.

$\alpha = T_1/T_2$	$a$	$b$	$\lambda$
0.1	20.63	0.09	0.003
0.2	21.80	-0.32	-0.003
0.3	23.05	-0.64	-0.008
0.4	22.99	-0.25	-0.001
0.5	23.82	-0.20	0.002
0.6	27.35	-1.15	-0.012
0.7	28.81	-1.03	-0.004
0.8	28.71	-0.41	0.027
0.9	15.86	5.38	0.020
1.0	0.36	62.78	1.108
1.1	2.99	-11.69	1.129
1.2	24.75	-17.22	0.911
1.3	58.21	-17.36	0.772
1.4	27.65	-11.85	0.837
1.5	8.95	0.41	0.964
1.6	0.68	25.30	1.443
1.7	0.26	61.08	1.564
1.8	0.22	61.01	1.600
1.9	1.10	21.04	1.292
2.0	0.28	60.92	1.531

Table 5.1: Correction to scaling results for  $Q_1 = 0.5$

At present, the critical exponent  $\lambda$  is obtained for  $Q_1 = 0.5$  by using the correction to scaling method. Note that  $\hat{C}$  will diverge as  $N \rightarrow \infty$  at a critical point ( $\lambda > 0$ ), otherwise it will approach a finite value ( $\lambda = 0$ ). The corresponding results are presented in the Table 5.1. These results show that second-order phase transitions occur at  $\alpha \geq 1$ . This is an evidence for the existence of a critical surface which contains the Baxter equilibrium critical line and its extension to  $\alpha > 1$  in Figure 5.1.

The value of the equilibrium critical exponent  $\lambda$  obtained from the exact Baxter equations (4.3) and (4.4) is  $\lambda = 1.10227$ . This compares favorably with our result  $\lambda = 1.108$ .

### 5.2.2 Two Temperature Variation:

$$(Q_1 = \delta Q_c, K_1 = \delta B(Q_c)) \text{ and } (Q_2 = Q_c/\delta, K_2 = B(Q_c)/\delta)$$

As mentioned for this case of the study, the effective energy parameters of the

dynamics of the system are chosen as proportional to the exact Baxter critical temperatures. The corresponding energy coupling constants are defined as

$$Q_1 = \delta Q_c \text{ and } K_1 = \delta B(Q_c) \text{ for sublattice-1,}$$

while

$$Q_2 = Q_c/\delta \text{ and } K_2 = B(Q_c)/\delta \text{ for sublattice-2,}$$

where  $\delta = \sqrt{1/\alpha} = \sqrt{T_2/T_1}$ .

Fluctuations  $\widehat{C}$  for two lattice sizes  $N = 20$  and  $N = 64$  are given in Figure 5.4. It is apparent that we need to use larger system sizes to understand the nature of the criticality.

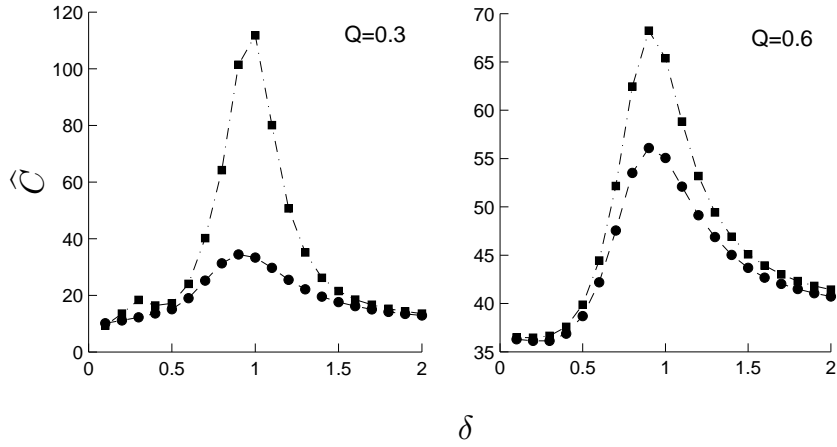


Figure 5.4: Plot of  $\widehat{C}$  versus  $\delta$  for different four spin coupling constant  $Q_1 = Q_{CB}$ . Symbols are as follows:  $N = 32(\bullet)$ ,  $64(\blacksquare)$ .

### 5.3 Discussion

We would like to point out that for the “single temperature variation” case of the problem, the obtained Monte Carlo data which show that the energy fluctuations of the system as presented by Figure 5.3, correspond to singularities for different values of temperature ratios,  $\alpha = \frac{T_1}{T_2} \geq 1$ . Here  $T_1$  refers to the fixed temperature on the critical Baxter line, while  $T_2$  varies.

For the well-known equilibrium limit ( $\alpha = 1$ ), there is a second-order phase transition and as the system size increases the fluctuations diverge. The singularity in the energy fluctuations of the system can be observed at this limit. On the other hand, for the non-equilibrium limits in which  $\alpha > 1$ , this singularity is much more dominant. This means that the second-order phase transition of the system extends to these temperature ratios. For the temperature ratios  $\alpha < 1$ , there are no observable singularities, and hence no phase transitions.

To understand the divergences of the energy fluctuations, correction to scaling is used. This yields an exponent which varies with the temperature ratio  $\alpha$  as shown in Table 5.1. As mentioned in section (5.2.1), the obtained value for this exponent is consistent with the exact equilibrium critical exponent.

In summary, there is a second order phase transition in the system for the temperature ratios  $\alpha \geq 1$  (that is  $T_1 \geq T_2$ ) and all the critical fixed points have different critical exponents.

When we investigate the criticality of the system for the “two temperature variation” case of the problem, the singularity in the energy fluctuations are seen only to be at the equilibrium critical point ( $\delta = 1$ ) as shown in Figure 5.4. However to obtain a comprehensive understanding for this case, further work is needed.

The preliminary results of the first case, namely “single temperature variation” indicates that there is a non-universal critical surface for the non-equilibrium eight-vertex model as shown schematically in Figure 5.5.

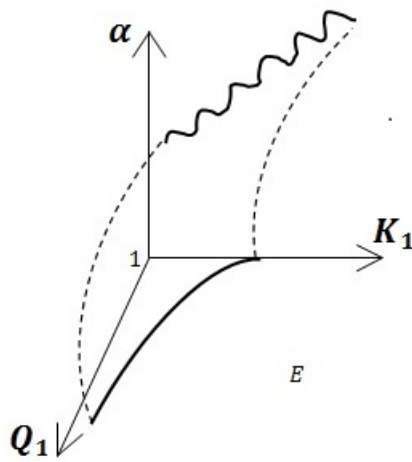


Figure 5.5: An illustration for the critical surface of the non-equilibrium eight vertex model. Here critical surface intersects the critical Baxter line indicated by the solid line at the equilibrium limit represented by  $E$  where  $\alpha = 1$  ( $T_1 = T_2$ ). Critical exponent varies along the critical surface.

# Chapter 6

## Summary and Conclusion

In this thesis, we study the non-equilibrium phase transitions of two different systems, each of them in contact with two heat baths, by using several methods. Both of these systems have spin exchange (Kawasaki) dynamics. Global phase diagrams and the corresponding critical exponents which are related to the universality features of these systems are obtained.

In chapter 3, the non-equilibrium critical properties of the two-finite temperature spin-1/2 Ising model with spin exchange dynamics are investigated through real-space renormalization group transformation (RSRG). We construct a new block-spin transformation which turns the original  $4 \times 4$  system into the renormalized  $2 \times 2$  system. This is the first attempt to use a non-Monte Carlo dynamical RSRG method for a non-equilibrium model with conserved dynamics. Although the RSRG transformation is conveniently applied to isotropic systems, there is reasonable agreement with the results of the previous studies (obtained by methods such as Monte Carlo simulations and the  $\epsilon$ -expansion). An extensive discussion on the validity of this proposed transformation is provided. For the first time in literature, the global phase diagram which includes the steady state, equilibrium and some certain limits of the system is presented. In addition, the corresponding critical exponents of this system are obtained for phase transitions at all limits and indicate the different universality class properties of the non-equilibrium phase transitions. The major flaw of this analysis is the equilibrium

result. This is because of the strong finite size effects of the system used in this study. We also provide an detailed explanation on this subject in Appendix A.

For the second work, steady state phase transitions and the universality behavior of the eight-vertex model, first introduced by R.J. Baxter [100] in equilibrium, is studied through four independent Monte Carlo simulations, each with  $60 \times 10^6$  Monte Carlo steps. The non-equilibrium eight-vertex model is constructed by using two interpenetrating spin-1/2 Ising models on square lattices, each in contact with different thermal baths. In order to avoid any anisotropies, spin exchanges are designed to occur within the sublattices instead of different directions.

In chapter 4, we analyze the limit at which one of the thermal baths coupled to the sublattices has an infinite temperature while the other one has a finite temperature. Monte Carlo simulations are carried out for the system sizes  $N = 32, 40, 80, 100$ . We apply finite size scaling to the Monte Carlo data for different system sizes. A spline interpolation is applied to the scaled data to obtain an error measure for the collapses. This study shows that as we increase the coupling between the corresponding sublattices, phase transitions occur at lower temperatures. This is a result of increased coupling of the finite temperature lattice (in which the transition occurs) to the infinite temperature lattice. At this limit the critical behavior of the non-equilibrium eight-vertex model is like that of the well-known equilibrium Ising model.

To obtain the full phase diagram of this model, we also study the finite temperature limits of this system. The system is investigated for two cases. In the “single temperature variation” case, one of the temperatures is fixed at the critical Baxter value while the other one varies. Monte Carlo simulations of the energy fluctuations for this case indicate that when the variable temperature is greater than or equal to the fixed one, second-order phase transitions occur for all those temperature values. These critical exponents are not universal, as is the case in equilibrium.

In the “two temperature variation” case, we analyze the system in contact with heat baths at finite temperatures displaced symmetrically from the critical Baxter values. Although further work is needed to reach a precise result, it can

be claimed that the second order phase transition occurs only when the system is in equilibrium.

Consequently, the critical surface of the eight-vertex model intersects the critical Baxter line as given by equation (4.2), and shown schematically in Figure 5.5. In this surface all the critical points have their own critical exponents. To sum up, although this system shows Ising-like behavior when one of the temperatures becomes very large, non-universal properties of the non-equilibrium eight-vertex model can be observed to extend around the equilibrium Baxter transition. This is the first study in literature that the non-universality of the non-equilibrium eight vertex model is reported.

# Bibliography

- [1] L. Onsager, “Crystal statistics. i. a two-dimensional model with an order-disorder transition,” *Physical Review*, vol. 65, pp. 117–149, 1944.
- [2] K. E. Bassler and Z. Rácz, “Bicritical point and crossover in a two-temperature, diffusive kinetic Ising model,” *Physical Review Letters*, vol. 73, pp. 1320–1323, 1994.
- [3] G. Ódor, “Universality classes in nonequilibrium lattice systems,” *Reviews of Modern Physics*, vol. 76, pp. 663–724, 2004.
- [4] P. Hohenberg and B. Halperin, “Theory of dynamic critical phenomena,” *Review of Modern Physics*, vol. 49, pp. 435–479, 1977.
- [5] B. Halperin, P. Hohenberg, and S. Ma, “Renormalization-group methods for critical dynamics: I. recursion relations and effects of energy conservation,” *Physical Review B*, vol. 10, pp. 139–153, 1974.
- [6] J. Gibbs, *Elementary principles in statistical mechanics*. New York: Scribner, 1902.
- [7] M. Henkel, H. Hinrichsen, and S. Lübeck, *Non-equilibrium phase transitions, Absorbing Phase Transitions*, vol. 1. New York: Springer, 2008.
- [8] H. E. Stanley, *Introduction to phase transitions and critical phenomena*. Oxford: Oxford University, 1971.
- [9] J. Yeomans, *Statistical Mechanics of the Phase Transitions*. New York: Oxford University Press, 1992.

- [10] S. K. Ma, *Modern theory of critical phenomena*. MA: Addison-Wesley, Reading, 1976.
- [11] M. E. Fisher, “The theory of equilibrium critical phenomena,” *Reports on Progress in Physics*, vol. 30, pp. 615–730, 1967.
- [12] L. P. Kadanof, W. Gotze, D. Hamblen, R. Hecht, E. A. S. Lewis, V. V. Palciauskas, M. Rayl, J. Swift, D. Aspnes, and J. Kane, “Static phenomena near critical points: theory and experiment,” *Reviews of Modern Physics*, vol. 39, pp. 395–431, 1967.
- [13] D. J. Amit, *Field theory, the Renormalization group and critical phenomena*. Singapore: 2nd edition, World Scientific, 1984.
- [14] L. P. Kadanoff, “Scaling laws for Ising models near  $t_c$ ,” *Physics*, vol. 2, pp. 263–272, 1966.
- [15] J. Marro, J. L. Lebowitz, and M. H. Kalos, “Computer simulation of the time evolution of a quenched model alloy in the nucleation region,” *Physical Review Letters*, vol. 43, p. 282285, 1979.
- [16] K. Binder and D. Stauffer, “Theory for the slowing down of the relaxation and spinodal decomposition of binary mixtures,” *Physical Review Letters*, vol. 33, pp. 1006–1009, 1974.
- [17] J. Marro and R. Dickman, *Nonequilibrium Phase Transitions in Lattice Systems*. U.K.: Cambridge University Press, 2005.
- [18] B. Derrida, A. Bray, and C. Godr che, “Non-trivial exponents in the zero temperature dynamics of the 1d Ising and Potts model,” *Journal of Physics A*, vol. 27, pp. L357–L361, 1994.
- [19] G. Grinstein, C. Jayaprakash, and Y. He, “Statistical mechanics of probabilistic cellular automata,” *Physical Review Letters*, vol. 55, pp. 2527–2530, 1985.
- [20] K. E. Bassler and B. Schmittmann, “Critical dynamics of nonconserved Ising-like systems,” *Physical Review Letters*, vol. 73, pp. 3343–3346, 1994.

- [21] B. Schmittman and R. K. P. Zia, *Phase Transitions and critical phenomena*. New York: Academic, 1996.
- [22] B. Schmittman and R. K. P. Zia, “Critical properties of a randomly driven diffusive system,” *Physical Review Letters*, vol. 66, pp. 357–360, 1991.
- [23] B. Schmittman, “Fixed-point Hamiltonian for a randomly driven diffusive system,” *Europhysics Letters*, vol. 24, pp. 109–114, 1993.
- [24] K. E. Bassler and Z. Rácz, “Existence of long-range order in the steady state of a two-dimensional, two-temperature xy model,” *Physical Review E*, vol. 52, pp. R9–R12, 1995.
- [25] W. Lenz, “Beiträge zum verständnis der magnetischen eigenschaften in festen körpern,” *Physikalische Zeitschrift*, vol. 21, pp. 613–615, 1920.
- [26] E. Ising, “Beitrag zur theorie des ferromagnetismus,” *Zeitschrift für Physik*, vol. 31, pp. 253–258, 1925.
- [27] R. J. Glauber, “Time dependent statistics of the Ising model,” *Journal of Mathematical Physics*, vol. 4, pp. 294–307, 1963.
- [28] K. Kawasaki, “Diffusion constants near the critical point for time-dependent Ising models. I,” *Physical Review*, vol. 145, pp. 224–230, 1966.
- [29] S. N. Majumdar, A. J. Bray, S. J. Cornell, and C. Sire, “Global persistence exponent for nonequilibrium critical dynamics,” *Physical Review Letters*, vol. 77, pp. 3704–3707, 1966.
- [30] W. Zwerger, “Critical slowing down of diffusion in an one-dimensional kinetic Ising model,” *Physics Letters A*, vol. 84, pp. 269–270, 1981.
- [31] P. Grassberger, “Damage spreading and critical exponents for “model A” Ising dynamics,” *Physica A*, vol. 214, pp. 547–559, 1995.
- [32] A. J. Jaster, J. Mainville, L. Schuelke, and B. Zheng, “Short-time critical dynamics of the three-dimensional Ising model,” *Journal of Physics A*, vol. 32, pp. 1395–1406, 1999.

- [33] D. Stauffer, “Flipping of magnetization in Ising models at  $T_c$ ,” *International Journal of Modern Physics C*, vol. 7, pp. 753–757, 1996.
- [34] B. Zheng, “Monte Carlo simulations of short-time critical dynamics,” *International Journal of Modern Physics B*, vol. 12, pp. 1419–1484, 1998.
- [35] B. Zheng, “Monte Carlo simulations of critical dynamics with conserved order parameter,” *Physics Letters A*, vol. 277, pp. 257–261, 2000.
- [36] B. Zheng, “Erratum to Monte Carlo simulations of critical dynamics with conserved order parameters: [phys. lett. a 277 (2000) 257],” *Physics Letters A*, vol. 282, p. 132, 2001.
- [37] H. J. Blöte, J. Heringa, A. Hoogland, and R. Zia, “Stability of Ising systems against non-Hamiltonian, symmetry breaking dynamics,” *International Journal of Modern Physics B*, vol. 5, pp. 685–695, 1990.
- [38] M. J. de Oliveira, J. F. F. Mendes, and M. A. Santos, “Nonequilibrium spin models with Ising universal behaviour,” *Journal of Physics A*, vol. 26, pp. 2317–2324, 1993.
- [39] M. A. Santos and S. Teixeira, “Anisotropic voter model,” *Journal of Statistical Physics*, vol. 78, pp. 963–970, 1995.
- [40] P. Tamayo, F. J. Alexander, and R. Gupta, “Two-temperature nonequilibrium Ising models: Critical behavior and universality,” *Physical Review E*, vol. 50, pp. 3474–3484, 1994.
- [41] M. Castro, R. Cuerno, A. Sánchez, and F. Domínguez-Adame, “Anomalous scaling in a nonlocal growth model in the Kardar-Parisi-Zhang universality class,” *Physical Review E*, vol. 57, pp. R2491–R2494, 1998.
- [42] M. C. Marques, “Critical behaviour of the non-equilibrium Ising model with locally competing temperatures,” *Journal of Physics A*, vol. 22, pp. 4493–4497, 1989.
- [43] M. C. Marques, “Nonequilibrium Ising model with competing dynamics: A mfrg approach,” *Physics Letters A*, vol. 145, pp. 379–382, 1990.

- [44] T. Tomé, M. J. de Oliveira, and M. A. Santos, “Non-equilibrium Ising model with competing glauber dynamics,” *Journal of Physics A*, vol. 24, pp. 3677–3686, 1991.
- [45] J. M. González-Miranda, P. L. Garido, J. Marro, and J. L. Lebowitz, “Nonequilibrium phase diagram of Ising model with competing dynamics,” *Physical Review Letters*, vol. 59, pp. 1934–1937, 1987.
- [46] P. L. Garrido, J. Marro, and J. M. González-Miranda, “Nonequilibrium Ising models with competing, reaction-diffusion dynamics,” *Physical Review A*, vol. 40, pp. 5802–5814, 1989.
- [47] E. Præstgaard, H. Larsen, and R. Zia, “Finite-size scaling in a two-temperature lattice gas: A Monte Carlo study of critical properties,” *Europhysics Letters*, vol. 25, pp. 447–452, 1994.
- [48] E. Præstgaard, B. Schmittmann, and R. Zia, “A lattice gas coupled to two thermal reservoirs: Monte Carlo and field theoretic studies,” *European Physical Journal B*, vol. 18, pp. 675–695, 2000.
- [49] P. Garrido, J. Lebowitz, C. Maes, and H. Spohn, “Long-range correlations for conservative dynamics,” *Physical Review A*, vol. 42, pp. 1954–1968, 1990.
- [50] J. Marro and A. Achahbar, “Anisotropic lattice gases,” *Journal of Statistical Physics*, vol. 90, pp. 817–826, 1998.
- [51] A. Achahbar, P. L. Garrido, J. Marro, and M. A. Muñoz, “Is the particle current a relevant feature in driven lattice gases?,” *Physical Review Letters*, vol. 87, pp. 195702–195706, 2001.
- [52] B. Schmittmann and R. Zia, *Phase Transitions and Critical Phenomena*. London: Academic, 1995.
- [53] H. Haken, *Synergetics*. New York: Springer, 1978.
- [54] H. Haken, *Advanced Synergetics*. New York: Springer, 1983.

- [55] C. Nicolis and I. Prigogine, *Self-Organization in Non-Equilibrium Systems*. London: Wiley, 1977.
- [56] W. Dieterich, P. Fulde, and I. Peschel, “Theoretical models for superionic conductors,” *Advanced Physics*, vol. 29, pp. 527–605, 1980.
- [57] S. Katz, J. Lebowitz, and H. Spohn, “Phase transitions in stationary nonequilibrium states of model lattice systems,” *Physical Review B*, vol. 28, pp. 1655–1658, 1983.
- [58] S. Katz, J. Lebowitz, and H. Spohn, “Nonequilibrium steady states of stochastic lattice gas models of fast ionic conductors,” *Journal of Statistical Physics*, vol. 34, pp. 497–537, 1984.
- [59] R. Zia and B. Schmittmann, “A possible classification of nonequilibrium steady states,” *Journal of Physics A*, vol. 39, pp. L407–L413, 2006.
- [60] R. Zia and B. Schmittmann, “Probability currents as principal characteristics in the statistical mechanics of non-equilibrium steady states,” *Journal of Statistical Mechanics*, vol. 2007, p. P07012, 2007.
- [61] J. Vallés and J. Marro, “Nonequilibrium phase transitions in stochastic lattice systems: Influence of the hopping rates,” *Journal of Statistical Physics*, vol. 43, pp. 441–461, 1986.
- [62] J. Vallés and J. Marro, “Nonequilibrium second-order phase transitions in stochastic lattice systems: A finite-size scaling analysis in two dimensions,” *Journal of Statistical Physics*, vol. 49, pp. 89–119, 1987.
- [63] J. Vallés and J. Marro, “Nonequilibrium discontinuous phase transitions in a fast ionic conductor model: Coexistence and spinodal lines,” *Journal of Statistical Physics*, vol. 49, pp. 121–137, 1987.
- [64] M. Zhang, J.-S. Wang, J. Lebowitz, and J. Vallés, “Power law decay of correlations in stationary nonequilibrium lattice gases with conservative dynamics,” *Journal of Statistical Physics*, vol. 52, pp. 1461–1478, 1988.

- [65] J.-S. Wang, K. Binder, and J. Lebowitz, “Computer simulation of driven diffusive systems with exchanges,” *Journal of Statistical Physics*, vol. 56, pp. 783–819, 1989.
- [66] J. Marro, J. Lebowitz, H. Spohn, and M. Kalos, “Nonequilibrium phase transition in stochastic lattice gases: Simulation of a three-dimensional system,” *Journal of Statistical Physics*, vol. 38, pp. 725–733, 1985.
- [67] H. van Beijeren and L. Schulman, “Phase transitions in lattice-gas models far from equilibrium,” *Physical Review Letters*, vol. 53, pp. 806–809, 1984.
- [68] J. Krug, J. Lebowitz, H. Spohn, and M. Zhang, “The fast rate limit of driven diffusive systems,” *Journal of Statistical Physics*, vol. 44, pp. 535–565, 1986.
- [69] K. Gawedzki and A. Kupiainen, “Critical behaviour in a model of stationary flow and supersymmetry breaking,” *Nuclear Physics B*, vol. 269, pp. 45–53, 1986.
- [70] K. Leung and J. Cardy, “Field theory of critical behavior in a driven diffusive system,” *Journal of Statistical Physics*, vol. 44, pp. 567–588, 1986.
- [71] H. Janssen and B. Schmittmann, “Field theory of critical behaviour in driven diffusive systems,” *Zeitschrift für Physik B: Condensed Matter*, vol. 64, pp. 503–514, 1986.
- [72] K. Hwang, B. Schmittmann, and R. K. P. Zia, “Three-point correlation functions in uniformly and randomly driven diffusive systems,” *Physical Review E*, vol. 48, pp. 800–809, 1993.
- [73] K. Leung, “Finite-size scaling of driven diffusive systems: Theory and Monte Carlo studies,” *Physical Review Letters*, vol. 66, pp. 453–456, 1991.
- [74] Z. Cheng, P. Garrido, J. Lebowitz, and J. Vallés, “Long-range correlations in stationary nonequilibrium systems with conservative anisotropic dynamics,” *Europhysics Letters*, vol. 14, pp. 507–513, 1991.
- [75] C. Sanlı, *Two-temperature Ising model at an exact limit*. PhD thesis, Bilkent University, 2008.

- [76] J. Marro, J. Vallés, and J. González-Miranda, “Critical behavior in nonequilibrium phase transitions,” *Physical Review B*, vol. 35, pp. 3372–3375, 1987.
- [77] B. Schmittmann, “Critical behavior of the driven diffusive lattice gas,” *International Journal of Modern Physics B*, vol. 4, pp. 2269–2306, 1990.
- [78] G. Grinstein, “Generic scale invariance in classical nonequilibrium systems (invited),” *Journal of Applied Physics*, vol. 69, pp. 5441–5446, 1991.
- [79] A. D. Masi, P. Ferrari, and J. Lebowitz, “Rigorous derivation of reaction-diffusion equations with fluctuations,” *Physical Review Letters*, vol. 55, pp. 1947–1949, 1985.
- [80] A. D. Masi, P. Ferrari, and J. Lebowitz, “Reaction-diffusion equations for interacting particle systems,” *Journal of Statistical Physics*, vol. 44, pp. 589–644, 1986.
- [81] R. Dickman, “Kinetic phase transitions and tricritical point in an Ising model with competing dynamics,” *Physics Letters A*, vol. 122, pp. 463–466, 1987.
- [82] T. Tomé and M. de Oliveira, “Self-organization in a kinetic Ising model,” *Physical Review A*, vol. 40, pp. 6643–6646, 1989.
- [83] M. Droz, Z. Rácz, and J. Schmidt, “One-dimensional kinetic Ising model with competing dynamics: Steady-state correlations and relaxation times,” *Physical Review A*, vol. 39, pp. 2141–2145, 1989.
- [84] J. Heringa, H. Shinkai, H. Blöte, A. Hoogland, and R. Zia, “Bistability in an Ising model with non-Hamiltonian dynamics,” *Physical Review B*, vol. 45, pp. 5707–5709, 1992.
- [85] H. Blöte, J. Heringa, A. Hoogland, and R. Zia, “Critical properties of nonequilibrium systems without global currents: Ising models at two temperatures,” *Journal of Physics A*, vol. 23, pp. 3799–3808, 1990.
- [86] J.-S. Wang and J. Lebowitz, “Phase transitions and universality in nonequilibrium steady states of stochastic Ising models,” *Journal of Statistical Physics*, vol. 51, pp. 893–906, 1988.

- [87] P. Garrido, A. Labarta, and J. Marro, “Stationary nonequilibrium states in the Ising model with locally competing temperatures,” *Journal of Statistical Physics*, vol. 49, pp. 551–568, 1987.
- [88] K. Wilson, “Renormalization group and critical phenomena. i. renormalization group and the kadanoff scaling picture,” *Physical Review B*, vol. 4, pp. 3174–3183, 1971.
- [89] S. Ma, “Renormalization group by Monte Carlo methods,” *Physical Review Letters*, vol. 37, pp. 461–464, 1976.
- [90] R. Swendsen, “Monte Carlo renormalization group,” *Physical Review Letters*, vol. 42, pp. 859–861, 1979.
- [91] J. Tobochnik, S. Sarker, and R. Cordery, “Dynamic Monte Carlo renormalization group,” *Physical Review Letters*, vol. 46, pp. 1417–1420, 1981.
- [92] M. Yalabik and J. Gunton, “Monte Carlo renormalization-group studies of kinetic Ising models,” *Physical Review B*, vol. 25, pp. 534–537, 1982.
- [93] U. Decker and F. Haake, “Renormalization group transformation for the master equation of a kinetic Ising chain,” *Zeitschrift für Physik B: Condensed Matter*, vol. 35, pp. 281–285, 1979.
- [94] Y. Achiam, “The critical dynamics and the real-space renormalization group,” *Physica A*, vol. 120, pp. 279–313, 1983.
- [95] G. Mazenko, M. Nolan, and O. Valls, “Real-space dynamic renormalization group. ii. simple examples,” *Physical Review B*, vol. 22, pp. 1275–1285, 1980.
- [96] N. Jan, L. Moseley, and D. Stauffer, “Dynamic Monte Carlo renormalization group,” *Journal of Statistical Physics*, vol. 33, pp. 1–11, 1983.
- [97] B. Zheng, “Monte Carlo simulations of critical dynamics with conserved order parameter,” *Physics Letters A*, vol. 277, pp. 257–261, 2000.
- [98] Y. Achiam and J. Kosterlitz, “Real-space renormalization group for critical dynamics,” *Physical Review Letters*, vol. 41, pp. 128–131, 1978.

- [99] T. Lookman, R. Pandey, N. Jan, D. Stauffer, L. Moseley, and H. Stanley, “Real-space renormalization group for kinetic gelation,” *Physical Review B*, vol. 29, pp. 2805–2807, 1984.
- [100] R. Baxter, “Eight-vertex model in lattice statistics,” *Physical Review Letters*, vol. 26, pp. 832–833, 1971.
- [101] N. Metropolis, A. Rosebluth, M. Rosebluth, and A. Teller, “Equation of state calculations by fast computing machines,” *Journal of Chemical Physics*, vol. 21, pp. 1087–1093, 1953.
- [102] M. E. Fisher, in *Critical Phenomena, Proceedings of the International School of Physics Enrico Fermi, Course LI, Varenna, Italy, 1970*, vol. p.1. New York: Academic Press.
- [103] M. Fisher and M. Barber, “Scaling theory for finite-size effects in the critical region,” *Physical Review Letters*, vol. 28, pp. 1516–1519, 1972.
- [104] Y. Imry and B. Bergman, “Critical points and scaling laws for finite systems,” *Physical Review A*, vol. 3, pp. 1416–1418, 1971.

# Appendix A

## Finite Size and Truncation Effects for the Non-Conserved RG Transformation

To investigate the validity of the RSRG method proposed in Chapter 3, the corresponding procedure is also applied to a system with non-conserved parameter near the equilibrium limit. All the characteristics of the RSRG transformation method and the assumptions we made (keeping the periodic boundary conditions in the original and also the renormalized systems, and having a renormalized system obeys the Markovian dynamics as well) in the chapter 4 are also considered in the calculations. Note that although the same transformation of the  $4 \times 4$  lattice to a  $2 \times 2$  lattice is obtained, this time, because of the non-conserved dynamics there are 16 spin configurations of the renormalized lattice (not just the 6 of them as in the previous study). Due to this situation, considerably large numbers of interactions may appear in the Hamiltonian of the system.

For various levels of truncations of the interactions in the system, the results of the corresponding system obtained by the RSRG transformation are presented in the Table A.1. A progressively lower level of the truncation of interaction

constants, keeping nearest-neighbor  $K_{nn}$ , next-nearest-neighbor  $K_{nnn}$ , and four-spin  $K_4$  product terms, is indicated in each line of the Table A.1. Respectively, the calculated values of the critical nearest neighbor interaction  $K_c$ , the fixed point values of the interaction constants  $K^*$ , and the critical exponent for the correlation length  $\nu$  are listed in the Table A.1. (Note that  $K_c$  flows into the fixed point under repeated the renormalization steps.) In addition for the fixed point values of the interaction constants, one can observe the level of truncation.

Consequently based on these calculations, it is understood that for the systems with non-conserved dynamics in the equilibrium limit, the proposed RSRG transformation obtains comparably good results as higher order interaction parameters are considered in the analysis. Especially for the system with the nearest and the next nearest neighbor interactions, the results are rather good. (However one can only regard the nearest neighbor interaction for the possible states of the renormalized systems in which the magnetization is conserved. For the same level of truncation, the accuracy results of the systems with the conserved and non-conserved order parameters are comparable.)

Table A.1: Near equilibrium limit, the RSRG results of the Ising model with non-conserved order parameter obtained through the transformation method presented in chapter 3. Different type of interactions are considered in each case.

<b>Type of interactions</b>	$K_c$	$K_{nn}^*$	$K_{nnn}^*$	$K_4^*$	$\nu$
Nearest neighbor	0.704	0.704	— — —	— — —	0.3797
Next nearest neighbor	0.4189	0.2989	0.08657	— — —	0.947
Four spin	0.4184	0.2999	0.08704	-0.001172	0.9256

# Appendix B

## Spline Interpolation

Let  $a, b \in \mathbb{R}$ , and define the spline as a piecewise polynomial curve function,  $C : [a, b] \rightarrow \mathbb{R}$ . Then let  $X_0 < X_1 < X_2 < \dots < X_n$  be an ordering of real numbers between  $a$  and  $b$  such that  $a = X_0$  and  $b = X_n$ . Then one can obtain  $n$  disjoint subintervals, each defined as  $[X_i, X_{i+1}]$  where  $i = 0 \dots n - 1$ . In each of these subintervals, the spline can be formulated by a polynomial function,  $F_i : [X_i, X_{i+1}] \rightarrow \mathbb{R}$ . This lead to

$$\begin{aligned} C_1(X) &= F_1(X), X_0 \leq X < X_1, \\ C_2(X) &= F_2(X), X_1 \leq X < X_2, \\ &\vdots \\ C_n(X) &= F_n(X), X_{n-1} \leq X \leq X_n. \end{aligned} \tag{B.1}$$

Note that, the total number of data points are equally distributed to these subintervals. Since the lengths of these intervals are not necessarily the same, the splines in our calculations are not uniform. The polynomial function is defined as,

$$F_i(X_i) = \alpha_{0i} + \alpha_{1i}X_i + \alpha_{2i}X_i^2 + \alpha_{3i}X_i^3, \tag{B.2}$$

in each interval. Essential smoothness between these curves depend on some certain conditions,

*i) Continuity of Displacement:* At the boundaries there must be intersection a point between the curve fragment. Thus, polynomial functions must be equal at border points,

$$F_i(X_i) = F_{i+1}(X_i). \quad (\text{B.3})$$

*ii) Continuity of First Derivative of Displacement:* The slopes of the curve splines must be equal at the boundary points. It is to say, the gradient must be continuous,

$$\frac{\partial F_i(X_i)}{\partial X_i} = \frac{\partial F_{i+1}(X_i)}{\partial X_i}. \quad (\text{B.4})$$

*iii) Continuity of Second Derivative of Displacement:* The splines must have the same curvatures at the boundaries,

$$\frac{\partial^2 F_i(X_i)}{\partial X_i^2} = \frac{\partial^2 F_{i+1}(X_i)}{\partial X_i^2}. \quad (\text{B.5})$$

In general, the error  $\varepsilon$  of the fit curve is determined by

$$\varepsilon = \sum_{i,j}^N (\alpha_{0i} + \alpha_{1i}q_{ij} + \alpha_{2i}q_{ij}^2 + \alpha_{3i}q_{ij}^3 - d_{ij})^2, \quad (\text{B.6})$$

where the corresponding subintervals and the data points are denoted by  $i$  and  $j$ , respectively. In equation (B.6), the  $x$  and  $y$  coordinates of the data are defined as  $q_{ij}$  and  $d_{ij}$ . Based on the constraints given in the equations (B.3), (B.4), (B.5), the minimization of the  $\varepsilon$  with respect to the parameters of  $\{\alpha\}$  can be carried out. Therefore the Lagrangian multipliers are needed to be added to the error term given in the equation B.6. As a result, the quantity turns into

$$\begin{aligned} \varepsilon = & \sum_{i,j}^N (\alpha_{0i} + \alpha_{1i}q_{ij} + \alpha_{2i}q_{ij}^2 + \alpha_{3i}q_{ij}^3 - d_{ij})^2 + \\ & \sum_i^N (\Lambda_{0i}(F_{i+1}(X_i) - F_i(X_i)) + \Lambda_{1i}(F'_{i+1}(X_i) - F'_i(X_i)) + \Lambda_{2i}(F''_{i+1}(X_i) - F''_i(X_i))), \end{aligned} \quad (\text{B.7})$$

where  $\Lambda_i$ 's are the Lagrange multipliers.

Consequently,  $\partial\varepsilon/\partial F$  is considered for the error analysis. Additional equations are described in order to minimize the error (for  $\partial\varepsilon/\partial F = 0$ ) as

$$\partial\varepsilon/\partial\alpha_{0i} = \sum_{i,j} [2E_1 + \Lambda_{0i}] = 0, \quad (\text{B.8})$$

$$\partial\varepsilon/\partial\alpha_{1i} = \sum_{i,j} [2E_1 q_{ij} + \Lambda_{0i} X_i + \Lambda_{1i}] = 0, \quad (\text{B.9})$$

$$\partial\varepsilon/\partial\alpha_{2i} = \sum_{i,j} [2E_1 q_{ij}^2 + \Lambda_{0i} X_i^2 + 2\Lambda_{1i} X_i + 2\Lambda_{2i}] = 0, \quad (\text{B.10})$$

$$\partial\varepsilon/\partial\alpha_{3i} = \sum_{i,j} [2E_1 q_{ij}^3 + \Lambda_{0i} X_i^3 + 3\Lambda_{1i} X_i^2 + 6\Lambda_{2i} X_i] = 0, \quad (\text{B.11})$$

where

$$E_1 = (\alpha_{0i} + \alpha_{1i} q_{ij} + \alpha_{2i} q_{ij}^2 + \alpha_{3i} q_{ij}^3 - d_{ij}), \quad (\text{B.12})$$

in addition to  $\partial\varepsilon/\partial\Lambda_i = 0$ .

The set of these parameters are needed to solve in order to obtain the required parameters of the curve function,

$$T\tilde{X} = Y, \quad (\text{B.13})$$

where  $\tilde{X}$  is the vector of all variables,  $Y$  is the vector of constants of the right-hand side of the equations B.9, B.10, B.11, B.11 which correspond to terms that do not contain factors of  $\alpha$ . The solution of this matrix equation gives the sets of the polynomial coefficients for each interval. Then, by using these parameters, one can obtain a smooth spline curve.

# Appendix C

## Code-1: RSRG Transformation

```
#include <stdio.h>
#include <math.h>
#include <stdlib.h>
#include <conio.h>

main(nfile,filenames)
int nfile; char *filenames[];
{
int d,r,s,t,i,j,k,n,mb,m,ier,E0,E1,bb[4],kk;
double b[12870][3],c[12870],eig[3],error[3];
double sum,rate,shift,temp,diff;

void sparse_symm_eig_v();

int a[16],y[16],y1[16],y2[16];
static int X[12870][16];
static double rateL[12870][32],dia[12870],rateLtrans[32][12870];
static int index[12870][32],indextrans[32][12870],symm[3][12870];
int num,count,adr,adrt,adrr,xref_state,yref_state;
```

```

int size=16;
int say,temp1,fark;
double oran1=1.0/3.0;
double oran2=1.0/6.0;
double coup16=16;
double coup24=24;
static double energy[12870],T[12870][6],bprime[6][3];
double coup,w,tot_offdia;
double diagonal,ust1,alt1,ust2,alt2;
double col1,col2,col3,col4;
double lin1,lin2,lin3,lin4;
double coupx,coupy,alpha_x,alpha_y,dif,ratio;

int sw[32][2]={
{0,1},{1,8},{8,9},{0,9},{2,3},{3,10},
{10,11},{2,11},{4,5},{5,12},{12,13},
{4,13},{6,7},{7,14},{14,15},{6,15},
{0,2},{2,4},{4,6},{0,6},{1,3},{3,5},
{5,7},{1,7},{8,10},{10,12},{12,14},
{8,14},{9,11},{11,13},{13,15},{9,15}
};

int Xref[8][2]={
{0,9},{2,11},{4,13},{6,15},{1,8},{3,10},{5,12},{7,14}
};

int Yref[8][2]={
{0,6},{1,7},{8,14},{9,15},{2,4},{3,5},{10,12},{11,13}
};

int nsw=32;

```

```

FILE *pr;
    pr=fopen ("indextrans 12870.txt", "w");

n = 12870; // size of operator
m = 6; // no of eigv to be determined
mb=3;
shift = 35.; // eigenvalue shift

coupx = 0.88; // nearest neighbor coupling in x direction
coupy = 0.88; // nearest neighbor coupling in y direction
alpha_x=3;
alpha_y=1;

s=0;

for(j=0;j<65536;j++) {
    num=j;
    say=0;
    for(i=15;i>=0;i--){
        int base=pow(2,i);
        int remain=num-base;
        if(remain>=0){
            a[15-i]=1;
            num=remain;
        }
        else{
            a[15-i]=-1;
            num=remain+base;
        }
        say=say+a[15-i];
    }
    if(say==0){
// Energy:

```

```

energy[s]= 0.5*(a[0]*(a[1]+a[2]+a[9]+a[6])+
a[1]*(a[8]+a[7]+a[0]+a[3])+
a[2]*(a[3]+a[0]+a[4]+a[11])+
a[3]*(a[2]+a[1]+a[10]+a[5])+
a[4]*(a[2]+a[5]+a[6]+a[13])+
a[5]*(a[4]+a[3]+a[12]+a[7])+
a[6]*(a[4]+a[7]+a[0]+a[15])+
a[7]*(a[1]+a[5]+a[6]+a[14])+
a[8]*(a[1]+a[10]+a[9]+a[14])+
a[9]*(a[8]+a[0]+a[11]+a[15])+
a[10]*(a[8]+a[12]+a[11]+a[3])+
a[11]*(a[10]+a[2]+a[13]+a[9])+
a[12]*(a[10]+a[14]+a[13]+a[5])+
a[13]*(a[11]+a[12]+a[15]+a[4])+
a[14]*(a[7]+a[12]+a[15]+a[8])+
a[15]*(a[13]+a[14]+a[9]+[6]));

```

```

// Construct "T" Transfer matrix:
diagonal=a[0]+a[3]+a[12]+a[15];
ust1=a[0]+a[1]+a[2]+a[3];
alt1=a[4]+a[5]+a[6]+a[7];
ust2=a[8]+a[9]+a[10]+a[11];
alt2=a[12]+a[13]+a[14]+a[15];
col1=a[0]+a[2]+a[4]+a[6];
col2=a[1]+a[3]+a[5]+a[7];
col3=a[8]+a[10]+a[12]+a[14];
col4=a[9]+a[11]+a[13]+a[15];
lin1=a[0]+a[1]+a[8]+a[9];
lin2=a[2]+a[3]+a[10]+a[11];
lin3=a[4]+a[5]+a[12]+a[13];
lin4=a[6]+a[7]+a[14]+a[15];

```

```

/// Certain Cases:
if(diagonal==0){
    if(ust1+alt1==8){
T[s][0]=1;  T[s][1]=0;  T[s][2]=0;
T[s][3]=0;  T[s][4]=0;  T[s][5]=0;
    }

    if(ust2+alt2==8){
T[s][0]=0;  T[s][1]=1;  T[s][2]=0;
T[s][3]=0;  T[s][4]=0;  T[s][5]=0;
    }

    if(alt1+alt2==8){
T[s][0]=0;  T[s][1]=0;  T[s][2]=1;
T[s][3]=0;  T[s][4]=0;  T[s][5]=0;
    }

    if(ust1+ust2==8){
T[s][0]=0;  T[s][1]=0;  T[s][2]=0;
T[s][3]=1;  T[s][4]=0;  T[s][5]=0;
    }

    if(col2+col3==8){
T[s][0]=0.5;  T[s][1]=0.5;  T[s][2]=0;
T[s][3]=0;  T[s][4]=0;  T[s][5]=0;
    }

    if(col1+col4==8){
T[s][0]=0.5;  T[s][1]=0.5;  T[s][2]=0;
T[s][3]=0;  T[s][4]=0;  T[s][5]=0;
    }

    if(lin2+lin3==8){

```

```
T[s][0]=0; T[s][1]=0; T[s][2]=0.5;
T[s][3]=0.5; T[s][4]=0; T[s][5]=0;
}
```

```
if(lin1+lin4==8){
T[s][0]=0; T[s][1]=0; T[s][2]=0.5;
T[s][3]=0.5; T[s][4]=0; T[s][5]=0;
}
}
```

```
if(ust1+alt2==8){
T[s][0]=0; T[s][1]=0; T[s][2]=0;
T[s][3]=0; T[s][4]=1; T[s][5]=0;
}
```

```
if(ust2+alt1==8){
T[s][0]=0; T[s][1]=0; T[s][2]=0;
T[s][3]=0; T[s][4]=0; T[s][5]=1;
}
```

///*Possible Cases:*

```
if(ust1>0){
    if(alt1>0){
T[s][0]=1; T[s][1]=0; T[s][2]=0;
T[s][3]=0; T[s][4]=0; T[s][5]=0;
}
}
```

```
    if(alt1<0){
        if(ust2>0){
T[s][0]=0; T[s][1]=0; T[s][2]=0;
T[s][3]=1; T[s][4]=0; T[s][5]=0;
}
}
```

```
        if(ust2<0){
```

```

T[s][0]=0; T[s][1]=0; T[s][2]=0;
    T[s][3]=0; T[s][4]=1; T[s][5]=0;
    }
    if(ust2==0){
        if(alt2>0){
            T[s][0]=0; T[s][1]=0; T[s][2]=0;
            T[s][3]=0; T[s][4]=1; T[s][5]=0;
        }
        if(alt2<0){
T[s][0]=0; T[s][1]=0; T[s][2]=0;
    T[s][3]=1; T[s][4]=0; T[s][5]=0;
    }
        if(alt2==0){
            if(coup16-energy[s]<energy[s]+coup24){
                T[s][0]=0; T[s][1]=0; T[s][2]=0;
                T[s][3]=1; T[s][4]=0; T[s][5]=0;
            } // T4=0
            if(coup16-energy[s]>energy[s]+coup24){
T[s][0]=0; T[s][1]=0; T[s][2]=0;
T[s][3]=0; T[s][4]=1; T[s][5]=0;
            } //T3=0
            if(coup16-energy[s]==energy[s]+coup24){
T[s][0]=0; T[s][1]=0; T[s][2]=0;
                T[s][3]=0.5; T[s][4]=0.5; T[s][5]=0;
            } //T3=T4=0.5
        }
    }
    if(alt1==0){
        if(ust2>0){
T[s][0]=0; T[s][1]=0; T[s][2]=0;
    T[s][3]=1; T[s][4]=0; T[s][5]=0;
    }

```

```

        if(ust2<0){
            if(alt2>0){
T[s][0]=0; T[s][1]=0; T[s][2]=0;
                T[s][3]=0; T[s][4]=1; T[s][5]=0;
            }
            if(alt2<0){
T[s][0]=1; T[s][1]=0; T[s][2]=0;
                T[s][3]=0; T[s][4]=0; T[s][5]=0;
            }
            if(alt2==0){
                if(coup16-energy[s]<energy[s]+coup24){
                    T[s][0]=1; T[s][1]=0; T[s][2]=0;
                    T[s][3]=0; T[s][4]=0; T[s][5]=0;
                } // T4=0
                if(coup16-energy[s]>energy[s]+coup24){
                    T[s][0]=0; T[s][1]=0; T[s][2]=0;
                    T[s][3]=0; T[s][4]=1; T[s][5]=0;
                }//T0=0
                if(coup16-energy[s]==energy[s]+coup24){
T[s][0]=0.5; T[s][1]=0; T[s][2]=0;
                    T[s][3]=0; T[s][4]=0.5; T[s][5]=0;
                } //T0=T4=0.5
            }
        }
        if(ust2==0){
            if(alt2>0){
                T[s][0]=0; T[s][1]=0; T[s][2]=0;
                T[s][3]=0; T[s][4]=1; T[s][5]=0;
            }
            if(alt2<0){
                T[s][0]=0.5; T[s][1]=0; T[s][2]=0;
                T[s][3]=0.5; T[s][4]=0; T[s][5]=0;
            }
        }
    }
}

```

```

    if(alt2==0){
        if(coup16-energy[s]<energy[s]+coup24){
            T[s][0]=0.5; T[s][1]=0; T[s][2]=0;
            T[s][3]=0.5; T[s][4]=0; T[s][5]=0;
        } // T4=0
        if(coup16-energy[s]>energy[s]+coup24){
            T[s][0]=0; T[s][1]=0; T[s][2]=0;
            T[s][3]=0; T[s][4]=1; T[s][5]=0;
        } //T0=T3=0
        if(coup16-energy[s]==energy[s]+coup24){
            T[s][0]=oran1; T[s][1]=0; T[s][2]=0;
            T[s][3]=oran1; T[s][4]=oran1; T[s][5]=0;
        } //T0=T4=T4=0.333333
    }
}
}
}
if(ust1<0){
    if(alt1>0){
        if(ust2>0){
T[s][0]=0; T[s][1]=0; T[s][2]=0;
            T[s][3]=0; T[s][4]=0; T[s][5]=1;
        }
        if(ust2<0){
            T[s][0]=0; T[s][1]=0; T[s][2]=1;
            T[s][3]=0; T[s][4]=0; T[s][5]=0;
        }
        if(ust2==0){
            if(alt2>0){
                T[s][0]=0; T[s][1]=0; T[s][2]=1;
                T[s][3]=0; T[s][4]=0; T[s][5]=0;
            }
            if(alt2<0){

```

```

        T[s][0]=0; T[s][1]=0; T[s][2]=0;
        T[s][3]=0; T[s][4]=0; T[s][5]=1;
    }
    if(alt2==0){
        if(coup16-energy[s]<energy[s]+coup24){
            T[s][0]=0; T[s][1]=0; T[s][2]=1;
            T[s][3]=0; T[s][4]=0; T[s][5]=0;
        }
        if(coup16-energy[s]>energy[s]+coup24){
            T[s][0]=0; T[s][1]=0; T[s][2]=0;
            T[s][3]=0; T[s][4]=0; T[s][5]=1;
        } //T2=0
        if(coup16-energy[s]==energy[s]+coup24){
            T[s][0]=0; T[s][1]=0; T[s][2]=0.5;
            T[s][3]=0; T[s][4]=0; T[s][5]=0.5;
        } //T2=T5=0.5
    }
}
if(alt1<0){
    T[s][0]=0; T[s][1]=1; T[s][2]=0;
    T[s][3]=0; T[s][4]=0; T[s][5]=0;
}
if(alt1==0){
    if(ust2>0){
        if(alt2>0){
            T[s][0]=0; T[s][1]=1; T[s][2]=0;
            T[s][3]=0; T[s][4]=0; T[s][5]=0;
        }
        if(alt2<0){
            T[s][0]=0; T[s][1]=0; T[s][2]=0;
            T[s][3]=0; T[s][4]=0; T[s][5]=1;
        }
    }
}

```

```

if(alt2==0){
    if(coup16-energy[s]<energy[s]+coup24){
        T[s][0]=0; T[s][1]=1; T[s][2]=0;
        T[s][3]=0; T[s][4]=0; T[s][5]=0;
    } // T5=0
    if(coup16-energy[s]>energy[s]+coup24){
        T[s][0]=0; T[s][1]=0; T[s][2]=0;
        T[s][3]=0; T[s][4]=0; T[s][5]=1;
    } //T1=0
    if(coup16-energy[s]==energy[s]+coup24){
        T[s][0]=0; T[s][1]=0.5; T[s][2]=0;
        T[s][3]=0; T[s][4]=0; T[s][5]=0.5;
    } //T1=T5=0.5
}
}
if(ust2<0){
    T[s][0]=0; T[s][1]=0; T[s][2]=1;
    T[s][3]=0; T[s][4]=0; T[s][5]=0;
}
if(ust2==0){
    if(alt2>0){
        T[s][0]=0; T[s][1]=0.5; T[s][2]=0.5;
        T[s][3]=0; T[s][4]=0; T[s][5]=0;
    }
    if(alt2<0){
        T[s][0]=0; T[s][1]=0; T[s][2]=0;
        T[s][3]=0; T[s][4]=0; T[s][5]=1;
    }
    if(alt2==0){
        if(coup16-energy[s]<energy[s]+coup24){
            T[s][0]=0; T[s][1]=0.5; T[s][2]=0.5;
            T[s][3]=0; T[s][4]=0; T[s][5]=0;
        } // T1=T2=0.5 T5=0
    }
}

```

```

        if(coup16-energy[s]>energy[s]+coup24){
            T[s][0]=0; T[s][1]=0; T[s][2]=0;
            T[s][3]=0; T[s][4]=0; T[s][5]=1;
        } //T1=T2=0 T5=1
        if(coup16-energy[s]==energy[s]+coup24){
            T[s][0]=0; T[s][1]=oran1; T[s][2]=oran1;
            T[s][3]=0; T[s][4]=0; T[s][5]=oran1;
        } //T1=T2=T5=0.333333
    }
}
}
if(ust1==0){
    if(alt1>0){
        if(ust2>0){
            T[s][0]=0; T[s][1]=0; T[s][2]=0;
            T[s][3]=0; T[s][4]=0; T[s][5]=1;
        }
        if(ust2<0){
            if(alt2>0){
                T[s][0]=0; T[s][1]=0; T[s][2]=1;
                T[s][3]=0; T[s][4]=0; T[s][5]=0;
            }
            if(alt2<0){
                T[s][0]=1; T[s][1]=0; T[s][2]=0;
                T[s][3]=0; T[s][4]=0; T[s][5]=0;
            }
            if(alt2==0){
                T[s][0]=0.5; T[s][1]=0; T[s][2]=0.5;
                T[s][3]=0; T[s][4]=0; T[s][5]=0;
            }
        }
    }
    if(ust2==0){

```

```

if(alt2>0){
    T[s][0]=0; T[s][1]=0; T[s][2]=1;
    T[s][3]=0; T[s][4]=0; T[s][5]=0;
}
if(alt2<0){
    if(coup16-energy[s]<energy[s]+coup24){
        T[s][0]=1; T[s][1]=0; T[s][2]=0;
T[s][3]=0; T[s][4]=0; T[s][5]=0;
    } // T5=0
    if(coup16-energy[s]>energy[s]+coup24){
        T[s][0]=0; T[s][1]=0; T[s][2]=0;
        T[s][3]=0; T[s][4]=0; T[s][5]=1;
    } //T0=0
    if(coup16-energy[s]==energy[s]+coup24){
        T[s][0]=0.5; T[s][1]=0; T[s][2]=0;
        T[s][3]=0; T[s][4]=0; T[s][5]=0.5;
    } //T0=T5=0.5
}
if(alt2==0){
    if(coup16-energy[s]<energy[s]+coup24){
        T[s][0]=0.5; T[s][1]=0; T[s][2]=0.5;
        T[s][3]=0; T[s][4]=0; T[s][5]=0;
    } // T5=0
    if(coup16-energy[s]>energy[s]+coup24){
        T[s][0]=0; T[s][1]=0; T[s][2]=0;
        T[s][3]=0; T[s][4]=0; T[s][5]=1;
    } //T0=T2=0
    if(coup16-energy[s]==energy[s]+coup24){
        T[s][0]=oran1; T[s][1]=0; T[s][2]=oran1;
        T[s][3]=0; T[s][4]=0; T[s][5]=oran1;
    } //T0=T2=T5=0.333333
}
}
}

```

```

}
if(alt1<0){
    if(ust2>0){
        if(alt2>0){
            T[s][0]=0; T[s][1]=1; T[s][2]=0;
            T[s][3]=0; T[s][4]=0; T[s][5]=0;
        }
        if(alt2<0){
            T[s][0]=0; T[s][1]=0; T[s][2]=0;
            T[s][3]=1; T[s][4]=0; T[s][5]=0;
        }
        if(alt2==0){
            T[s][0]=0; T[s][1]=0.5; T[s][2]=0;
            T[s][3]=0.5; T[s][4]=0; T[s][5]=0;
        }
    }
    if(ust2<0){
        T[s][0]=0; T[s][1]=0; T[s][2]=0;
        T[s][3]=0; T[s][4]=1; T[s][5]=0;
    }
    if(ust2==0){
        if(alt2>0){
            if(coup16-energy[s]<energy[s]+coup24){
                T[s][0]=0; T[s][1]=1; T[s][2]=0;
                T[s][3]=0; T[s][4]=0; T[s][5]=0;
            } // T4=0
            if(coup16-energy[s]>energy[s]+coup24){
                T[s][0]=0; T[s][1]=0; T[s][2]=0;
                T[s][3]=0; T[s][4]=1; T[s][5]=0;
            }
        } //T1=0
        if(coup16-energy[s]==energy[s]+coup24){
            T[s][0]=0; T[s][1]=0.5; T[s][2]=0;
            T[s][3]=0; T[s][4]=0.5; T[s][5]=0;
        }
    }
}

```

```

        } //T1=T4=0.5
    }
    if(alt2<0){
        T[s][0]=0; T[s][1]=0; T[s][2]=0;
        T[s][3]=1; T[s][4]=0; T[s][5]=0;
    }
    if(alt2==0){
        if(coup16-energy[s]<energy[s]+coup24){
            T[s][0]=0; T[s][1]=0.5; T[s][2]=0;
            T[s][3]=0.5; T[s][4]=0; T[s][5]=0;
        } // T4=0 T1=T3=0.5
        if(coup16-energy[s]>energy[s]+coup24){
            T[s][0]=0; T[s][1]=0; T[s][2]=0;
            T[s][3]=0; T[s][4]=1; T[s][5]=0;
        } //T1=T3=0
        if(coup16-energy[s]==energy[s]+coup24){
            T[s][0]=0; T[s][1]=oran1; T[s][2]=0;
            T[s][3]=oran1; T[s][4]=oran1; T[s][5]=0;
        } //T1=T3=T4=0.333333
    }
}
}
if(alt1==0){
    if(ust2>0){
        if(alt2>0){
            T[s][0]=0; T[s][1]=1; T[s][2]=0;
            T[s][3]=0; T[s][4]=0; T[s][5]=0;
        }
        if(alt2<0){
            if(coup16-energy[s]<energy[s]+coup24){
                T[s][0]=0; T[s][1]=0; T[s][2]=0;
                T[s][3]=1; T[s][4]=0; T[s][5]=0;
            } // T5=0

```

```

    if(coup16-energy[s]>energy[s]+coup24){
        T[s][0]=0; T[s][1]=0; T[s][2]=0;
        T[s][3]=0; T[s][4]=0; T[s][5]=1;
    } //T3=0
    if(coup16-energy[s]==energy[s]+coup24){
        T[s][0]=0; T[s][1]=0; T[s][2]=0;
        T[s][3]=0.5; T[s][4]=0; T[s][5]=0.5;
    } //T3=T5=0.5
}
if(alt2==0){
    if(coup16-energy[s]<energy[s]+coup24){
        T[s][0]=0; T[s][1]=0.5; T[s][2]=0;
        T[s][3]=0.5; T[s][4]=0; T[s][5]=0;
    } // T5=0 T1=T3=0.5
    if(coup16-energy[s]>energy[s]+coup24){
        T[s][0]=0; T[s][1]=0; T[s][2]=0;
        T[s][3]=0; T[s][4]=0; T[s][5]=1;
    } //T1=T3=0
    if(coup16-energy[s]==energy[s]+coup24){
        T[s][0]=0; T[s][1]=oran1; T[s][2]=0;
        T[s][3]=oran1; T[s][4]=0; T[s][5]=oran1;
    } //T1=T3=T5=0.333333
}
}
if(ust2<0){
    if(alt2>0){
        if(coup16-energy[s]<energy[s]+coup24){
            T[s][0]=0; T[s][1]=0; T[s][2]=1;
            T[s][3]=0; T[s][4]=0; T[s][5]=0;
        } // T4=0
        if(coup16-energy[s]>energy[s]+coup24){
            T[s][0]=0; T[s][1]=0; T[s][2]=0;
            T[s][3]=0; T[s][4]=1; T[s][5]=0;
        }
    }
}

```

```

    } //T2=0
    if(coup16-energy[s]==energy[s]+coup24){
        T[s][0]=0; T[s][1]=0; T[s][2]=0.5;
        T[s][3]=0; T[s][4]=0.5; T[s][5]=0;
    } //T2=T4=0.5
}
if(alt2<0){
    T[s][0]=1; T[s][1]=0; T[s][2]=0;
    T[s][3]=0; T[s][4]=0; T[s][5]=0;
}
if(alt2==0){
    if(coup16-energy[s]<energy[s]+coup24){
        T[s][0]=0.5; T[s][1]=0; T[s][2]=0.5;
        T[s][3]=0; T[s][4]=0; T[s][5]=0;
    } // T4=0 T0=T2=0.5
    if(coup16-energy[s]>energy[s]+coup24){
        T[s][0]=0; T[s][1]=0; T[s][2]=0;
        T[s][3]=0; T[s][4]=1; T[s][5]=0;
    } //T0=T2=0
    if(coup16-energy[s]==energy[s]+coup24){
        T[s][0]=oran1; T[s][1]=0; T[s][2]=oran1;
        T[s][3]=0; T[s][4]=oran1; T[s][5]=0;
    } //T1=T3=T5=0.333333
}
}
if(ust2==0){
    if(alt2>0){
        if(coup16-energy[s]<energy[s]+coup24){
            T[s][0]=0; T[s][1]=0.5; T[s][2]=0.5;
            T[s][3]=0; T[s][4]=0; T[s][5]=0;
        } // T4=0
        if(coup16-energy[s]>energy[s]+coup24){
            T[s][0]=0; T[s][1]=0; T[s][2]=0;

```

```

        T[s][3]=0; T[s][4]=1; T[s][5]=0;
    } //T2=T1=0
    if(coup16-energy[s]==energy[s]+coup24){
        T[s][0]=0; T[s][1]=oran1; T[s][2]=oran1;
        T[s][3]=0; T[s][4]=oran1; T[s][5]=0;
    } //T1=T2=T4=0.333333
}
if(alt2<0){
    if(coup16-energy[s]<energy[s]+coup24){
        T[s][0]=0.5; T[s][1]=0; T[s][2]=0;
        T[s][3]=0.5; T[s][4]=0; T[s][5]=0;
    } // T5=0
    if(coup16-energy[s]>energy[s]+coup24){
        T[s][0]=0; T[s][1]=0; T[s][2]=0;
        T[s][3]=0; T[s][4]=0; T[s][5]=1;
    } //T0=T3=0
    if(coup16-energy[s]==energy[s]+coup24){
        T[s][0]=oran1; T[s][1]=0; T[s][2]=0;
        T[s][3]=oran1; T[s][4]=0; T[s][5]=oran1;
    } //T0=T3=T5=0.333333
}
if(alt2==0){
    if(coup16-energy[s]<energy[s]+coup24){
        T[s][0]=0.25; T[s][1]=0.25; T[s][2]=0.25;
        T[s][3]=0.25; T[s][4]=0; T[s][5]=0;
    } // T4=T5=0
    if(coup16-energy[s]>energy[s]+coup24){
        T[s][0]=0; T[s][1]=0; T[s][2]=0;
        T[s][3]=0; T[s][4]=0.5; T[s][5]=0.5;
    } //T0=T1=T2=T3=0
    if(coup16-energy[s]==energy[s]+coup24){
        T[s][0]=oran2; T[s][1]=oran2; T[s][2]=oran2;
        T[s][3]=oran2; T[s][4]=oran2; T[s][5]=oran2;
    }
}

```

```

        }
    }
}

// Constructing the X matrix with the size of 70x8

    for(i=0;i<size;i++)    X[s][i]= (a[i]+1)/2;
    s++;
}
}

for(d=0;d<1;d++){
printf("%d th trial",d);
printf("\n");
printf(" Kp_x = %f\n",coupx);
printf(" Kp_y = %f\n",coupy);
printf("Alpha_y= %f\n",alpha_y);
printf("Alpha_x= %f\n",alpha_x);
diff=0;
for(i=0;i<n;i++){
    for(j=0;j<32;j++) {
        rateL[i][j]=0;
        index[i][j]=-1;
        rateLtrans[j][i]=0;
        indextrans[j][i]=-1;
    }
}

for(i=0;i<n;i++){
adrr=0;
adr=0;

```

```

adrt=0;
tot_offdia=0;
////////////////////////////////////

for(t=0;t<16;t++) y1[t]=X[i][t];
for(t=0;t<16;t++) y2[t]=X[i][t];

for(r=0;r<8;r++){
    temp1=y1[Xref[r][0]];
    y1[Xref[r][0]]=y1[Xref[r][1]];
    y1[Xref[r][1]]=temp1;

    temp1=y2[Yref[r][0]];
    y2[Yref[r][0]]=y2[Yref[r][1]];
    y2[Yref[r][1]]=temp1;
}
for(t=0;t<n;t++){
    say=0;
    for(r=0;r<16;r++){
        if(y1[r]==X[t][r]) say++;
    }
    if(say==16) {
        xref_state=t;
        break;
    }
}

symm[0][i] = xref_state;
symm[1][i] = xref_state;

for(t=0;t<n;t++){
    say=0;
    for(r=0;r<16;r++){

```

```

        if(y2[r]==X[t][r]) say++;
    }
    if(say==16){
        yref_state=t;
        break;
    }
}

symm[2][i] = yref_state;

////////////////////////////////////

    for(r=0;r<nsw;r++) {
// i_th row of the X matrix transforms into the y_th array
        for(t=0;t<16;t++)    y[t]=X[i][t];
// f the spins are not same;
        if(y[sw[r][0]]!=y[sw[r][1]]){
// spin exchange occurs according to the switch matrix
            temp1=y[sw[r][0]];
            y[sw[r][0]]=y[sw[r][1]];
            y[sw[r][1]]=temp1;

            for(j=0;j<n;j++){
                adrt=0;
                adrr=0;
                count=0;
                for(t=0;t<16;t++) {
                    if(y[t]!=X[j][t]) break;
                    count++;
                }
            }
// Constructing the L matrix...

```

```

if(count==16) {

    fark=sw[r][0]-sw[r][1];
    if(abs(fark)%2==0)
        w = alpha_y*(1-tanh((coupy*(energy[i]-energy[j]))/2));
    else
        w = alpha_x*(1-tanh((coupx*(energy[i]-energy[j]))/2));

    if(rateLtrans[adrr][j]==0)
        rateLtrans[adrr][j]=w;
    else{
        for(t=0;t<32;t++){
            if(rateLtrans[t][j]==0) break;
            adrr++;
        }
        rateLtrans[adrr][j]=w;
    }

    if(indextrans[adrt][j]==-1)
        indextrans[adrt][j]=i;
    else{
        for(t=0;t<32;t++){
            if(indextrans[t][j]==-1) break;
            adrt++;
        }
        indextrans[adrt][j]=i;
    }
    rateL[i][adr] = w;
    tot_offdia=tot_offdia+w;
    index[i][adr]=j;
    adr++;
    break;
}

```

```

        }
    }
}
dia[i]=shift-tot_offdia;
}
// initialization:
for(i=0;i<n;i++){
    for(j=0;j<mb;j++){
        b[i][j]=1.;
        for(j=1;j<mb;j++){
            if(symm[j][i] < i) b[i][j] = -1.;
            else if(symm[j][i] == i) b[i][j] = 0.;
        }
    }
}

sparse_symm_eig_v(n,mb,32,indextrans,dia,rateLtrans,symm,b,c,eig,error);

/// Prime matrix size of 4x4 from Vec x T

for(i=0;i<m;i++){
    for(j=0;j<mb;j++){
        bprime[i][j]=0;
        for(k=0;k<n;k++){
            bprime[i][j]=bprime[i][j]+(T[k][i]*b[k][j]);}
    }
}

printf("Olusan b prime matrix: ");
printf("\n");

for(i=0;i<m;i++){
    for(j=0;j<mb;j++){
        printf("%f ",bprime[i][j]);}
    printf("\n");
}

```

```

}

coup_x = 0.125*log(bprime[0][0]/bprime[4][0]);
coup_y = 0.125*log(bprime[2][0]/bprime[4][0]);

alpha_x = ((-0.25*(eig[1]-shift))*(1+(bprime[0][0]/bprime[4][0])));
alpha_y = ((-0.25*(eig[2]-shift))*(1+(bprime[2][0]/bprime[4][0])));
ratio = (eig[1]-shift)*(bprime[0][0]+bprime[4][0])/
        ((eig[2]-shift)*(bprime[2][0]+bprime[4][0]));
printf(" Kp_x = %f\n", coup_x);
printf(" Kp_y = %f\n", coup_y);
printf("Alpha_y= %f\n", alpha_y);
printf("Alpha_x= %f\n", alpha_x);
printf("Ratio: %f\n", ratio);
printf("\n");
printf("\n");

if(alpha_y > alpha_x){
    alpha_x/=alpha_y;
    alpha_y=1.0;
}
else if(alpha_x >= alpha_y){
    alpha_y/=alpha_x;
    alpha_x=1.0;
}

}

fclose(pr);
system("pause");
}

```

```

void sparse_symm_eig_v(n,m,q,indextrans,dia,rateLtrans,symm,b,c,eig,error)
int n; int m; int q; int indextrans[32][12870] ; double dia[12870] ;
double rateLtrans[32][12870]; int symm[3][12870]; double b[12870][3];
double c[12870]; double eig[3]; double error[3];
{
/*
This is a routine to find the largest m eigenvalues and the corresponding
right eigenvectors (with defined symmetries) of an n x n sparse matrix
(with n >= m and q non-diagonal elements in addition to diagonal elements).
The symmetric (assumed to be even for 0'th eigenvector and odd for the
remaining ones) elements are given in the array symm.

The method used is repeated
multiplications, where the largest eigenvalue dominates.
This version finds the left as well as right eigenvectors.
Normalization of b is such that sum_i(b[i][i]*b[i][i])=1
Ld[n] are the diagonal elements // dia[n]
Lwt[q][n] are the non-diagonal elements for transitions to state t
Lit[q][n] are the indices corresponding to the non-diagonal elements
i.e.    L_{n, Lit[q][n]} = Lwt[q][n]
symm[m][n] contains the index of the (anti)symmetric element
b[n][m] contains the m right-eigenvectors on return
c[n] is a buffer array
eig[m] contains the m eigenvalues on return
error[m] contains the average absolute error on return

by Cemal Yalabik, Physics Dept, Bilkent University, Ankara, Turkey
yalabik@fen.bilkent.edu.tr
*/
int i,j,ii,jj,kk,mm,m_list;
double projl,projr,sl,sr,err,prod;

```

```

printf("entering eigens loop\n");
for(kk=0;kk<m;kk++){ // for the m eigenvalues to be determined

    m_list=1;
    for(mm=0;mm<200000;mm++){ // repeated multiplication part

        sr = 0.;
        for(i=0;i<n;i++){
            sr += b[i][kk]*b[i][kk]; // find size
        }
        sr = sqrt(sr);
        for(i=0;i<n;i++){ b[i][kk] /= sr;} // normalize

        for(i=0;i<n;i++){ // apply operator
            if(kk == 0 && symm[0][i] < i){
                c[i] = c[symm[0][i]]; continue;}
            else if(kk != 0 && symm[kk][i] < i){
                c[i] = -c[symm[kk][i]]; continue;}
            else if(kk != 0 && symm[kk][i] == i){
                c[i] = 0.; continue;}

            c[i] = dia[i]*b[i][kk];

            for(j=0;j<q;j++){
                ii=indextrans[j][i];
                if(ii == -1) break;
                c[i] += rateLtrans[j][i]*b[ii][kk];
            }
        }

        sr=0.;prod=0.;
        // find new size
        for(i=0;i<n;i++){sr += c[i]*c[i];prod+=b[i][kk]*c[i];}

```

```

    sr = sqrt(sr);

    err=0.;
    for(i=0;i<n;i++){    // find total absolute error
        err += fabs(sr*b[i][kk]-c[i]);
        b[i][kk] = c[i]/sr; // normalize
    }
    // err = err/(n+n);
    if(mm == m_list){
        m_list = m_list+m_list;
    }

    if(err < 1e-8){break;}

} // mm-loop

eig[kk] = sr;
error[kk] = err;

printf("found eigens %d in %d iterations: %lf with error %le\n",
       kk,mm,eig[kk],error[kk]);

} // kk-loop

return;
}

```

# Appendix D

## Code-2: Monte Carlo Simulations

```
#include<stdio.h>
#include<stdlib.h>
#include<math.h>
#include<time.h>
#define N 100 // Size of the lattice

int main()
{
int m,n,i,j,a,NN;
int loop,mcs,mcs_begin,size,half,say;
int temp,stp;
int E,q;
int lattice1[N][N],lattice2[N][N];
int im1[N],ip1[N],ip2[N];
int E_K1,E_Q1,near1a,near2a,near4_1a,near4_2a;
int E_K2,E_Q2,near1b,near2b,near4_1b,near4_2b;
int rand(),maxint;
int n_eq,n_sample,n_record,count1;
double E1_avg,E1_2_avg,Egy1;
double E2_avg,E2_2_avg,Egy2;
```

```

double E3_avg,E3_2_avg,Egy3;
double tot1_energy,tot2_energy,tot3_energy;
double cv1,cv2,cv3;
double K1,K2,Jq,Q1,Q2,r;
double rr;
double table1[13][13],table2[13][13];
double R;
FILE *analyze; analyze=fopen("analyze.txt","w");
FILE *stop;
FILE *read; read=fopen("read.txt","r");
FILE *write;

if(read==NULL) {
    printf("Error: File can not open\n");
}
else{
    fscanf(read,"%lf %lf %lf %lf %d %d %d %d",&r,&K1,&K2,
           &Jq,&mcs_begin,&n_eq,&n_sample,&n_record);

    if(mcs_begin == 1){
        E1_avg=0.; E1_2_avg=0.;
        E2_avg=0.; E2_2_avg=0.;
        E3_avg=0.; E3_2_avg=0.; count1=0;
    }else{
        fscanf(read,"%d %lf %lf %lf %lf %lf %lf %d %lf %lf %lf",&NN,
               &E1_avg,&E1_2_avg,
               &E2_avg,&E2_2_avg,
               &E3_avg,&E3_2_avg,
               &count1,
               &cv1,&cv2,&cv3);
        if(N != NN){
            printf("incompatible temporary file - stopping!\n");

```

```

        exit(1);
    }
}

printf("System initialize:\n");
printf("r= %lf\n K1= %lf\n K2= %lf\n Jq= %lf\n mcs_begin= %d\n
        n_eq= %d\n n_sample= %d\n n_record= %d\n N= %d\n E1_avg= %lf\n
        E1_2_avg= %lf\n E2_avg= %lf\n E2_2_avg= %lf\n E3_avg= %lf\n
        E3_2_avg= %lf\n count1= %d\n cv1= %lf\n cv2= %lf\n cv3= %lf\n",
        r,K1,K2,Jq,
        mcs_begin,n_eq,n_sample,n_record,N,
        E1_avg,E1_2_avg,
        E2_avg,E2_2_avg,
        E3_avg,E3_2_avg,count1,
        cv1,cv2,cv3);
}

Q1=Jq*K1; // Four spin coupling
Q2=Jq*K2;

maxint=~(1<<(8*sizeof(int)-1));
R=(1.0-r)/2.0;
size=N*N;
half=size/2;

//tables for exchange dynamics of A_ atoms and B atoms

for(i=0;i<=13;i++)
    for(j=0;j<=13;j++){

        table1[i][j]=0.0;
        table2[i][j]=0.0;

```

```

    }

for(i=0;i<13;i=i+2){
    E=i-6;          // -6 -4 -2 0 2 4 6
    for(j=0;j<13;j=j+2){
        q=j-6;
        table1[i][j]=exp((-2*E)*K1+(-2*q)*Q1);
        table2[i][j]=exp((-2*E)*K2+(-2*q)*Q2);
    }
}

//borders
for(i=0;i<N;i++){ im1[i]=i-1;   ip1[i]=i+1;   ip2[i]=i+2; }
im1[0]=N-1;   ip1[N-1]=0;   ip2[N-2]=0;   ip2[N-1]=1;

if(mcs_begin == 1){

// Setting spin_1/2 random lattice1 and lattice2 with zero magnetization
for(i=0;i<N;i++)
    for(j=0;j<N;j++) {
        lattice1[i][j]=1;
        lattice2[i][j]=1; }

for(a=0;a<half;a++){
    say=0;
    while(say==0){
        while( (i=N*(((double)rand())/maxint)) == N ){;}
        while( (j=N*(((double)rand())/maxint)) == N ){;}
        if(lattice1[i][j]==1){
            say=1;
            lattice1[i][j]=-1;
        }
    }
}

```

```

    }
}
for(a=0;a<half;a++){
    say=0;
    while(say==0){
        while( (i=N*(((double)rand())/maxint)) == N ){;}
        while( (j=N*(((double)rand())/maxint)) == N ){;}
        if(lattice2[i][j]==1){
            say=1;
            lattice2[i][j]=-1;
        }
    }
}

}else{

    for(i=0;i<N;i++)
        for(j=0;j<N;j++)
            fscanf(read,"%d %d",&lattice1[i][j],&lattice2[i][j]);

}

fclose(read);

////////////////////////////////MCS PROCEDURE //////////////////////////////////
for(mcs=mcs_begin;;mcs++){

//////////////////////////////// Start 1-MCS loop //////////////////////////////////
    for(loop=0;loop<size;loop++){
        say=0;
        while(say==0){
            //Choose the (m,n) site randomly between 0 and N-1
            while( (n=N*(((double)rand())/maxint)) == N ){;}
            while( (m=N*(((double)rand())/maxint)) == N ){;}

```

```

//Choose a parameter between 0 and 1
// (to determine the type of the current dynamic)

rr=(((double)rand())/maxint);

//Begin procedure
if(rr<R){ //exchange between A atoms
    if( 0.5 > (((double)rand())/maxint) ) { //exchange in x direction
        if(lattice1[m][n]!=lattice1[m][ip1[n]]){
            say=1;
near1a=(lattice1[im1[m]][n]+lattice1[ip1[m]][n]
        +lattice1[m][im1[n]]);

near2a=(lattice1[im1[m]][ip1[n]]+lattice1[ip1[m]][ip1[n]]
        +lattice1[m][ip2[n]]);

near4_1a=(lattice1[im1[m]][n]*
        (lattice2[im1[m]][n]*lattice2[im1[m]][im1[n]])
        +lattice1[m][im1[n]]*
        (lattice2[im1[m]][im1[n]]*lattice2[m][im1[n]])
        +lattice1[ip1[m]][n]*
        (lattice2[m][im1[n]]*lattice2[m][n]));

near4_2a=(lattice1[im1[m]][ip1[n]]*
        (lattice2[im1[m]][n]*lattice2[im1[m]][ip1[n]])
        +lattice1[ip1[m]][ip1[n]]*
        (lattice2[m][n]*lattice2[m][ip1[n]])
        +lattice1[m][ip2[n]]*
        (lattice2[im1[m]][ip1[n]]*lattice2[m][ip1[n]]));

E_K1=lattice1[m][n]*(near1a-near2a);
E_Q1=lattice1[m][n]*(near4_1a-near4_2a);

```

```

        if(table1[E_K1+6][E_Q1+6]>(((double)rand())/maxint)){
            temp=lattice1[m][n];
            lattice1[m][n]=lattice1[m][ip1[n]];
            lattice1[m][ip1[n]]=temp;
        }
    }
} // 0.5 closed
else{ // exchange in y direction
if(lattice1[m][n]!=lattice1[ip1[m]][n]){
    say=1;

near1a=(lattice1[im1[m]][n]+lattice1[m][ip1[n]]
        +lattice1[m][im1[n]]);

near2a=(lattice1[ip2[m]][n]+lattice1[ip1[m]][im1[n]]
        +lattice1[ip1[m]][ip1[n]]);

near4_1a=(lattice1[im1[m]][n]*
        (lattice2[im1[m]][n]*lattice2[im1[m]][im1[n]])
+lattice1[m][im1[n]]*
        (lattice2[im1[m]][im1[n]]*lattice2[m][im1[n]])
+lattice1[m][ip1[n]]*
        (lattice2[im1[m]][n]*lattice2[m][n]));

near4_2a=(lattice1[ip1[m]][im1[n]]*
        (lattice2[m][im1[n]]*lattice2[ip1[m]][im1[n]])
+lattice1[ip2[m]][n]*
        (lattice2[ip1[m]][im1[n]]*lattice2[ip1[m]][n])
+lattice1[ip1[m]][ip1[n]]*
        (lattice2[m][n]*lattice2[ip1[m]][n]));

E_K1=lattice1[m][n]*(near1a-near2a);
E_Q1=lattice1[m][n]*(near4_1a-near4_2a);

```

```

        if(table1[E_K1+6][E_Q1+6]>=(((double)rand())/maxint)){
            temp=lattice1[m][n];
            lattice1[m][n]=lattice1[ip1[m]][n];
            lattice1[ip1[m]][n]=temp;
        }
    }
} //else (for y direction) closed

} // if(rr<R) closed
else{ //exchange between B atoms
    if( 0.5 > (((double)rand())/maxint) ){ // exchange in x direction
        if(lattice2[m][n]!=lattice2[m][ip1[n]]){
            say=1;
near1b=(lattice2[im1[m]][n]+lattice2[ip1[m]][n]
        +lattice2[m][im1[n]]);

near2b=(lattice2[im1[m]][ip1[n]]+lattice2[ip1[m]][ip1[n]]
        +lattice2[m][ip2[n]]);
near4_1b=(lattice2[im1[m]][n]*
        (lattice1[m][n]*lattice1[m][ip1[n]])
        +lattice2[m][im1[n]]*
        (lattice1[m][n]*lattice1[ip1[m]][n])
        +lattice2[ip1[m]][n]*
        (lattice1[ip1[m]][ip1[n]]*lattice1[ip1[n]][n]));

near4_2b=(lattice2[im1[m]][ip1[n]]*
        (lattice1[m][ip1[n]]*lattice1[m][ip2[n]])
        +lattice2[ip1[m]][ip1[n]]*
        (lattice1[ip1[m]][ip1[n]]*lattice1[ip1[m]][ip2[n]])
        +lattice2[m][ip2[n]]*
        (lattice1[m][ip2[n]]*lattice1[ip1[m]][ip2[n]]));

```

```

E_K2=lattice2[m][n]*(near1b-near2b);
E_Q2=lattice2[m][n]*(near4_1b-near4_2b);

if(table2[E_K2+6][E_Q2+6]>(((double)rand())/maxint)){
    temp=lattice2[m][n];
    lattice2[m][n]=lattice2[m][ip1[n]];
    lattice2[m][ip1[n]]=temp;
}
}
} //0.5 closed
else{ // exchange in y direction between B atoms
    if(lattice2[m][n]!=lattice2[ip1[m]][n]){
        say=1;
near1b=(lattice2[im1[m]][n]+lattice2[m][ip1[n]]
        +lattice2[m][im1[n]]);

near2b=(lattice2[ip2[m]][n]+lattice2[ip1[m]][im1[n]]
        +lattice2[ip1[m]][ip1[n]]);

near4_1b=(lattice2[im1[m]][n]*
        (lattice1[m][n]*lattice1[m][ip1[n]])
        +lattice2[m][im1[n]]*
        (lattice1[m][n]*lattice1[ip1[m]][n])
        +lattice2[m][ip1[n]]*
        (lattice1[m][ip1[n]]*lattice1[ip1[m]][ip1[n]]));

near4_2b=(lattice2[ip1[m]][im1[n]]*
        (lattice1[ip1[m]][n]*lattice1[ip2[m]][n])
        +lattice2[ip2[m]][n]*
        (lattice1[ip2[m]][n]*lattice1[ip2[m]][ip1[n]])
        +lattice2[ip1[m]][ip1[n]]*

```

```

        (lattice1[ip1[m]][ip1[n]]*lattice1[ip2[m]][ip1[n]]));

    E_K2=lattice2[m][n]*(near1b-near2b);
    E_Q2=lattice2[m][n]*(near4_1b-near4_2b);

    if(table2[E_K2+6][E_Q2+6]>=(((double)rand())/maxint)){
        temp=lattice2[m][n];
        lattice2[m][n]=lattice2[ip1[m]][n];
        lattice2[ip1[m]][n]=temp;
    }
}

} // else closed
} // exchange between B atoms "closed"

} // while closed

} //End 1_MCS loop
//////////////////////////////// End 1-MCS loop //////////////////////////////////

//////////////// Compute physical quantities //////////////////
if(mcs >= n_eq){
    if((mcs-n_eq)%n_sample==0){
        tot1_energy =0.0;
        tot2_energy =0.0;
        tot3_energy =0.0;
        count1=count1+1;
        for(i=0;i<N;i++) for(j=0;j<N;j++){

Egy1=lattice1[i][j]*(lattice1[ip1[i]][j]+lattice1[i][ip1[j]]);

Egy2=lattice2[i][j]*(lattice2[ip1[i]][j]+lattice2[i][ip1[j]]);

```

```

Egy3=(lattice1[i][j]*lattice1[im1[i]][j]*
      lattice2[im1[i]][im1[j]]*lattice2[im1[i]][j])
+(lattice1[i][j]*lattice1[i][ip1[j]]*
      lattice2[im1[i]][j]*lattice2[i][j]);

    tot1_energy+=Egy1;
    tot2_energy+=Egy2;
    tot3_energy+=Egy3;
}
E1_avg+=tot1_energy;      E1_2_avg+=tot1_energy*tot1_energy;
E2_avg+=tot2_energy;      E2_2_avg+=tot2_energy*tot2_energy;
E3_avg+=tot3_energy;      E3_2_avg+=tot3_energy*tot3_energy;
}

////////////////////////////////////End - energy fluctuations////////////////////////////////////

if((mcs-n_eq)%n_record == 0){

    write=fopen("write.txt","w");

    cv1 = ( E1_2_avg/count1 - ( (E1_avg/count1)*(E1_avg/count1) ) ) / size;
    cv2 = ( E2_2_avg/count1 - ( (E2_avg/count1)*(E2_avg/count1) ) ) / size;
    cv3 = ( E3_2_avg/count1 - ( (E3_avg/count1)*(E3_avg/count1) ) ) / size;

    fprintf(write,"%lf\n %lf\n %lf\n %lf\n %d\n %d\n %d\n %d\n %d\n %lf\n
              %lf\n %lf\n %lf\n %lf\n %d\n %lf\n %lf\n %lf\n",
            r,K1,K2,Jq,
            mcs,n_eq,n_sample,n_record,N,
            E1_avg,E1_2_avg,
            E2_avg,E2_2_avg,
            E3_avg,E3_2_avg,
            count1,

```

```

        cv1,cv2,cv3);

for(i=0;i<N;i++)
    for(j=0;j<N;j++)
        fprintf(write,"%d %d ",lattice1[i][j],lattice2[i][j]);

fprintf(write," \n");

fflush(write);
fclose(write);
fprintf(analyze,"%d %f %f %f\n",mcs,cv1,cv2,cv3);

stop=fopen("stop_file.txt","r");
if(stop==NULL) {
    printf("Error: stop File can not open\n");
}
else{
    fscanf(stop,"%d",&stp);
}

if(stp==1) exit(1);
fclose(stop);

}
if(mcs==40000000) exit(1);

} // End of if mcs>n_eq

////////////////////////////////////
} // End MCS

```

```
//////////////////////////////////// End MCS procedure //////////////////////////////////////
```

```
fflush(analyze);
```

```
fclose(analyze);
```

```
return;
```

```
}
```

# Appendix E

## Code-3: Finite Size Scaling

```
#include<stdio.h>
#include<stdlib.h>
#include<math.h>
#include<conio.h>
#define N 80 // total number of data points(x,y)

main(nfile,filenames)
int nfile; char *filenames[];
{

FILE *results;
results=fopen("results.txt","r");
FILE *fit;
fit=fopen("FIT.txt","w");
FILE *err;
err=fopen("error.txt","w");
FILE *fss;
fss=fopen("FSS_org.txt","w");
FILE *n100;
n100=fopen("N100.txt","w");
```

```

FILE *n80;
n80=fopen("N80.txt","w");
FILE *n40;
n40=fopen("N40.txt","w");
FILE *n32;
n32=fopen("N32.txt","w");

int i,j,k,a,b,n,count;
int num_points,interval;
int low,high;
int dd,nn,mm,fact,ier;
double ctrl,func,func2,fmax,diff,error,std_dev,jj;
double lambda,gg;

interval=10;
error=0.0;

printf("Please enter gg and lambda values:\n");
scanf("%lf %lf",&gg, &lambda);
printf("gg= %lf lambda=%lf\n",gg,lambda);

num_points=N/interval; // total data point in each interval=16
nn=(7*interval)-3;
mm=1;
double orginal[N][2],data[N][2];
double T[nn][nn];
double Y[nn][1];
double x[interval+1];
double arr[N][2];

void gelg(); void quicksort();
double sum(); double sum_y();

```

```

for(i=0;i<N;i++){
    for(j=0;j<2;j++){
        fscanf(results,"%lf",&original[i][j]);
        data[i][j]=0.0;
    }
}
//////// Finite-Size Scaling (FSS)////////////////////////////////////

for(i=0;i<20;i++){ // N100
data[i][0]=(original[i][0]-0.45)*pow(100,lambda);
data[i][1]=(original[i][1]-gg)/pow(100,(2.0*lambda-2.0));
fprintf(n100,"%lf      %lf\n",data[i][0],data[i][1]);
}
for(i=20;i<40;i++){ // N80
data[i][0]=(original[i][0]-0.44)*pow(80,lambda);
data[i][1]=(original[i][1]-gg)/pow(80,(2.0*lambda-2.0));
fprintf(n80,"%lf      %lf\n",data[i][0],data[i][1]);
}
for(i=40;i<60;i++){ // N40
data[i][0]=(original[i][0]-0.43)*pow(40,lambda);
data[i][1]=(original[i][1]-gg)/pow(40,(2.0*lambda-2.0));
fprintf(n40,"%lf      %lf\n",data[i][0],data[i][1]);
}
for(i=60;i<N;i++){ // N32
data[i][0]=(original[i][0]-0.43)*pow(32,lambda);
data[i][1]=(original[i][1]-gg)/pow(32,(2.0*lambda-2.0));
fprintf(n32,"%lf      %lf\n",data[i][0],data[i][1]);
}
// Sort the data according to the x-axis
quicksort(data,0,(N-1));

for(i=0;i<N;i++){

```

```

        for(j=0;j<2;j++){ fprintf(fss,"%lf      ",data[i][j]);}
        fprintf(fss,"\n");
        fflush(fss);
    }

    //////////// END-FSS ////////////////////////////////////////////

    x[0]=data[0][0];
    x[interval]=data[N-1][0];
    for(i=1;i<interval;i++){
        x[i]=(data[num_points*i][0]+data[(num_points*i)-1][0])/2.0;
    }

    //for(i=0;i<(interval+1);i++) printf("%lf\n",x[i]);

    for(i=0;i<nn;i++){
        for(j=0;j<nn;j++){ T[i][j]=0.0; }
    }

    //////////// Symmetric parts - with 5 alpha ////////////////////////////////////////////
    a=0;
    b=num_points;
    for(k=0;k<nn;k=k+7){
        for(i=0;i<4;i++){
            for(j=0;j<4;j++){
                dd=i+j;
                T[i+k][j+k]=2.0*sum(a,b,dd,data);
            }
        }
        a=a+num_points;
        b=b+num_points;
    }

```

```

}
////////// asymmetric parts://////////
n=0;
for(k=0;k<(nn-4);k=k+7){
    for(i=0;i<4;i++){
        T[i+k][4+k]=pow(x[n+1],i);
        T[4+k][i+k]=T[i+k][4+k];
        T[4+k][i+k+7]= -T[i+k][4+k];
        T[i+k+7][4+k]= -T[i+k][4+k];
    }
    for(i=1;i<4;i++){
        T[i+k][5+k]=(i*pow(x[n+1],(i-1)));
        T[5+k][i+k]=T[i+k][5+k];
        T[5+k][i+k+7]= -T[i+k][5+k];
        T[i+k+7][5+k]= -T[i+k][5+k];
    }
    for(i=2;i<4;i++){
        fact=1;
        for(j=1;j<=i;j++){ fact*=j; }
        T[i+k][6+k]=(fact*pow(x[n+1],(i-2)));
        T[6+k][i+k]=T[i+k][6+k];
        T[6+k][i+k+7]= -T[i+k][6+k];
        T[i+k+7][6+k]= -T[i+k][6+k];
    }
    n++;
}
//////////

for(i=0;i<nn;i++){ Y[i][0]=0.0; }
a=0;
b=num_points;
for(k=0;k<nn;k=k+7){
    for(i=0;i<4;i++){

```

```

                                Y[k+i] [0]=2.*sum_y(a,b,i,data);
                                }

a=a+num_points;
b=b+num_points;
}
////////////////////////////////////

gelg(nn,mm,T,Y,&ier);

//// PLOT & ERROR //////////////////////////////////////
fmax=0.0;
ctrl=0.0;
k=0;
for(i=0;i<interval;i++){
    for(j=0;j<=10;j++){
        jj=(x[i]*(10-j)+x[i+1]*j)/10.;
        fprintf(fit,"%lf    ",jj);
        func=Y[k] [0]+(Y[k+1] [0]*jj)+(Y[k+2] [0]*pow(jj,2.0))
                +(Y[k+3] [0]*pow(jj,3.0));

        if(ctrl==0.0){
            if(jj >= 0.0){fmax=func; ctrl=jj;}
        }
        fprintf(fit,"%lf\n",func);
        fflush(fit);

    }
    k=k+7;
}

////// Deviation //////////////////////////////////////

diff=0.0;

```

```

count=0;
k=14; // reason: starting from the 2nd interval
a=16; // reason: starting from the 2nd interval
b=num_points+16; //8 points in each interval
// for(i=0;i<interval;i++){
for(i=2;i<7;i++){ // from the interval2 to the interval7
                // (central 5 interval with 40 points)
    for(j=a;j<b;j++){
//    if(abs(data[j][0]) <= 5.0){
        count++;
        func2=Y[k][0]+(Y[k+1][0]*data[j][0])+(Y[k+2][0]*pow(data[j][0],2.0))
                +(Y[k+3][0]*pow(data[j][0],3.0));

        diff += pow( fabs(data[j][1]-func2),2.0);

    } // }
    a=a+num_points;
    b=b+num_points;
    k=k+7;
}

std_dev=0.0;
error=0.0;
std_dev = (diff/count);
error=sqrt(std_dev)/fabs(fmax);
printf("diff: %lf\n number_of_points: %d\n std_dev: %lf\n
      (x0,f_max): %lf %lf\n ERROR: %lf\n",
      diff,count,std_dev,ctrl,fmax,error);

fprintf(err,"diff: %lf\n number_of_points: %d\n std_dev: %lf\n
      f_max: %lf\n ERROR: %lf\n",diff,count,std_dev,fmax,error);

```

```

fclose(err);
fclose(fit);
fclose(fss);
fclose(n100);
fclose(n80);
fclose(n40);
fclose(n32);
fclose(results);
getch();
return 0;
}

```

```

double sum(int a, int b, int dd, double c[80][2]) // q^dd
{
    int i,j;
    double top;
    top=0.0;
    for(i=a;i<b;i++){
        top += pow(c[i][0],dd); // sum_Xi
    }
    return top;
}

```

```

double sum_y(int a, int b, int dd, double c[80][2]) // q^dd
{
    int i,j;
    double top;
    top=0.0;
    for(i=a;i<b;i++){
        top += c[i][1]*pow(c[i][0],dd); // // sum_Xi
    }
    return top;
}

```

```

}

void gelg(n,m,a,b,ier)
int n; int m; double a[n][n]; double b[n][m]; int *ier;
{
/*
c
c this is a subroutine to solve a system of linear equations
c a(n,n) is the coefficient matrix      (destroyed)
c b(n,m) is the "right hand side" matrix (solution on return)
c ier is returned as a non-zero value if matrix a is ill defined
c by Cemal Yalabik, Physics Dept, Bilkent University, Ankara, Turkey
c   yalabik@fen.bilkent.edu.tr
*/
    int i,j,k,irow;
    double big,raa,aa,tt,fabs();
    *ier=0;
    for(i=0;i<n;i++){
// find the largest element in this coulumn:
        if(i == n-1){
            irow=n-1;
            big=fabs(a[n-1][n-1]);
        }
        else{
            big=-1.;
            for(j=i;j<n;j++){
                raa=fabs(a[j][i]);
                if(raa <= big){continue;}
                big=raa;
                irow=j;
            }
        }
    }
    if(big == 0.){

```

```

        *ier=i;
        return;
    }
// interchange the pivot row
    aa=1./a[irow][i];
    for(j=i;j<n;j++){
        tt=a[irow][j];
        a[irow][j]=a[i][j];
        a[i][j]=tt*aa;
    }
    for(j=0;j<m;j++){
        tt=b[irow][j];
        b[irow][j]=b[i][j];
        b[i][j]=tt*aa;
    }
// eliminate the remaining elements on this column
    for(j=0;j<n;j++){
        if(i == j){continue; }
        aa=a[j][i];
        for(k=i;k<n;k++){
            a[j][k]=a[j][k]-aa*a[i][k];
        }
        for(k=0;k<m;k++){
            b[j][k]=b[j][k]-aa*b[i][k];
        }
    }
}
return;
}

/* sort everything inbetween 'low' <-> 'high' */
void quicksort(double arr[N][2],int low,int high)
{

```

```

int i = low;
int j = high;
int y = (low+high)/2;
double row = 0.0;
double col = 0.0;

/* compare value */
double z = arr[y][0];

/* partition */
do {
    /* find member above ... */
    while(arr[i][0] < z) i++;

    /* find element below ... */
    while(arr[j][0] > z) j--;

if(i <= j) {
    /* swap two elements */
    row = arr[i][0];
    col = arr[i][1];

    arr[i][0] = arr[j][0];
    arr[i][1] = arr[j][1];
    arr[j][0] = row;
    arr[j][1] = col;
    i++;
    j--;
}
} while(i <= j);

/* recurse */
if(low < j)

```

```
quicksort(arr, low, j);

if(i < high)
    quicksort(arr, i, high);
}
```